CUMULONIMBUS CONVECTION IN SHEAR

by

Mitchell William Moncrieff.

Department of Meteorology,

Imperial College of Science and Technology.

A Thesis Submitted for the

Degree of Doctor of Philosophy

in the University of London.

ABSTRACT

A steady, two-dimensional dynamical model of cumulonimbus convection in shear is developed, based on a particular observational description.

A conservative quantity, fundamental in this type of finite-amplitude convective overturning is found and used to formulate an eigenvalue problem for the streamfunction, defined in terms of two nondimensional numbers - a Richardson Number and a density-scaling parameter. Solution of the asymptotic form defines the height of the steering-level and also the remote flow. Using real data to evaluate the nondimensional numbers, the height of the steering-level and the propagation speed of particular convective systems compare favourably with the corresponding observed values.

The transformation between the compressible and incompressible solutions for finite-amplitude flow contrasts with that associated with linear theory.

Heat and momentum fluxes are quantified and are contrary to the usual conceptions of mesoscale transport mechanisms. These could be used to parameterise cumulonimbus convection in global numerical models. A measure of the transport efficiency of cumulonimbus convection compared to smaller scale processes is obtained.

The two-dimensional problem is approached from free-boundary and initial-value viewpoints, the main difficulty in the former being the prescription of appropriate dynamical boundary conditions at the updraught/downdraught interface. With pressure continuous, $-1.62 \leqslant Ri \leqslant 0.75$ is shown to be a necessary condition for the existence of solutions to the free-boundary problem, and for steady, two-dimensional, wet-adiabatic overturning; this type

of overturning demands an interface sloping downshear.

Using the initial-value problem as a guide, an alternative dynamic boundary condition is defined, modelling a physical process in the updraught/downdraught boundary layer; this process is associated with an interface which slopes upshear.

A momentum budget indicates that further physical processes could be featured in an extension to three space dimensions, giving grounds for future research.

LIST OF CONTENTS

CHAPTER I — INTRODUCTION

The recognition of structure in convective systems has led to significant developments in meteorology over recent years. For instance, the structure of large-scale slantwise convection, particularly in relation to the poleward transfer of heat and momentum, has been evident for many years and is important for the maintenance of climate on the global scale. Only comparatively recently however, in conjunction with the development of global atmospheric modelling, has a more precise theory of smaller scale transfer become necessary. The necessity arises because the fluxes of heat and momentum from low to high levels are crucial for the maintenance of the available potential energy of the global atmosphere and hence the maintenance of the large scale eddies which effect most of the large-scale heat and momentum transfer. This implies close interaction between all scales of atmospheric motion and indeed the models of cumulonimbus convection in shear developed in later chapters reflect this philosophy in that they are expressed in terms of parameters which can be measured on the synoptic scale.

Before proceeding with the development of specific dynamical models of cumulonimbus convection in sheared flow, it is enlightening to review the problem from the meteorological viewpoint and also briefly discuss work which is mathematically relevant.

1.1 — THE DESCRIPTIVE APPROACH

Serious study of cumulonimbus convection from the descriptive viewpoint has been going on for the greater part of a century, among the earlier descriptive models being those by Möller (1884), Davies (1894), Wegener (1911), Brooks (1922),

Simpson (1924), Letzmann (1930), Suckstorff (1939) and Findeisen (1940). These were extremely qualitative and progress was hampered mainly due to difficulty in collecting data from upper levels. It was not until the development of aircraft robust enough to traverse storm areas and more particularly the application of radar to descriptive meteorology, that systematic and comprehensive data could be obtained.

The first intensive study using these techniques was the Thunderstorm Project, conducted in Ohio and Florida. The results of this study published by Byers and Braham (1949), did much to quantify updraught and downdraught speed and area, cloud-top height, storm propagation speed, time evolution etc. However, the storms examined during the Thunderstorm Project were probably not typical of the more severe variety found in the mid-western states of America, which have a high frequency of very large hail. The storms studied in the Thunderstorm Project had a low proportion of hail, and were not so severe in terms of updraught speed. It is interesting to note that in general the shear was generally less than 10^{-3} s^{-1}, at least a factor of three smaller than that considered typical of severe storm situations.

The mid-latitude severe storm, characterised by its giant hailstones, intense rainfall and strong squalls is distinctive from the more sporadic and less intense 'heat storm', a common feature of summer afternoons. Not only is the intensity of these severe storms much greater but also their duration, since they can last for at least twelve hours often during the night, contrasting with the 'heat storm' which usually decays when the buoyant sources provided by solar heating of the surface, die out in the evening. These cumulonimbi characteristically

travel several hundreds of kilometres during their lifetime, while the 'heat storm' is a much more localised and slower moving phenomenon. Stationary severe storms are however found occasionally, but this feature will be discussed more fully in chapter III.

Prohaska (1907) was among the first observers to record that mid-latitude severe storms are characteristic of frontal regions and that they travel at the speed of the usually substantial mid-level wind. Much later Wichmann (1951) noted from glider experience that updraught speeds as large as 20 - 30 m s^{-1} were maintained over a number of kilometres, and also that in such cases strong shear was usually present in the undisturbed flow. The correlation of strong mid-level winds with storm occurrence was noted by Fawbush and Miller (1953), who advised that strong winds at 500 mb and 700 mb was a reliable prediction of storm severity.

Aided by rainfall data, Newton (1959) tracked the movement of individual storms over several hundred kilometres for periods of the order of twelve hours, noting that the storm tracks were on the average 20 degrees to the right of the mean 850 mb - 500 mb wind direction.

Although the occurrence of severe storms had previously been correlated with strong shear in the troposphere, Newton (1959) was the first to include this feature into a descriptive model for the maintenance of a severe storm and the observed regeneration on the right flank. However, after a systematic study including intensive radar analysis of the Wokingham Storm of 9 July 1959, Ludlam and Browning (1962) produced the first descriptive model suggesting that not only is wind-shear important for the maintenance of the overturning, but also for the occurrence of

large hail and the intensity of the downdraught circulation. Since the description of the severe storm given by Ludlam and Browning suggested the form of the dynamical model developed in the following chapters, it is worthwhile presenting this description in some detail. Greater detail of the other descriptions can be found in papers by the particular authors listed in the references or in a more concise form in Meteorological Monographs, Vol.5.

From their detailed observational study of cumulonimbi working and propagating in zones of marked wind-shear, Ludlam and Browning suggest that their detailed data is consistent with a quasi-steady, wet-adiabatic relative flow consisting of two distinct branches. In one branch, low-level potentially warm air enters the front of the system forming an updraught, where buoyancy is generated due to the latent heat released by the condensation of water vapour. The other branch is a downdraught of comparable intensity, maintained by the cooling of potentially cold mid-level air entering at high-levels from the rear, by the evaporation of rain falling from the updraught branch. It is also inferred from observational evidence that the updraught slopes backwards over the downdraught. This orientation is emphasised because rain falling from the updraught can fall directly into and maintain the downdraught by evaporative cooling, and moreover hail can circulate in the updraught and thus grow to the observed large size. Fig.(1.1) is a diagrammatic representation of this descriptive model. Consequently, cumulonimbi working in a sheared airstream is visualised as being an extreme form of steady, organised convection in which mixing is unimportant, in contrast with cumulus convection which is a process dominated by mixing.

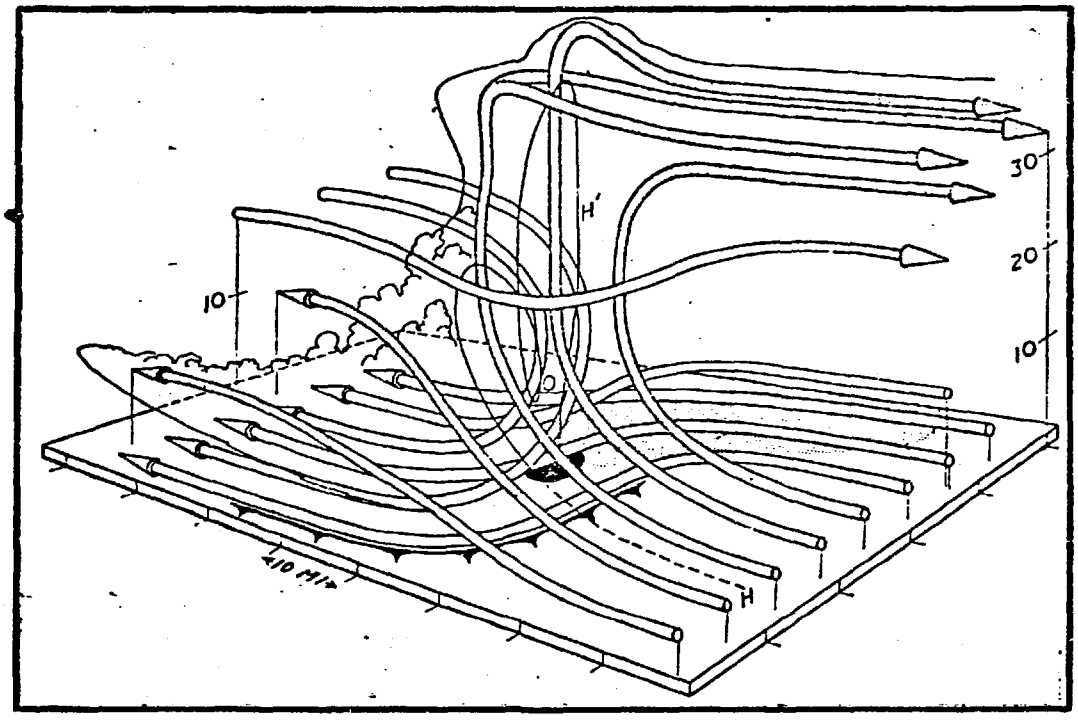

FIG. 1.1.1 — THREE-DIMENSIONAL DESCRIPTION OF THE RELATIVE FLOW WITHIN THE WOKINGHAM STORM. THE PATH HOH' IS THE SUGGESTED TRAJECTORY OF A PARTICLE WHICH BECOMES A LARGE HAILSTONE. (FROM BROWNING & LUDLAM (1962)).

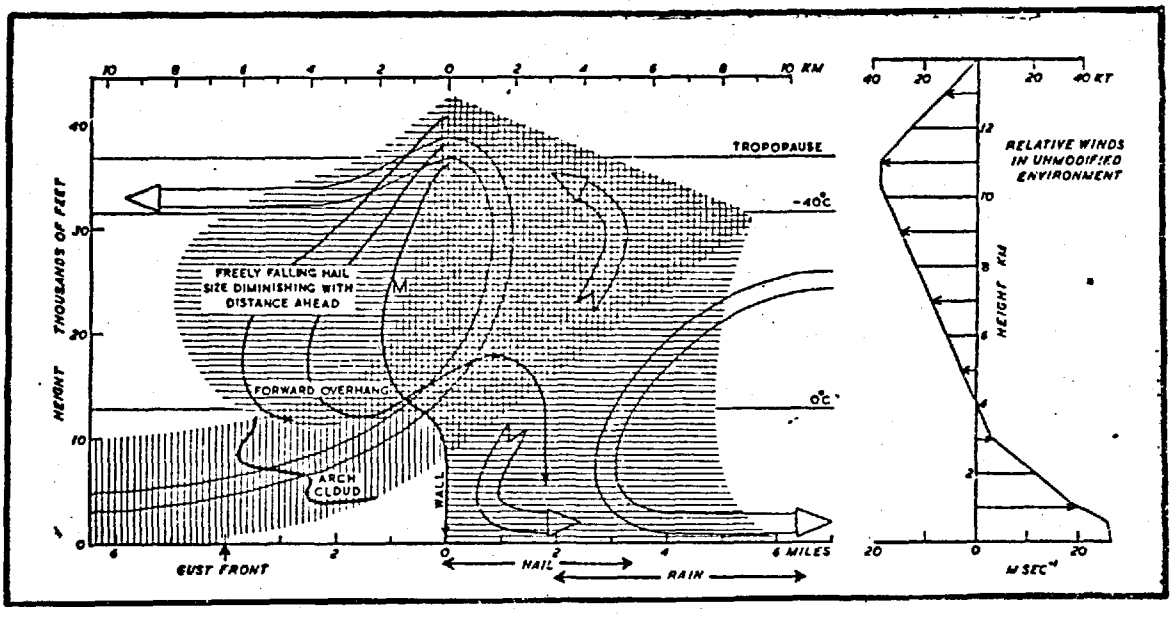

FIG. 1.1.2 — VERTICAL SECTION THROUGH THE WOKINGHAM STORM ALONG THE DIRECTION OF PROPAGATION, WHICH IS FROM RIGHT TO LEFT IN THIS FIGURE. THE FLOW IS RELATIVE TO COORDINATES MOVING AT THE STORM SPEED IN BOTH FIGURES. (FROM BROWNING & LUDLAM).

Severe storms can persist in situations where the amount of available potential energy, as measured by the positive area on a tephigram is rather small, with an intensity comparable to those on occasions with a significantly larger amount of available potential energy. (For instance compare the tephigrams of the Wokingham and Horsham Storms in chapter III.) This suggests that the shear or the available potential energy alone may not be the important parameter for cumulonimbus convection in shear, but rather a relationship between these two parameters. Subsequently it will be shown that this is indeed the case, the important parameter being a Richardson Number.

A dynamical model of cumulonimbus convection in shear based on the above descriptive model has at least to quantify the factors determining the propagation of the system and the important question of the orientation of the updraught/downdraught boundary. Moreover, as far as global atmospheric models are concerned, the main question to be answered is not the detailed forms of the individual cloud systems, but rather the effect which these mesoscale phenomena have on the synoptic scale, particularly their role in the vertical transfer of heat and momentum. These points define the main subject matter of this thesis.

1.2 — THE MATHEMATICAL APPROACH

Compared to observational work done on cumulonimbus convection in shear, the amount of work adopting a dynamical approach is small. Regarding convection in shear in general, theoretical approaches can be classified into two distinct categories.

First, linearised perturbation analysis has been extensively

used to examine the dynamical stability of the basic flow, including the classical problem of the dynamical stability of statically stable shear flow and the more recent studies of the statically unstable problem. Since the resulting boundary-value problem is linear and usually analytically tractable some progress has been made on the analytical treatment.

Second, the finite amplitude problem which is the most relevant in cumulonimbus convection because particles undergo vertical displacement comparable to the depth of the system. Due to the intractable nonlinearity of the equations, this problem requires some degree of numerical solution, whether it is a purely numerical initial-value problem or as in this thesis a partly numerical, partly analytic eigenvalue problem.

Although only the finite amplitude approach is directly relevant to the cumulonimbus problem, a brief summary of the linearised theory is interesting because in both approaches the form of the convection is classified into regimes determined largely by a Richardson Number. However, the resemblance between the linearised and finite amplitude motion is superficial and the approaches really define distinct classes of motion.

1.2.1 — SUMMARY OF THE LINEARISED THEORY OF CONVECTION IN SHEAR

The dynamical stability of neutrally stratified, inviscid shear flow has been studied since Rayleigh (1880). If the velocity of an unbounded homogeneous fluid changes discontinuously at a free-surface, then this surface is dynamically unstable for perturbations of all wavelengths, but the short waves grow fastest. The introduction of a transition layer stabilises the short waves provided the undisturbed vorticity gradient changes sign across the shear layer, while if the vorticity gradient

does not change sign all waves are stable.

(a) Statically Stable Flow

If the undisturbed shear flow is stratified, then the mathematical problem of determing the stability criterion is much more difficult due to the singular form of the differential equation (of hypergeometric form). In the Helmholtz problem, where both the velocity and density change discontinuously at a free-surface, with the denser fluid underneath giving a statically stable flow, short waves of wave number λ satisfying

$$\lambda > \frac{2g(\rho_2 - \rho_1)}{(\rho_1 + \rho_2)} \Big/ (U_2 - U_1)^2$$

are unstable, while the long waves are stable. (Subscripts [1] and [2] denote upper and lower fluid respectively.)

Taylor (1931) considered the stability of shear flow in a semi-infinite region bounded below by a rigid surface. He dealt with constant shear and stratification in the undisturbed flow, finding that the flow is stable if the Richardson Number (Ri) satisfies $Ri > 1/4$, while if $0 < Ri < 1/4$ no harmonic waves can exist.

Case and Dyson (1960), adopting an initial-value problem approach with the same undisturbed flow as Taylor, showed that if $0 < Ri < 1/4$ an arbitrary initial perturbation behaves like $t^{\frac{1}{2}[(1-4Ri)^{\frac{1}{2}}-1]}$ as $t \to \infty$, proving the flow stable.

Goldstein (1931) was concerned with the dynamical stability of a three-layered, unbounded fluid having a continuous density and velocity profile, but with discontinuities in the undisturbed vorticity at the two free-surfaces. He found that the flow is dynamically unstable if $0 < Ri < 1/4$ and stable if $Ri > 1/4$.

Drazin (1958) considered flow in which the undisturbed

density, velocity and vorticity are everywhere continuous in an unbounded region. He obtained a critical Richardson Number of 1/4, agreeing with Goldstein's result. Presumably the vorticity discontinuities in Goldstein's model do not influence the stability criterion.

Miles (1961) proved that sufficient conditions for the stability of a heterogeneous shear flow that $\frac{du}{dz} \neq 0$ and that the local Richardson Number satisfies $Ri(z) > 1/4$ at every point in a bounded region. Howard (1961) proved the more general result that a sufficient condition for dynamical stability is $Ri > 1/4$.

Consequently, it is well established that a statically stable shear flow is dynamically stable for any velocity profile if $Ri > 1/4$, while if $0 < Ri < 1/4$ the flow may or may not be stable depending on the velocity profile. Moreover, the above brief summary indicates that the justification for having discontinuities in the velocity, density or vorticity is non-trivial at least from the point of view of dynamical stability. It will be seen later that prescribing a dynamical boundary condition which implies discontinuities of velocity, temperature, vorticity and pressure is not a trivial problem to justify either.

(b) Statically Unstable Flow

The meteorologically significant linear theory of unstably stratified shear flow was studied by Kuo(1963). He shows that if the stratification is unstable, three-dimensional perturbations are more likely to be dynamically unstable than two-dimensional perturbations, contrasting with stably stratified shear flow which exhibits the opposite effect. Consequently, in determining the stability criteria in the unstably stratified case, it is

necessary to include the transverse wavenumber. Moreover, in order to explicitly determine the preferred scale of the transverse motion, Kuo finds it necessary to include the dissipation of heat and momentum in his analysis. He defines the stability regimes in terms of a modified Richardson Number $\overline{J} = (1 + \frac{K_2}{K_1})\,Ri$, where K_1 and K_2 are the wavenumbers in the direction of and transverse to the shear respectively. Kuo shows that in unsheared, statically unstable, inviscid flow, perturbations of all wavenumbers are dynamically unstable, while in the sheared case provided that $0 > \overline{J} > -2$, the short waves are stable. He also shows that $\overline{J} < -2$ is a sufficient condition for instability in a semi-infinite region with constant undisturbed shear — that is, <u>all</u> waves are unstable if $\overline{J} < -2$. (Remember that Howard showed that all waves are stable if $Ri > 1/4$.) For bounded regions an analogous result holds if -2 is replaced by -0.75. Fig.(1.2) shows the complete set of regimes of dynamical stability/instability for constant undisturbed shear.

Thus for small negative Ri, two-dimensional perturbations (that is $K_2 = 0$ with variations in the shear direction only) are stable, but three-dimensional perturbations ($K_2 \neq 0$) are unstable if $\overline{J} = (1 + K_2/K_1)Ri < -2$. In fact Kuo showed that the most preferred motion corresponds to large $\overline{J}$, with the consequence that if $-2 < Ri < 0$ long roll-clouds (altocumulus) with $K_1 << K_2$ will develop, so that their axis will be parallel to the shear vector. If however $-Ri$ is large, so that both the two- and three-dimensional perturbations are unstable, the growing disturbances will be characteristically three-dimensional with the clouds forming longitudinally and transversely spaced rolls, their orientation being dependent on the ratio K_1/K_2.

FIG. 1.2 — STABILITY REGIMES OF SMALL AMPLITUDE PERTURBATIONS IN FLOW OF CONSTANT UNDISTURBED SHEAR. (after Kuo)

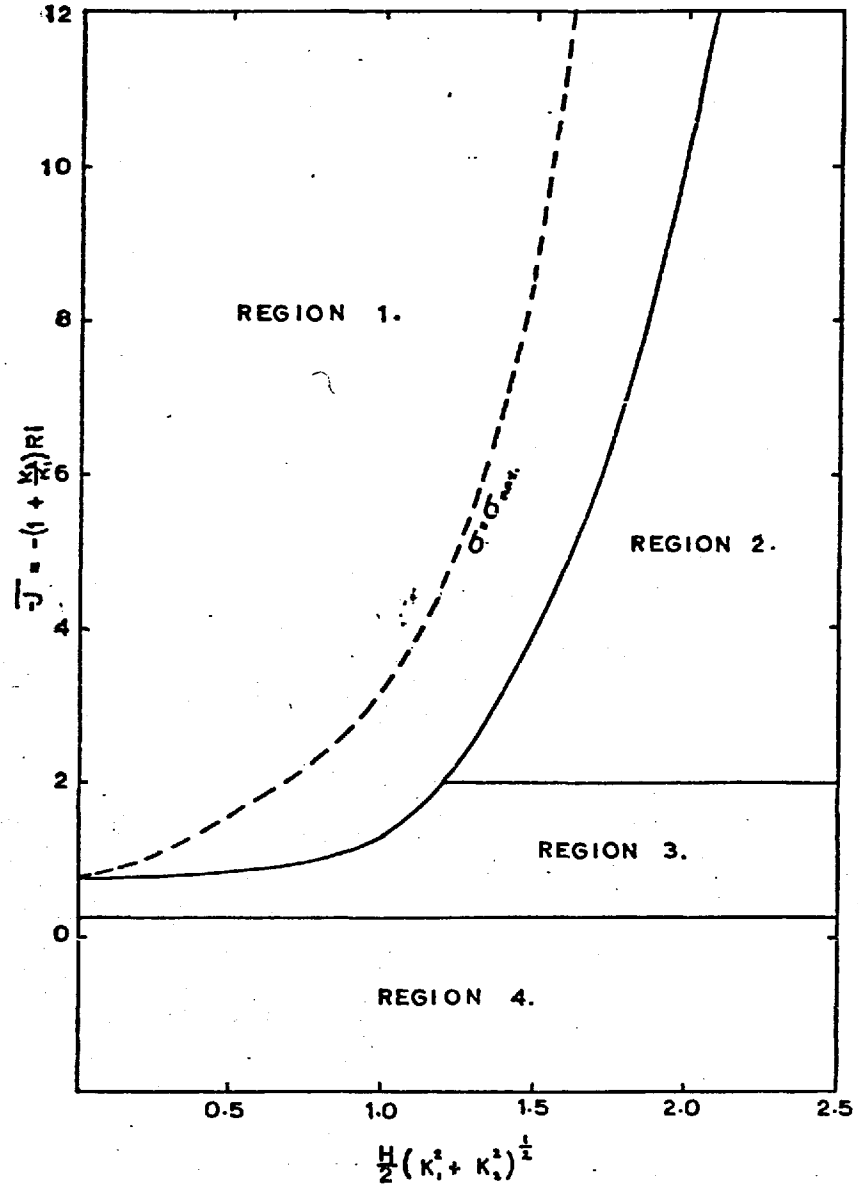

REGION 1 – Unstable long waves, stationary relative to the mid-level flow with a wavelength of maximum amplification rate.

REGION 2 – Unstable short waves, propagating relative to the flow at all levels with almost uniform growth rates.

REGION 3 – Stable waves. No eigensolutions exist in this region and initial perturbations behave asymptotically like $t^{\frac{1}{2}[(1-4J)^{\frac{1}{2}}-1]}$.

REGION 4 – Neutrally stable internal gravity waves.

From the above discussion on the stability of shear flow, it is evident that if the flow is stably stratified with $0 < Ri < 1/4$ and d^2u/dz^2 changes sign in the shear layer, since two-dimensional flow ($K_2 = 0$) is the most unstable, billow clouds with their axes perpendicular to the shear vector will be the dominant convective regime. If however, the flow is unstably stratified with $-2 < Ri < 0$ ($-0.75 < Ri < 0$ in bounded regions), then roll-clouds with their axes parallel to the shear vector will be the dominant regime.

In later chapters it will be shown that within a limited range of Richardson Number, ($-1.62 \leqslant Ri \leqslant 0.75$) when the convection is of finite amplitude, steady overturning with axes perpendicular to the shear vector is the preferred class of motion. This is one example of a contrast between finite amplitude and linearised theories of convection in shear, others will arise in later analysis.

1.2.2 — FINITE AMPLITUDE APPROACHES TO CUMULONIMBUS CONVECTION IN SHEAR

A two-dimensional, numerical simulation of cumulonimbus convection in shear has been attempted by Takeda (1966). For initial conditions, Takeda assumes the existence of a model cloud stationary at 5 km with respect to flow of undisturbed shear satisfying $\frac{\partial}{\partial z}(\rho u) \sim$ constant. This 'cloud' is of two distinct halves. The upshear half has a high liquid water content, with a maximum of 10 g m^{-3} at the same temperature as the undisturbed fluid. The downshear half has a water content consistent with a cloud droplet distribution (0.4 g m^{-3}), and there is a constant temperature excess of 0.5°C over the undisturbed flow. Since the model equations include the effects of condensation, evaporation and the drag of water drops, this

initialisation is essentially equivalent to defining a heat source on the downshear side and a heat sink on the upshear side, stationary with respect to the undisturbed flow at 5 km. The use of cyclic inflow/outflow boundary conditions in this model means, however, that the simulated convection must not proceed for a time longer than that taken by the fastest internal gravity wave to travel from the source region to the lateral boundaries, otherwise the solution will be affected, especially the development of the steering level. Now if U and C are the speeds of the undisturbed flow and the phase speed of a gravity wave, then

$$U \pm C = \left[\frac{gB}{\lambda^2 + \nu^2 + 1/4H_o^2}\right]^{1/2}$$

and the longest waves given by $\lambda = 2\pi/L$, $\nu = 2\pi/H$, (where H = vertical scale and 2L = horizontal scale) are the fastest. For the model $gB \simeq 10^{-4}$ s^{-2} $H/L \simeq 1/2$, so

$$(U \pm C)_{max} = \frac{H}{2\pi}\left[\frac{gB}{1 + H^2/L^2 + 1/4H_o^2}\right]^{1/2} \simeq 17 \text{ m s}^{-1}$$

Since $U_{max} \simeq 30$ m s^{-1}, this means that the simulated time should not exceed about 9 minutes. Consequently the solutions at 10 minutes and more particularly 15 minutes should be treated with some suspicion. In fact the solution at 10 minutes does reflect interference due to the lateral boundary condition. Moreover the condensation occurring behind the downdraught is more likely to be caused by this effect than Takeda's proposed meteorological explanation.

Takeda's conclusions are rather qualitative. He states that if the shear is too intense for a given amount of available potential energy then the development of the convective system

will be adversely affected, but some degree of shear is necessary to organise the release of potential energy, particularly by establishing strong horizontal convergence in the lowest part of the updraught. Takeda's solutions indicate that the updraught/downdraught boundary is almost perpendicular. However, although the evaporation of rain on the upshear side maintains a downdraught, a considerable part of this downdraught air consists of low-level air from the lowermost kilometre. This is very suspect because in the meteorological problem, this air is thought to form the main part of the updraught. He suggests that a connection between the intensity of the wind shear and the supply of available potential energy is possibly important, but unfortunately does not investigate this aspect.

The first study introducing the concept of a Richardson Number in cumulonimbus convection in shear was that by Green and Pearce (1962). For an assumed steady, inviscid, two-dimensional flow, consistent with the descriptive model of Ludlam and Browning, Pearce calculates the vorticity distribution and by using the vorticity equation the distribution of $\frac{\partial \theta'}{\partial x}$, and on integrating, the distribution of $\theta' - \theta'_0$ (where θ' is the deviation of the potential temperature from the undisturbed value, and θ'_0 is the value at the interface) can be found. By assuming that the flow along a given streamline in the updraught conserves its wet-bulb temperature, it is possible to find the departure of the wet-bulb temperature from its adiabatic value along the other streamlines. Pearce found that the flow was broadly consistent with a wet-adiabatic updraught, together with evaporative cooling of the downdraught air, presumably by rain falling from the assumed backward-sloping updraught. It is interesting that Pearce found that the inflow air in the lower

part of the updraught has to be cooled in order to maintain steady flow. This aspect will be compared to the solutions obtained in chapter V.

Green also restricts the problem to two-dimensional, steady, inviscid flow, finding that the incompressible problem is determined by a non-dimensional number of the form of, but not identically, a Richardson Number. He finds that the steering-level of the incompressible problem is determined as an eigenvalue of an eigenvalue problem (a special case of Eq.(3.6)), and that the remote flow is largely independent of the detailed flow within the storm. Without explicitly examining the detailed flow within the system, Green infers that provided continuity of pressure can adequately model the effect of the updraught/downdraught boundary layer, the interface must be orientated with the updraught lying underneath the downdraught.

Consequently the individual approaches of Green and Pearce give conflicting results regarding the orientation of the interface: Pearce assuming a backward sloping interface and deducing the heat sources and sinks necessary to maintain the flow, Green determining from dynamical considerations that with the pressure continuous, the interface must be orientated in the opposite sense. Resolution of the discrepancy between these two approaches is the subject of chapters IV and V.

Although the analysis of the following chapters is primarily concerned with cumulonimbus convection in shear, the formulation of the problem makes this analysis relevant to other scales of convection in sheared flow, in particular regarding the propagation of mid-latitude squall-lines and precipitation belts associated with cold front regions. For instance, the description of squall-lines by Lempfert and Corless (1910) is remarkably

consistent with Ludlam and Browning's description of severe storms. Moreover, the observed steering levels of precipitation belts given by Harper and Beimers (1958) is consistent with the theoretical values obtained in chapter III. Another possible application of the analysis is in modelling the form and propagation of convective circulations in the sub-cloud layer, giving insight into the dynamical structure of this region, in particular in relation to the heat and momentum transfers.

CHAPTER II — THE GENERAL FORMULATION OF THE STEADY MODELS

2.1 — THE EQUATIONS OF MOTION AND MODELLING APPROXIMATIONS

In their general form, the equations of momentum, mass continuity and energy are difficult to solve analytically. In order to obtain solutions and yet retain the essential physics, it is necessary to simplify the equations rather carefully. The first part of this simplification results in the well-known Boussinesq equations. These are obtained from the full equations of motion by supposing, as is characteristic of tropospheric motion, that at a given point the deviations of p and ρ from the static state $p_o(z)$ and $\rho_o(z)$ are small. Consequently let

$$p(x,y,z,t) = p_o(z) + \delta p$$

$$\rho(x,y,z,t) = \rho_o(z) + \delta\rho$$

$$\phi(x,y,z,t) = \phi_o(z) + \delta\phi$$

where the log-potential temperature ϕ satisfies

$$\phi = \frac{1}{\gamma}\ln p - \ln\rho$$

and p_o and ρ_o are in static equilibrium with

$$\frac{dp_o}{dz} = -\rho_o g \ .$$

With the understanding that $\left|\frac{\delta p}{p_o}\right| << 1$ and $\left|\frac{\delta\rho}{\rho_o}\right| << 1$,

$$\delta\phi = \frac{\delta p}{\gamma p_o} - \frac{\delta\rho}{\rho_o} + O(\delta^2)$$

and with these approximations the momentum equation,

$$\frac{D\underset{\sim}{v}}{Dt} + f\underset{\sim}{k}\wedge\underset{\sim}{v} + \frac{1}{\rho}\nabla p + g\underset{\sim}{k} = 0 \qquad \text{——(1.1)}$$

may be written as

$$\frac{D\underset{\sim}{v}}{Dt} + f\underset{\sim}{k}\wedge\underset{\sim}{v} + \nabla\left(\frac{\delta p}{\rho_o}\right) - \left(g\delta\phi + \frac{d\phi_o}{dz}\cdot\frac{\delta p}{\rho_o}\right)\underset{\sim}{k} = O(\delta^2) \simeq 0 \qquad \text{——(1.2)}$$

To the same order of approximation the continuity equation,

$$\frac{\partial \rho}{\partial t} + \text{div}(\rho \underset{\sim}{v}) = 0 \qquad \text{——(1.3)}$$

may be written as

$$\frac{\partial}{\partial t}(\delta\rho) + \text{div}(\rho_o \underset{\sim}{v}) = 0 \qquad \text{——(1.4)}$$

Similarly the energy equation,

$$\frac{D\phi}{Dt} = Q(x,y,z,t) \qquad \text{——(1.5)}$$

becomes

$$\frac{D}{Dt}(\delta\phi) + w\frac{d\phi_o}{dz} = Q(x,y,z,t) \qquad \text{——(1.6)}$$

In Eq.(1.4), $\frac{\partial}{\partial t}(\delta\rho)$ may be neglected compared to $\text{div}(\rho_o \underset{\sim}{v})$, eliminating the elastic compressibility and hence sound waves from the system. However, when this is done, the frequency equation for the linearised system is found to contain a spurious term unless the term $\frac{d\phi_o}{dz} \cdot \frac{\delta p}{\rho_o}$ is negelcted as well.

Consequently, the complete set of equations is now in the Boussinesq form,

$$\frac{D\underset{\sim}{v}}{Dt} + f\underset{\sim}{k} \wedge \underset{\sim}{v} + \nabla\left(\frac{\delta p}{\rho_o}\right) - g\delta\phi\underset{\sim}{k} = 0 \qquad \text{——(1.7)}$$

$$\text{div}(\rho_o \underset{\sim}{v}) = 0 \qquad \text{——(1.8)}$$

$$\frac{D}{Dt}(\delta\phi) + w\frac{d\phi_o}{dz} = Q \qquad \text{——(1.9)}$$

The Boussinesq approximation, in which the inertial effects of density variation are neglected compared to the buoyancy effects, has been analysed and the frequency given by their solution are in close agreement with the solution of the exact equations. Consequently, at least for tropospheric

motion, the Boussinesq approximation can be used with confidence.

Now if in addition, the flow is restricted to a two-dimensional (independent of the y-coordinate) and steady form, it will be shown that it is possible to integrate the fully nonlinear equations and obtain a general result which can be used to study a model of cumulonimbus convection in shear. It is not surprising that the problem is extremely nonlinear and therefore in conjunction with the analytic approach, numerical methods have to be used to obtain solutions.

2.2 — FORMAL INTEGRATION OF THE BOUSSINESQ EQUATIONS IN STEADY, TWO-DIMENSIONAL, INVISCID FLOW

In this section the fully nonlinear vorticity, continuity and energy equations are integrated in steady, two-dimensional, inviscid flow, a procedure which yields a conservative quantity which is extremely useful in the subsequent analysis.

For the purpose of integration along streamlines, it is convenient to transform the variables from the (x,z) coordinate system to the (ψ,z) system, where ψ is a streamfunction.

2.2.1 — THE TRANSFORMATION (x,z) $\longrightarrow$ (ψ,z)

Because u and w satisfy the continuity equation Eq.(1.8), it is possible to define a streamfunction ψ to satisfy

$$u = \frac{1}{\rho}\frac{\partial \psi}{\partial z} \quad ; \qquad w = -\frac{1}{\rho}\frac{\partial \psi}{\partial x} \qquad \text{———(2.1)}$$

If h(x,z) is an arbitrary differentiable function of x and z, then

$$\left(\frac{\partial h}{\partial x}\right)_z = \left(\frac{\partial h}{\partial \psi}\right)_z \left(\frac{\partial \psi}{\partial x}\right)_z = -\rho w \left(\frac{\partial h}{\partial \psi}\right)_z$$

and

$$\left(\frac{\partial h}{\partial z}\right)_x = \left(\frac{\partial h}{\partial z}\right)_\psi + \left(\frac{\partial h}{\partial \psi}\right)_z \left(\frac{\partial \psi}{\partial z}\right)_x = \left(\frac{\partial h}{\partial z}\right)_\psi + \rho u \left(\frac{\partial h}{\partial \psi}\right)_z$$

The transformation is therefore defined by

$$\left.\begin{aligned}\left(\frac{\partial}{\partial x}\right)_z &= -\rho w\left(\frac{\partial}{\partial \psi}\right)_z \\ \left(\frac{\partial}{\partial z}\right)_x &= \left(\frac{\partial}{\partial z}\right)_\psi + \rho u\left(\frac{\partial}{\partial \psi}\right)_z\end{aligned}\right\} \qquad \text{——(2.2)}$$

The transformation given by Eq.(2.2) has been used in laminar boundary layer theory, but here it will be used in flows in which the baroclinic effect is important, rather than the viscous forces characteristic of boundary layers.

2.2.2 — VERTICAL TRANSPORT OF AN ARBITRARY QUANTITY IN TERMS OF A TOTAL DERIVATIVE

In later analysis it is convenient to write $wh(\psi,z)$ in terms of a total derivative, where h is an arbitrary function of z and ψ. Suppose that for steady flow, some function $g(\psi,z)$ exists such that

$$\begin{aligned} wh(\psi,z) &= \frac{Dg}{Dt} \\ &= u\left(\frac{\partial g}{\partial x}\right)_z + w\left(\frac{\partial g}{\partial z}\right)_x , \\ &= -\rho u w\left(\frac{\partial g}{\partial \psi}\right)_z + w\left[\left(\frac{\partial g}{\partial z}\right)_\psi + \rho u\left(\frac{\partial g}{\partial \psi}\right)_z\right], \quad \text{by Eq.(2.2)} \\ &= w\left(\frac{\partial g}{\partial z}\right)_\psi \end{aligned}$$

So g is defined by the simple partial differential equation,

$$\begin{aligned} \left(\frac{\partial g}{\partial z}\right)_\psi &= h(\psi,z) \\ \therefore \qquad g(z,\psi) &= f_n(\psi) + \int_{s=0}^{s=z} h\left(\psi(x,z),s\right) ds , \end{aligned}$$

where the integrand is understood to be at constant ψ, and $f_n(\psi)$ is an arbitrary function of ψ.

$$\therefore \qquad wh(\psi,z) = \frac{D}{Dt}\int_{s=0}^{s=z} h_p\left(\psi(x,z),s\right) ds , \qquad \text{——(2.3)}$$

where h_p denotes the value of h following a particle of fluid, and the property, $\frac{D}{Dt} f_n(\psi) = 0$ in steady flow has been used.

2.2.3 — THE FORMAL INTEGRATION

Taking the curl of Eq.(1.7), the y-component of the vorticity equation can be shown to be

$$\frac{D\eta}{Dt} + \eta \operatorname{div} \underset{\sim}{v} - (\underset{\sim}{\zeta} \cdot \nabla) v + g \frac{\partial \phi}{\partial x} = 0 \qquad \text{———(2.4)}$$

where $\underset{\sim}{\zeta} = \left(\frac{\partial w}{\partial y} - \frac{\partial v}{\partial z}, \frac{\partial u}{\partial z} - \frac{\partial w}{\partial x}, \frac{\partial v}{\partial x} - \frac{\partial u}{\partial y} + f \right)$. Since the motion is assumed to be two-dimensional in the sense that it is independent of the y-coordinate, Eq.(2.4) simplifies to

$$\frac{D\eta}{Dt} + \eta \operatorname{div} \underset{\sim}{v} - f \frac{\partial v}{\partial z} + g \frac{\partial \phi}{\partial x} = 0 \qquad \text{———(2.5)}$$

Now if $f << \frac{D}{Dt}$, so that the flow is of large Rossby number, a condition which is satisfied by severe storms to an approximation of about 10%, Eq.(2.5) simplifies further to

$$\frac{D\eta}{Dt} + \eta \operatorname{div} \underset{\sim}{v} + g \frac{\partial \phi}{\partial x} = 0 \qquad \text{———(2.6)}$$

which by continuity can be written as

$$\frac{D}{Dt}\left(\frac{\eta}{\rho}\right) + \frac{1}{\rho} \cdot \frac{\partial \phi}{\partial x} = 0 \qquad \text{———(2.7)}$$

Since the flow is steady, ψ constant defines a trajectory so the log-potential temperature can be written in terms of a function F such that

$$\phi(x,z) = f_n(\psi,z) = F(\psi, z-z_o) \qquad \text{———(2.8)}$$

where $z_o(\psi)$ is the height of the inflow streamline remote from the storm. So using Eq.(2.2),

$$\frac{D}{Dt}\left(\frac{\eta}{\rho}\right) - w\left(\frac{\partial F}{\partial \psi}\right)_z = 0 \qquad \text{———(2.9)}$$

and further by Eq.(2.3)

$$\frac{D}{Dt}\left\{\frac{\eta}{\rho} - \int_{z_o}^{z}\left(\frac{\partial F}{\partial \psi}\right)_z dz\right\} = 0 \qquad \text{———(2.10)}$$

Integrating Eq.(2.10),

$$\frac{\eta}{\rho} = G(\psi) + \int_{z_o}^{z}\left(\frac{\partial F}{\partial \psi}\right)_z dz \qquad \text{———(2.11)}$$

where $G(\psi)$ is a function of ψ specified by the inflow conditions. Consequently Eq.(2.10) shows that in steady, inviscid, two-dimensional flow the quantity

$$X = \frac{\eta}{\rho} - \int_{z_o}^{z}\left(\frac{\partial F}{\partial \psi}\right) dz \qquad \text{———(2.12)}$$

is conserved by a particle of fluid.

One of the most useful conserved quantities in three-dimensional, inviscid, adiabatic flow is the potential vorticity $Q = \frac{\zeta}{\rho}\cdot\nabla\phi$, but in two-dimensional motion Q vanishes and is therefore useless. The quantity X can be thought of as the fundamental quantity which replaces potential vorticity in two-dimensional, steady overturning. Of the two terms in X, the first contains the effect of compressibility, which decreases the vorticity of a particle on rarefaction. The second term demands that the vorticity of a particle increases with the tilt of the isentropic surfaces relative to the particle path — a baroclinic effect. These two are in fact opposing effects in steady, buoyant, convective overturning, since on ascent the vorticity is increased by the baroclinicity, and decreased by the compressibility.

Although X is not the potential vorticity Q, it is nevertheless closely related to it in the sense that the

baroclinicity and compressibility can be identified in both. In the subsequent analysis, particularly chapter III, the quantity X will be extremely useful in obtaining fairly general results for steady overturning.

2.3 – THE GENERAL FORM OF THE BOUNDARY CONDITIONS

The differential equation for the streamfunction obtained from Eq.(2.11) is elliptic and therefore along fixed boundaries, it is sufficient to prescribe the streamfunction. However one of the boundaries, the interface between updraught and downdraught, is a free-boundary and characteristic of free-boundary problems in general, in addition to the kinematic condition that the free-boundary is a streamline, an additional (dynamic) boundary condition must be prescribed. This constraint effectively determines the shape of the free-boundary. This dynamic boundary condition will be discussed at length in chapters IV and V, where the boundary layer between updraught and downdraught will be investigated in detail. A comprehensive treatment of free-boundary problems, including some existence and uniqueness theorems can be found in "The Encyclopedia of Physics" Vol.IX - Fluid Dynamics III pp.311-438.

Throughout, rigid boundaries will be assumed at the top $z = H$ and the bottom $z = 0$, and since models for which inflow and outflow are on the same side are discussed, the streamfunction is necessarily constant along $z = 0$, $z = H$ and the free-boundary.

The conditions at the inflow/outflow boundaries are determined as asymptotic solutions of the full two-dimensional problem, this partly being the content of chapter III. Further detail on the determination of this boundary condition will be discussed there.

CHAPTER III — ASYMPTOTIC SOLUTIONS

In this chapter the conservative quantity X derived in the preceding chapter will be used to define an eigenvalue problem for the streamfunction, the asymptotic solution of which defines both the height of the steering-level (appearing as an eigenvalue) and the remote flow field. The speed of propagation of the system can be defined if the steering-level is known, since by definition the steering-level is the height at which the fluid speed equals the travel speed of the system. The propagation speeds obtained in this manner, using real data to define the relevant parameters, will be compared to the observed values. Moreover, it will be shown that the remote flow field and steering-level can be used to calculate heat and momentum fluxes by cumulonimbus convection in a form which could be of use in numerical simulation models of the global atmosphere, a field where it is becoming increasingly obvious that some such dynamical representation of these fluxes is essential.

3.1 — THE EIGENVALUE PROBLEM

Since the y-component of the vorticity is given in terms of the streamfunction as

$$\eta = \frac{\partial}{\partial x}\left(\frac{1}{\rho}\frac{\partial \psi}{\partial x}\right) + \frac{\partial}{\partial z}\left(\frac{1}{\rho}\frac{\partial \psi}{\partial z}\right)$$

using Eq.(2.11), this gives a partial differential equation for the streamfunction as

$$\frac{1}{\rho}\frac{\partial}{\partial x}\left(\frac{1}{\rho}\frac{\partial \psi}{\partial x}\right) + \frac{1}{\rho}\frac{\partial}{\partial z}\left(\frac{1}{\rho}\frac{\partial \psi}{\partial z}\right) = G(\psi) + \int_{z_o}^{z}\left(\frac{\partial F}{\partial \psi}\right) dz \qquad \text{——(3.1)}$$

The functions F and G are in fact determined by conditions remote from the storm. Suppose that the height of the steering-level z_*

is known, and that fluid below z_* has not been through the convective system. If the undisturbed shear is known, the asymptotic streamfunction $\psi(x=\infty,z)$ can be constructed, starting at $z=z_*$. With these values of ψ, $F(\psi,0)$ can be found from the ϕ distribution and also $F(\psi,z-z_o)$ if for instance, wet-adiabatic ascent is assumed for each particle. Since G is simply asymptotically equal to the undisturbed shear, the determination of z_* is the crucial part of the problem. Fig.(3.1) shows $F(\psi,z)$ for a particular occasion.

Following each streamline through the system and out to large distances again, assuming that gravity waves are smoothed out or absent, then the x-variation can again be neglected, and Eq.(3.1) becomes a differential equation for the outflow

$$\frac{1}{\rho}\frac{\partial}{\partial z}\left(\frac{1}{\rho}\frac{\partial\psi}{\partial z}\right) \sim G(\psi) + \int_{z_o}^{z}\left(\frac{\partial F}{\partial \psi}\right)dz \qquad \text{——(3.2)}$$

(where $\sim$ is taken as representing asymptotic equality).

The boundary conditions are that ψ and $\rho u = \frac{\partial\psi}{\partial z}$ should be continuous at $z=z_*$, the first by definition and continuity, and the second from considering the energy of a particle entering just below and leaving just above $z=z_*$. If the fluid flowing in at the bottom $z=0$ is to flow out at the top $z=H$, then ψ must take the same value at these limits, a condition that can only be satisfied in general if z_* is correctly chosen. Consequently, z_* is determined as an eigenvalue of the differential equation (3.2).

3.2 — FINAL INTEGRATION OF THE ASYMPTOTIC VORTICITY EQUATION

In principle Eq.(3.2) could be solved numerically for quite arbitrary functions F and G, but fairly general results can be obtained for simple forms of these functions. Consequently

FIG. 3.1 — ILLUSTRATIONS OF THE PARCEL LOG-POTENTIAL TEMPERATURE $F(\psi, z-z_0)$ IN OBSERVED AND MODEL CONDITIONS FOR $\psi = Az_s^2$.

(a) OBSERVED (WOKINGHAM STORM)

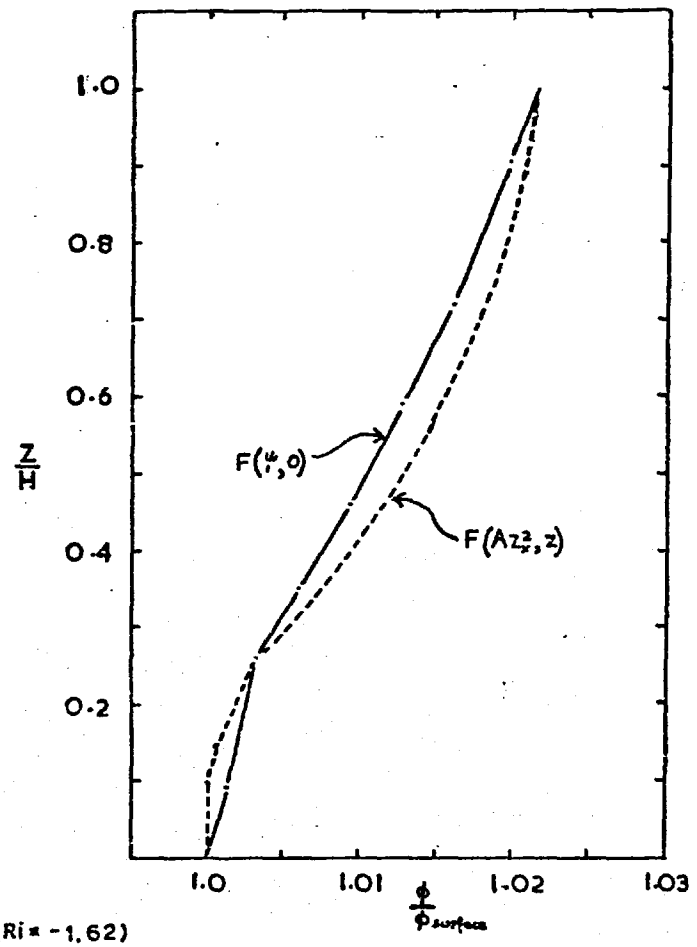

(b) MODEL (Ri = -1.62)

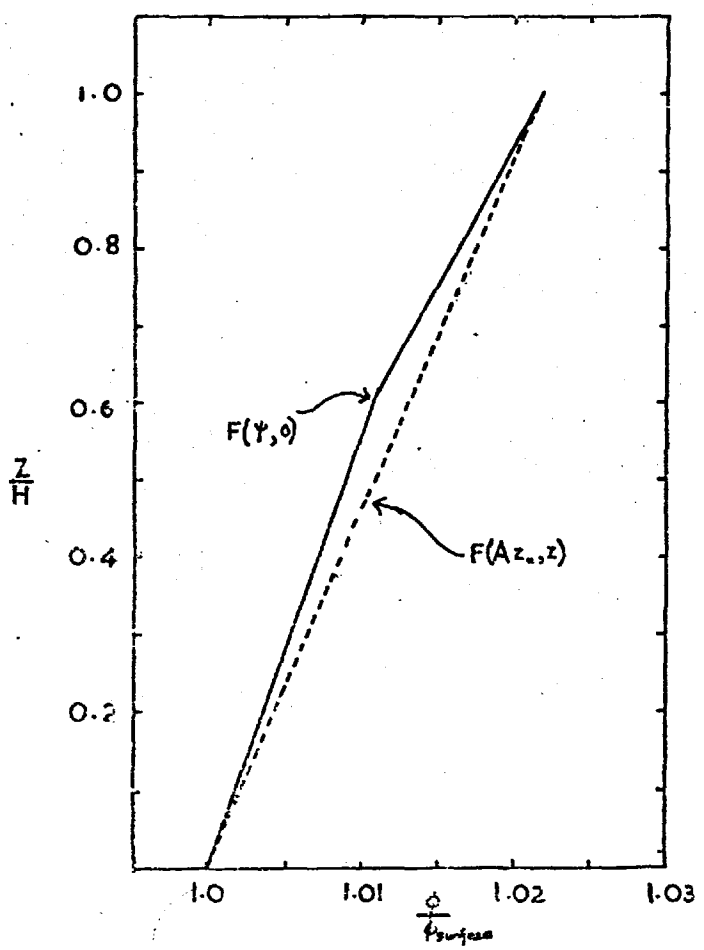

it is assumed that the shear and the static stability of the inflowing undisturbed fluid remote from the system are constant, with $\frac{\partial u}{\partial z_o} \sim 2A$ and $\frac{\partial \phi}{\partial z_o} \sim B$ where A and B are constants. Then

$$\phi \sim Bz_o + \phi(x=\infty, z=0) \quad \text{and} \quad \frac{\partial \psi}{\partial z_o} \sim 2A\rho(z_o - z_*)$$

Thus assuming that $\rho(z) = \rho_S \exp(-z/H_o)$, with ρ_S constant, and using the boundary conditions $\psi \sim \frac{\partial \psi}{\partial z} \sim 0$ at $z_o = z_*$,

$$\psi \sim 2A\rho_S H_o \left\{ (H_o - z_o - z_*) \exp(-z_o/H_o) - H_o \exp(-z_*/H_o) \right\} \qquad \text{———(3.3)}$$

which defines $z_o(\psi)$.

Now suppose that as any parcel is displaced upwards, its gradient of log-potential temperature is positive and constant. This is a crude way of representing a wet-adiabatic process simulating the release of potential energy.

$$\therefore \quad \left(\frac{\partial \phi}{\partial z}\right)_\psi = \gamma$$

$$\therefore \quad \phi(x,z) = F(\psi, z-z_o) = \gamma z + f_n(\psi)$$

and since the inflow log-potential temperature is $\phi = Bz_o + \phi(x=\infty, z=0)$

$$F(\psi, z-z_o) = Bz_o + \gamma(z-z_o) + \text{constant} \qquad \text{———(3.4)}$$

Substituting into Eq.(3.2),

$$\frac{1}{\rho}\frac{\partial}{\partial z}\left(\frac{1}{\rho}\frac{\partial \psi}{\partial z}\right) \sim g(B-\gamma)\int_{z_o}^{z} \frac{\partial z_o}{\partial \psi}\, dz + G(\psi), \qquad \text{———(3.5)}$$

where z is any point on ψ remote from the system. Putting $z = z_o$ defines G as

$$G(\psi) = 2A/\rho(z_o)$$

Consequently,

$$\frac{1}{\rho}\frac{\partial}{\partial z}\left(\frac{1}{\rho}\frac{\partial \psi}{\partial z}\right) \sim \frac{2A}{\rho_o} + \frac{g(\gamma - B)(z - z_o)}{2A\rho(z_o)(z_* - z_o)}, \qquad \text{———(3.6)}$$

where z_o is the function of ψ defined by Eq.(3.3).

Together with the boundary conditions given in section 3.1, Eq.(3.6) defines the eigenvalue problem explicitly.

3.2.1 — INCOMPRESSIBLE SOLUTIONS

Due to its extreme nonlinearity, the eigenvalue problem defined by Eq.(3.6) and its boundary conditions has in general to be solved by numerical methods. If, however the gross variation of density with height is neglected, analytic solutions exist in a simple form. In this case the inflow streamfunction is defined by

$$\psi \sim A(z_o - z_*)^2 \qquad \text{——(3.7)}$$

giving the inflow height $z_o(\psi)$ as

$$z_o \sim z_* - \left(\frac{\psi}{A}\right)^{1/2} \qquad \text{——(3.8)}$$

Substituting for z_o in Eq.(3.6), but keeping ρ constant, shows that this equation is satisfied if on outflow

$$\psi \sim \beta^2 A(z - z_*)^2 \qquad \text{——(3.9)}$$

where

$$\beta(\beta - 1) = \frac{g(\gamma - B)}{4A^2} = R \text{ (say)} \qquad \text{——(3.10)}$$

and this solution satisfies the upper boundary condition if in addition

$$z_* = \beta H/(1 + \beta) \qquad \text{——(3.11)}$$

The parameter R is a measure of the available potential to available kinetic energy of the system (i.e. a measure of the Richardson Number). However, it is important to realise that even when the Richardson Number is defined as the ratio of available potential to available kinetic energy, it is still dependent on the nature of the process which defines availability. If, for instance, the momentum and potential temperature of a slab are thoroughly mixed by interchanging parcels of air

it can be shown that the ratio potential to kinetic energy is given by 2Ri where $Ri = g \frac{\partial \phi}{\partial z} \Big/ \left(\frac{\partial u}{\partial z}\right)^2$, but if the momentum is smoothed out (by pressure forces say) while the temperature is advected then the ratio is given by 4Ri. This distinction is brought out in the discussion of the maintenance versus generation of shearing turbulence.

Taking the scalar product of $\underset{\sim}{v}$ and the momentum equation, it can be shown that

$$\frac{1}{2} \underset{\sim}{v}_2^2 \sim \frac{1}{2} \underset{\sim}{v}_1^2 + \int_{z_o}^{z} g(\phi_p - \phi)\, dz \qquad \text{——(3.12)}$$

where $\underset{\sim}{v}_1$ and $\underset{\sim}{v}_2$ are the inflow and outflow velocities respectively, and ϕ_p and ϕ are the parcel and undisturbed log-potential temperatures. The Richardson Number for steady overturning is defined as the negative of the ratio of the two terms on the R.H.S. of Eq.(3.12). (The choice of sign is to make $Ri < 0$ if the flow is statically unstable, in order to be consistent with convention.) In general, Ri will be a function of z_o, and R and Ri are not simply related. For instance, for the incompressible problem $Ri = -RH/\sqrt{V/A}$, but this is inconvenient and therefore the relationship corresponding to $z_* = 0$ is chosen, i.e. $Ri = -RH/z_*$.

If the flow is neutrally buoyant (isentropic and dry-adiabatic), then $R = 0$, $\beta = 1$ and the steering-level is at the middle of the layer ($z_* = \frac{1}{2}H$), with flow symmetrically approaching and receding below and above this level, with no vorticity generation. This picture suggests that there might be quite a vigorous convective overturning even with no available potential energy (see chapter IV, section 4.3).

If the flow is buoyant, $R > 0$, $\beta > 1$ and the outflow at the top is faster and more sheared than the inflow at the bottom, because of the work done and the vorticity generated by the buoyancy forces (but note the qualification of section 3.2.2), and the steering-level is raised above the middle level. It is

remarkable that the outflow shear is constant in this special case, and convenient both from the point of view of finding as well as describing the form of the solution, because the asymptotic flow can be completely described by z_*/H and the ratio of outflow to inflow shear β^2, as a function of Ri.

3.2.2 — COMPRESSIBLE SOLUTIONS

In this section, the modification that the gross variation of density with height has on the solutions is discussed. Although incompressible models give insight into the dynamics, it is usually necessary to take the variation of density with height into account when making comparisons with the atmosphere.

The only two effects that can change the y-component of the vorticity of a particle in two-dimensional, inviscid overturning (the baroclinic and compressibility effects) are found to be equally important when the height-scale of the convective overturning is comparable with the density scale-height ($H_o = 7.3$ km). In the analysis of severe convective storms, which usually extend at least up to the tropopause, $H/H_o \sim 1$ and it is therefore essential to take the height variation of density into account. This section is therefore concerned with the solutions of the compressible problem. Sometimes the effect of density stratification can be accounted for by a scaling procedure. For instance, linearised perturbation solutions for an incompressible model of gravity waves give realistic predictions provided that the dependent variables are first multiplied by $\rho^{1/2}$. In this section the fully nonlinear, compressible problem is solved, and it is interesting to observe that in the resulting finite amplitude overturning, this $\rho^{1/2}$ transformation between the compressible and incompressible solutions is not appropriate. A transformation that is valid for this finite amplitude motion will be presented later.

3.2.2.1 — DENSITY VARIATION FOR NEUTRAL STRATIFICATION

The effect of density variation can be demonstrated simply when the stratification is neutral ($B = \gamma$). In this situation, the kinetic energy of the updraught is derived from the kinetic energy of the inflow fluid, the baroclinic effect vanishes and Eq.(2.11) shows that η/ρ is conserved along streamlines, and the outflow shear is therefore reduced by a factor of $\frac{\rho(z_o)}{\rho(z)}$. Consequently, the general effect of density stratification is to decrease the outflow shear, in the opposite sense due to the action of buoyancy, while at the same time the steering-level must be lowered in order to satisfy mass continuity. The implicit relationship between the variables z_o, z and ψ makes analytic completion of the solution difficult, so this is approached numerically.

3.2.2.2 — A LOCAL ANALYTIC SOLUTION IN THE NEIGHBOURHOOD OF $z = z_*$

From the numerical point of view, the nonlinearity of the eigenvalue problem defined by Eq.(3.6) and its boundary conditions is not in itself a great complication since there is no difficulty in finding accurate, convergent, iterative numerical schemes for solving elliptic equations. However, being second order in ψ, Eq.(3.6) requires starting values defined at $z = z_*$ and $z = z_* + h$, where h is the mesh length. $\psi(x=\infty, z=z_*)$ can be obtained direct from the boundary condition on ψ, but it is not easy to get $\psi(x=\infty, z=z_*+h)$ accurate to better than first order, (which is easily obtained using the boundary conditions, continuity of ψ and $\frac{\partial \psi}{\partial z}$ at z_* and a first order Taylor expansion around z_*) because $z = z_*$ is a singular point of the differential equation and so it is not possible to get a second order correction by direct use of the equation. Since

it is important to get the starting values as accurate as possible in numerical work, a local analytic solution was found for ψ in the neighbourhood of $z = z_*$. The solution is given to the approximation that the flow is incompressible in the neighbourhood of z_* —that is $h/H_o << 1$ where h is the mesh length, and this is a justifiable approximation since h was chosen so that $h/H_o = O(0.01)$. It may be argued that h could have been made small enough to make the first order starting condition acceptable, but in that case the accuracy of the starting values is purely numerical in nature, whereas in the procedure adopted here the dynamical nature of the approximation is explicit. (incompressibility in the neighbourhood of $z = z_*$)

Now from Eq.(3.6), the differential equation for the streamfunction is

$$\frac{1}{\rho}\frac{\partial}{\partial z}\left(\frac{1}{\rho}\frac{\partial \psi}{\partial z}\right) \sim \frac{1}{\rho(z_o)}\left\{1 + R\,\frac{(z - z_o)}{(z_* - z_o)}\right\} \qquad \text{———(3.13)}$$

and taking $\rho(z) = \rho_s \exp(-z/H_o)$, where ρ_s is constant,

$$\frac{\partial^2 \psi}{\partial z^2} + \frac{H}{H_o}\frac{\partial \psi}{\partial z} \sim \left\{1 + R\,\frac{(z - z_o)}{(z_* - z_o)}\right\}\exp\left(\frac{z_o - 2z}{H_o}\right) \qquad \text{———(3.14)}$$

In the range $z_* \leqslant z \leqslant z_* + h$, where h is the mesh length

$$\frac{z - z_o}{z_* - z_o} \simeq \frac{h + k}{k} = \frac{1 + r}{r} \qquad \text{———(3.15)}$$

where $r = k/h$ and $z_* - k$ is the inflow height of the streamline $\psi(x = \infty, z = z_* + h)$. Note that if the flow is incompressible over the whole range $0 \leqslant z \leqslant H$, then $r = \beta$ where β is defined by Eq.(3.11). Consequently in the range $z_* \leqslant z \leqslant z_* + h$, the approximate equation, (exact for the incompressible problem) defines the local streamfunction:

$$\frac{\partial^2 \psi}{\partial z^2} + \frac{H}{H_o}\frac{\partial \psi}{\partial z} \simeq \left\{1 + R\,\frac{(1 + r)}{r}\right\}\exp\left(\frac{z_o - 2z}{H_o}\right)$$

$$\simeq \left\{1 + R\,\frac{(1 + r)}{r}\right\}\exp\left(\frac{-h(1 + r) - z}{H_o}\right) \qquad \text{———(3.16)}$$

Since $h \ll H_o$, a condition that can always be satisfied by appropriate choice of mesh length, the local streamfunction is given by the following standard second order linear differential equation.

$$\frac{\partial^2 \psi}{\partial z^2} + \frac{H}{H_o}\frac{\partial \psi}{\partial z} \simeq C \exp(-z/H_o) \qquad \text{———(3.17)}$$

where $C = C(R, z_*) = 1 + R\frac{(1+r)}{r}$. With starting conditions, continuity of ψ and $\partial\psi/\partial z$ at $z = z_*$, this solution is

$$\left.\begin{aligned} \psi &\sim a + (b - CzH_o)\exp(-z/H_o) \\ \text{where} \quad a &= \psi(x=\infty, z=z_*) + CH_o^2 \exp(-z_*/H_o) \\ b &= CH_o(z_* - H_o) \end{aligned}\right\} \qquad \text{———(3.18)}$$

Consequently, provided that $r(R, z_*)$ can be defined as a function of R and z_*, the local solution is explicitly defined.

Determination of $r(R, z_*)$

The value of r for a given R and z_* is determined through the use of the energy relationship given by Eq.(3.12). In the context of this section

$$\phi_p - \phi = \begin{cases} (\gamma - B)(z - z_o) & 0 \leqslant z \leqslant z_* \\ (\gamma - B)\left\{z_o + \frac{z_*}{H - z_*}(z - z_*)\right\} & z_* \leqslant z \leqslant H \end{cases}$$

———(3.19)

After some manipulation it can be shown that

$$\frac{\underset{\sim}{v}_2^2}{\underset{\sim}{v}_1^2} = 1 + R\left(1 + \frac{z_* r^2}{H - z_*} - 2r\right) \qquad \text{———(3.20)}$$

Since continuity of mass, together with the assumption of incompressibility in $z_* - k \leqslant z \leqslant z_* + h$ requires that

$$\overline{|\underset{\sim}{v}|}^{[z_*-k, z_*]}_{k} = \overline{|\underset{\sim}{v}|}^{[z_*, z_*+h]}_{h} \ , \qquad \text{———(3.21)}$$

it follows that r is given by the appropriate root of the quartic equation.

$$q^4 - (1+R)q^2 - 2Rq + R\frac{z_*}{H - z_*} = 0 \qquad \text{———(3.22)}$$

For the range of R and z_* of interest, Eq.(3.22) has two real roots, one less than unity and the other greater than unity. The former is physically acceptable if $R < 0$, and the latter if $R > 0$. If $R = 0$ then it is physically obvious that the roots are equal.

Note that in particular if $r = \frac{z_*}{H - z_*}$, Eq.(3.22) reduces to

$$q^3 - (1+R)q - R = 0$$

i.e. $q^2 = 1 + R(1 + 1/q)$, the solution of which is $r = \beta$, where β is as defined by Eq.(3.11) in the solution of the incompressible problem.

3.2.2.3 — η/ρ CONSTANT ON INFLOW

If the inflow vorticity satisfies $\eta/\rho = 2A$, with A constant, and if in particular the fluid is neutrally stratified, ($\gamma = B$) Eq.(3.6) reduces to the linear form

$$\frac{1}{\rho}\frac{\partial}{\partial z}\left(\frac{1}{\rho}\frac{\partial \psi}{\partial z}\right) \sim 2A \qquad \text{———(3.23)}$$

With the density profile given by $\rho(z) = \rho_s \exp(-z/H_o)$ the solution of Eq.(3.23) subject to the usual boundary conditions is

$$\left.\begin{aligned} \psi &\sim AH_o^2\left\{\exp(-z/H_o) - \exp(-z_*/H_o)\right\}^2 \\ 2\exp(-z_*/H_o) &= 1 + \exp(-H/H_o) \end{aligned}\right\} \qquad \text{———(3.24)}$$

Therefore in this particular case, the steering-level is located at the height where the density is the arithmetic mean of the extreme outflow and inflow densities. Moreover, the compressible solution can also be expressed as a modification of the incompressible

solution. Letting δz_* and δu denote the difference between the compressible and incompressible solutions:

$$\left.\begin{aligned} \delta z_* &= -H_o \ln(\cosh H/2H_o) \\ \delta u(z) &= 2AH_o\left\{\exp\left(\frac{z_* - z}{H_o}\right) + \frac{(z - z_*)}{H_o} - 1\right\} \end{aligned}\right\} \qquad (3.25)$$

This is the only case where an analytic solution to the compressible problem has been found.

3.2.2.4 — INFLOW VORTICITY CONSTANT

The full eigenvalue problem represented by Eq.(3.6) and the boundary conditions was solved numerically for a representative range of values of the parameters H/H_o and $R = g(\gamma - B)/4A^2$. The results of the computations are displayed in Figs.(3.2, 3.3, 3.4).

Remarkably, the effect of density variation is in the opposite sense to that in many deep systems. It is well established both theoretically and by observation, that the specific kinetic energy $\rho \underset{\sim}{v}^2$ is practically independent of height, in particular for sound waves propagating upwards, for gravity waves extending to great heights as in tidal oscillations and for the large-scale motion - particularly that of very great wavelength that extend up to very high levels. Thus in these systems, the decreasing density allows larger velocities at upper levels, whereas here the velocities relative to the incompressible system decrease upwards. The main distinction between these two classes of system is that in the first the vertical displacement of fluid particles is not comparable with the density scale height (whereas the penetration of energy is), but in the system at present under discussion, the fluid particles themselves undergo vertical displacement comparable to the density scale height.

FIG. 3.2.1 — THE STEERING-LEVEL AS A FUNCTION OF THE NONDIMENSIONAL NUMBER R IN ISOPLETHS OF H/H_0.

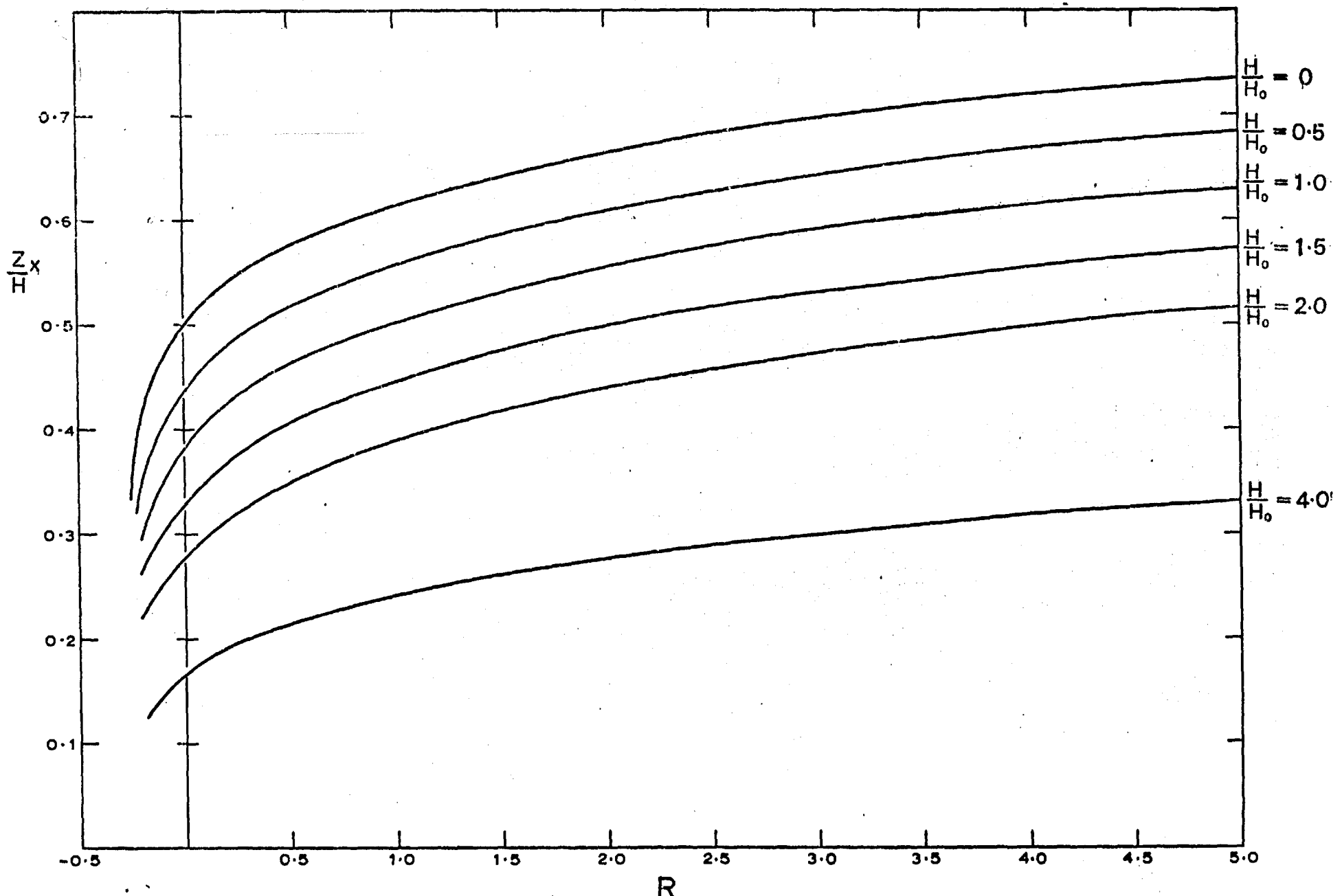

FIG. 3.2.2 — THE STEERING-LEVEL AS A FUNCTION OF RICHARDSON NUMBER IN ISOPLETHS OF H/H_0.

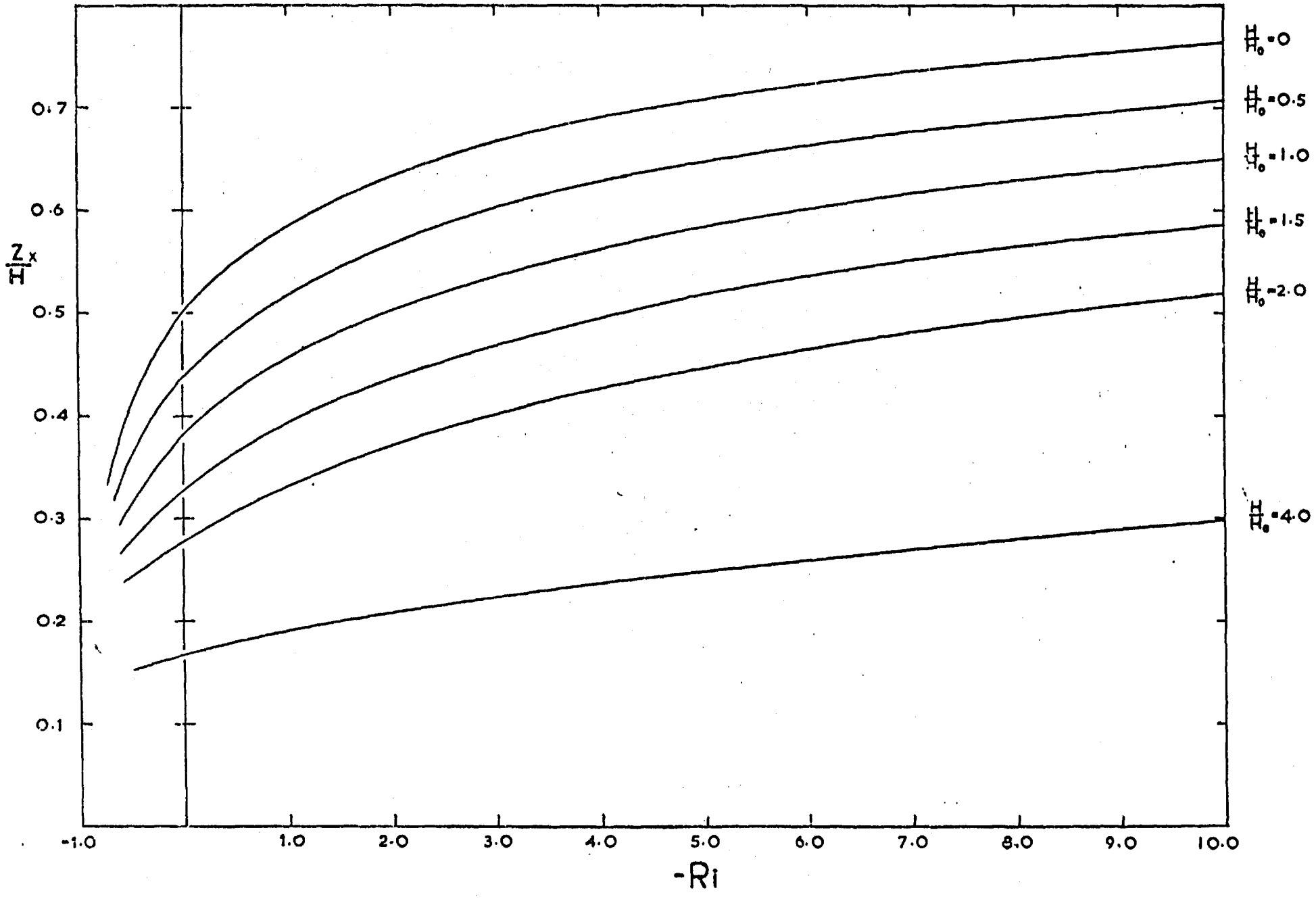

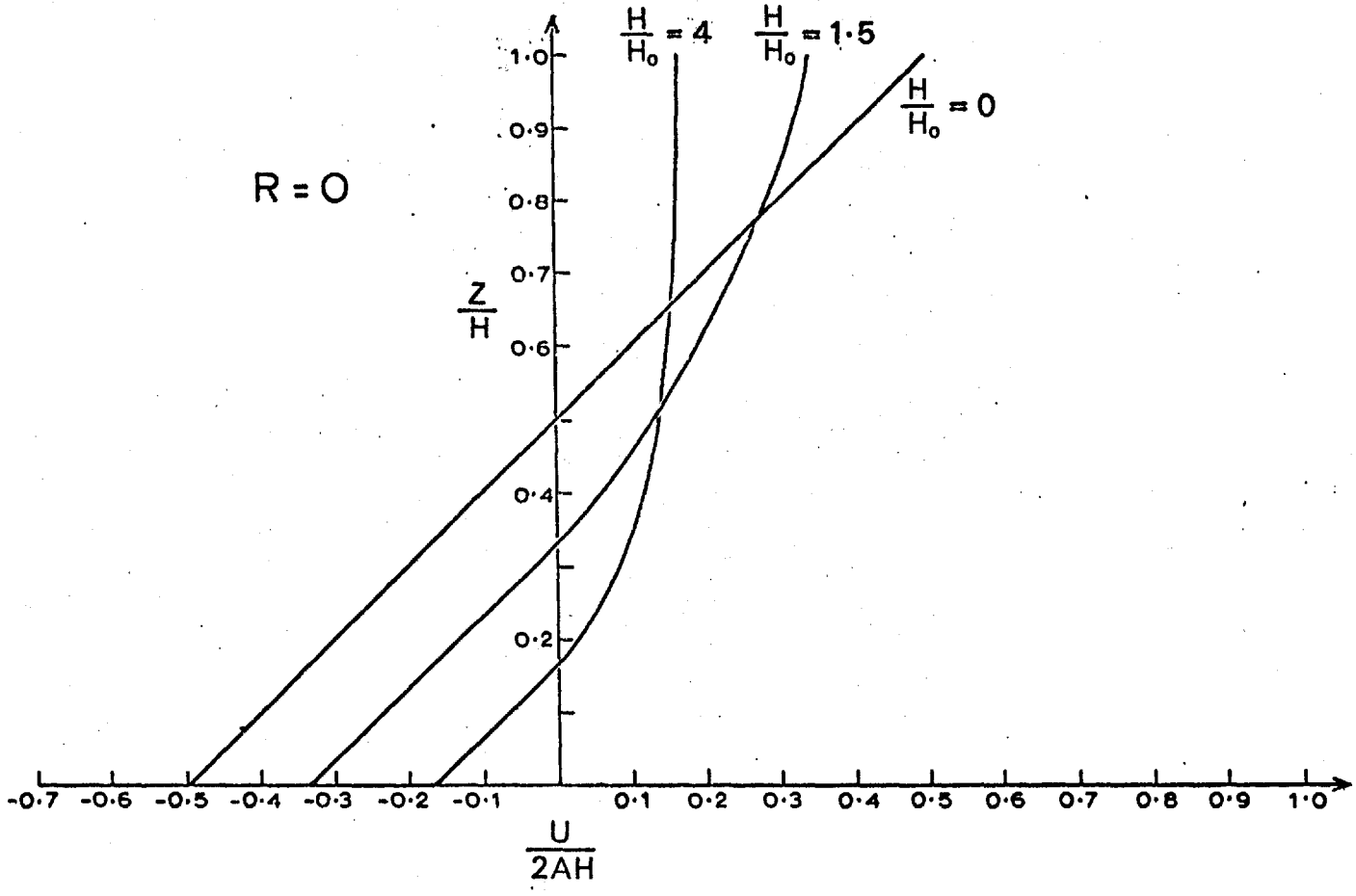

FIG. 3.3 — PROFILES OF INFLOW & OUTFLOW SPEED FOR DISCRETE VALUES OF H/H_0 AND $Ri = 0$

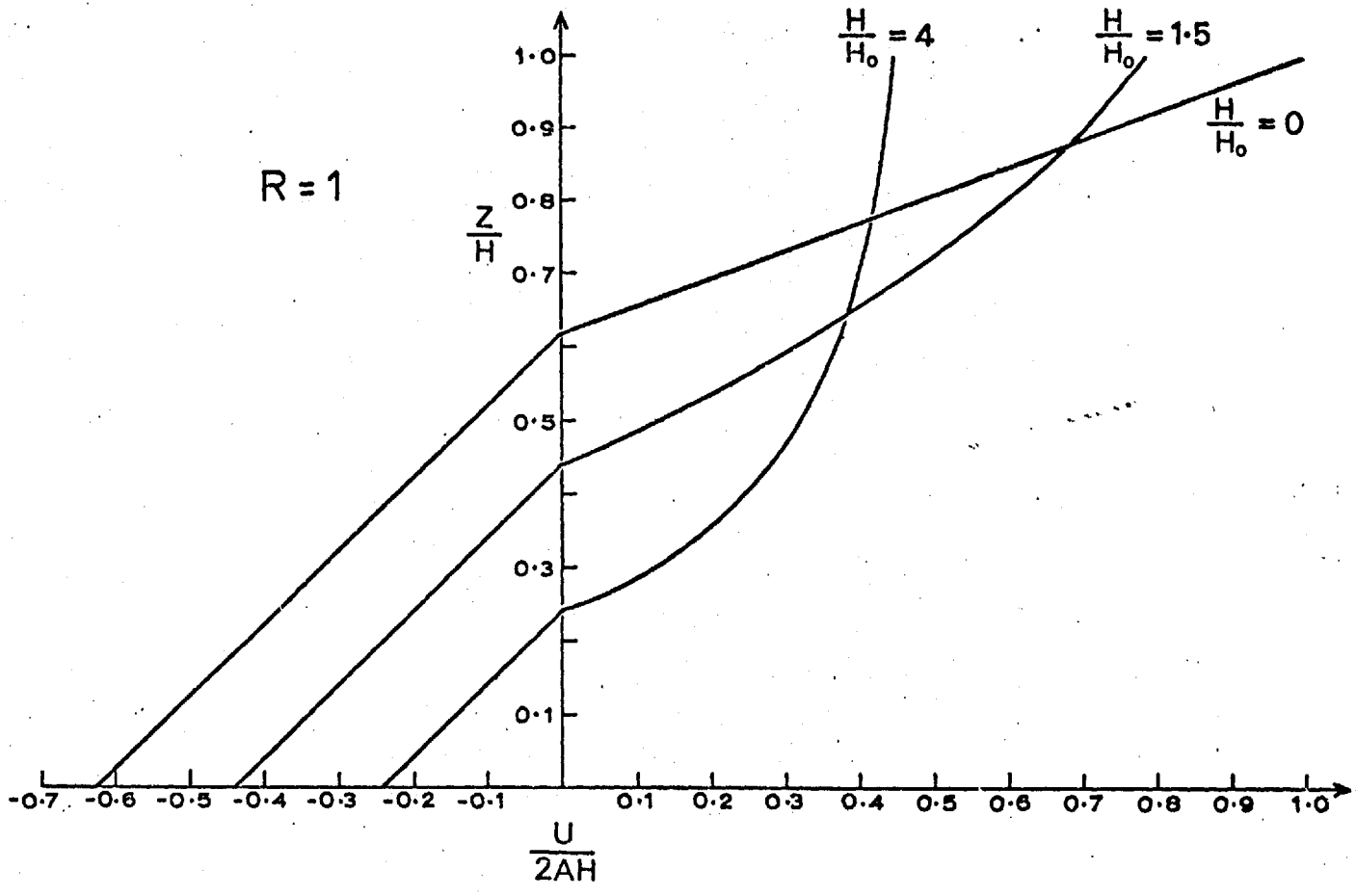

FIG. 3.4 — PROFILES OF INFLOW & OUTFLOW SPEED FOR DISCRETE VALUES OF H/H_o AND $Ri = -1.62$ $(R = 1)$.

These solutions are accurate to about 0.1%, but at the expense of trivial accuracy, empirical formulae for the compressible solutions in terms of the incompressible solutions have been obtained. Examining the solutions in Fig.(3.2) in the range $0 \leqslant H/H_o \leqslant 2$ and for $0 \leqslant R \leqslant 5$, the depression of the steering-level by the density stratification is to good approximation a linear function of H/H_o and independent of R. Moreover there is a close relationship with Eq.(3.25), where $\delta z_* = -H^2/8H_o + O(H^4/8H_o^3)$. However, the inflow vorticity is different in this case, and in fact the following empirical formula for the depression of the steering-level is more accurate

$$\delta z_* \simeq -0.11\, H^2/H_o$$

The corresponding outflow speeds are of the form of a linear function of height, divided by a power of the density. After some manipulation it is found that:

$$\delta u(z) \simeq \begin{cases} -2A\delta z_* & 0 \leqslant z \leqslant z_* \\ 2A[(z - z_*)(\beta^2 \exp(-z/2H_o) - 1) - \delta z_*] & z_* \leqslant z \leqslant z_* + |\delta z_*| \\ 2A\beta^2[(z - z_*)\left(\exp(-z/2H_o) - 1\right) - \delta z_*] & z_* + |\delta z_*| \leqslant z \leqslant H \end{cases} \qquad \text{———(3.26),}$$

where β^2 is the ratio of the outflow to inflow shear given in the incompressible solutions by Eq.(3.10). The accuracy of the above empirical formulae is about 1% - 5% for δz_* and about 5% - 10% for δu, for a range of $0 \leqslant R \leqslant 5$ and $0 \leqslant H/H_o \leqslant 2$. These empirical formulae are therefore of acceptable accuracy for application in severe storm conditions.

3.3 — A MODEL FOR SYSTEMS WHERE $H >> H_o$

Here the extreme effect of density variation on the system

is examined, contrasting with the incompressible solutions dealt with in section 3.2.1 which demonstrated the extreme effect of baroclinicity on the motion. It can be seen from Eq.(3.6) that the outflow shear is of the form of $\exp\left\{-\frac{(z-z_o)}{H_o}\right\}$ multiplied by a bounded function of z and ψ. Therefore for $z \sim H$ and $H >> H_o$, $\frac{\partial u}{\partial z} \sim 0$ —that is there is block outflow in upper levels. This suggests the model shown in Fig.(3.5), for the extreme case where $H >> H_o$.

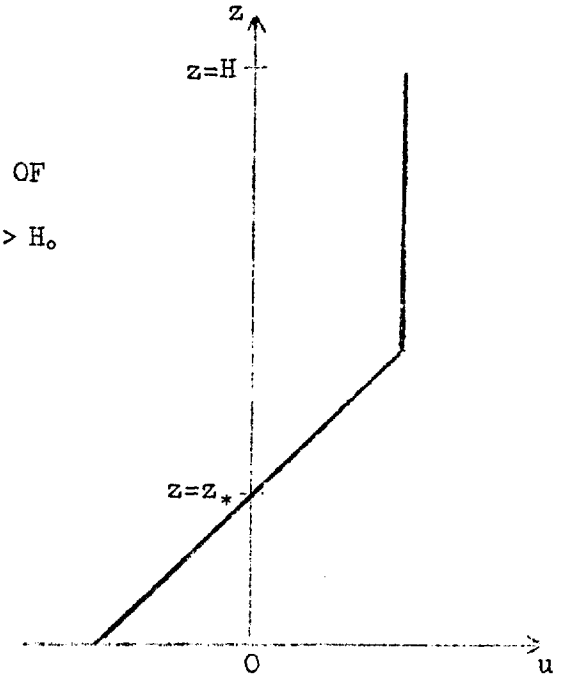

FIG. 3.5 — SCHEMATIC DIAGRAM OF REMOTE FLOW FOR $H >> H_o$

If for this model $u(x=\infty, z=H)$ can be determined, then the steering-level $z=z_*$ may be directly obtained by integrating the mass-continuity equation. The solutions of section 3.2.2.4 suggest that $u(x=\infty, z=H) \simeq u_o(x=\infty, z=0) = 2Az_*$ is a reasonable approximation (i.e. the effect of density on the extreme outflow speed almost exactly counteracts the gain in outflow speed due to the work done by buoyancy forces on ascent).

The steering-level is therefore given by the solution of the following simple integral equation for z_*.

$$\int_{2z_*}^{H} z_* \exp(-z/H_o)dz = -\int_{0}^{2z_*} (z - z_*) \exp(-z/H_o)dz \qquad \text{———(3.27)}$$

That is, the solution of the following transcendental equation in z_*;

$$\exp(-2z_*/H_o) + z_*/H_o\left(1 - \exp(-H/H_o)\right) - 1 = 0 \qquad \text{———(3.28)}$$

Comparison of the solution of this equation for $H = 4H_o$ with the numerical solution of the exact equation, Eq.(3.6), shows that the steering-level is given to an accuracy of about 5% by the above simple model for extreme compressibility.

3.4 — APPLICATION OF COMPRESSIBLE SOLUTIONS: CASE STUDIES OF CONVECTIVE SYSTEMS

In comparing with a real, observed system it is more convenient to determine the Richardson Number (Ri) using an appropriate ascent curve on a tephigram and the wind profiles, rather than try to directly estimate an equivalent value for R. The theory has been used to estimate the height of the steering-levels and consequently the propagation speeds of severe convective storms, squall-lines and the precipitation belts associated with cold fronts by using real data to calculate Ri and H/H_o and subsequently using the solutions given by Fig.(3.2) to find the corresponding value of z_*.

3.4.1 — THE WOKINGHAM STORM

This storm, which occurred on the 9th July 1959 over S.E. England, was the subject of intensive analysis including detailed radar studies by Ludlam and Browning. The details of this study are given by Browning (1962), and in a more condensed form by Browning and Ludlam (1962). The thermodynamic state and the velocity profile of the undisturbed flow are shown in Fig.(3.6) and from these data, $Ri = -2.3$ and $H/H_o = 1.5$. (For real storms H is defined as being the height of the intersection

of the undisturbed temperature profile with the wet-adiabatic corresponding to the mean θ_w of the surface boundary layer of depth one kilometre.) Note that for this occasion the low-level inflow air cannot become positively buoyant until it has ascended to a considerable height ($\simeq$ 3 km), and consequently in the updraught below this level, the kinetic energy of the inflow air is converted into potential energy - in fact some 75% of the inflow kinetic energy is disposed of in this way. This negative area must of course be included in the calculation of the Richardson Number. Moreover, detailed theoretical study of flow within convective storms (chapter V) suggests that this region is of considerable importance in determining the orientation of the updraught/downdraught boundary layer and hence to maintenace of the steady overturning. The predicted height of the steering-level, 4.85 km, and the predicted propagation speed 17.5 m s^{-1} compare favourably with the observed values of 5 km and 18 m s^{-1}.

3.4.2 — THE HORSHAM STORM

The detailed synoptic analysis of this storm, which occurred over S.E. England on 5th September 1958, and was most intense in the vicinity of Horsham in Sussex, is given by Carlson (1965). The data shown in Fig.(3.7) defines a Richardson Number of -14.5 and a density-scaling parameter $H/H_o = 1.6$. The largeness of the Richardson Number is due to a combination of a very large positive area and relatively small shear on this occasion. Despite this rather untypically large Richardson Number, the theory gives the height of the steering-level as 6.8 km and a propagation speed of 12 m s^{-1} precisely the observed values.

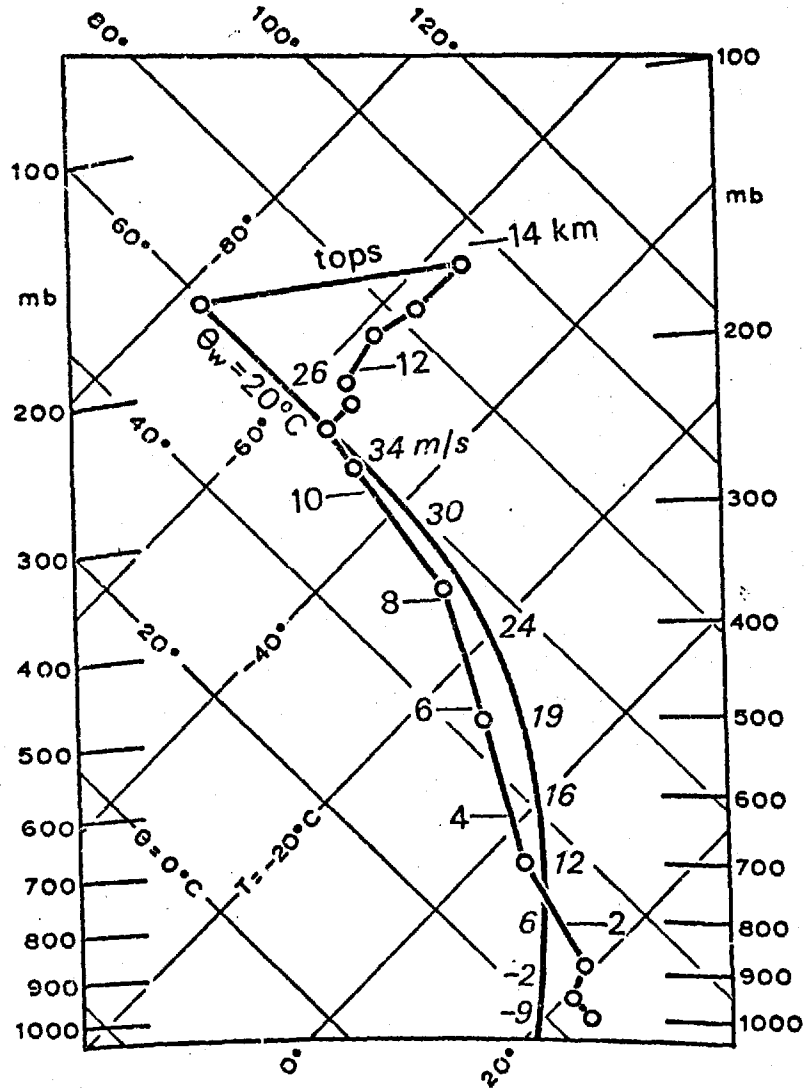

FIG. 3.6 — THE WOKINGHAM STORM

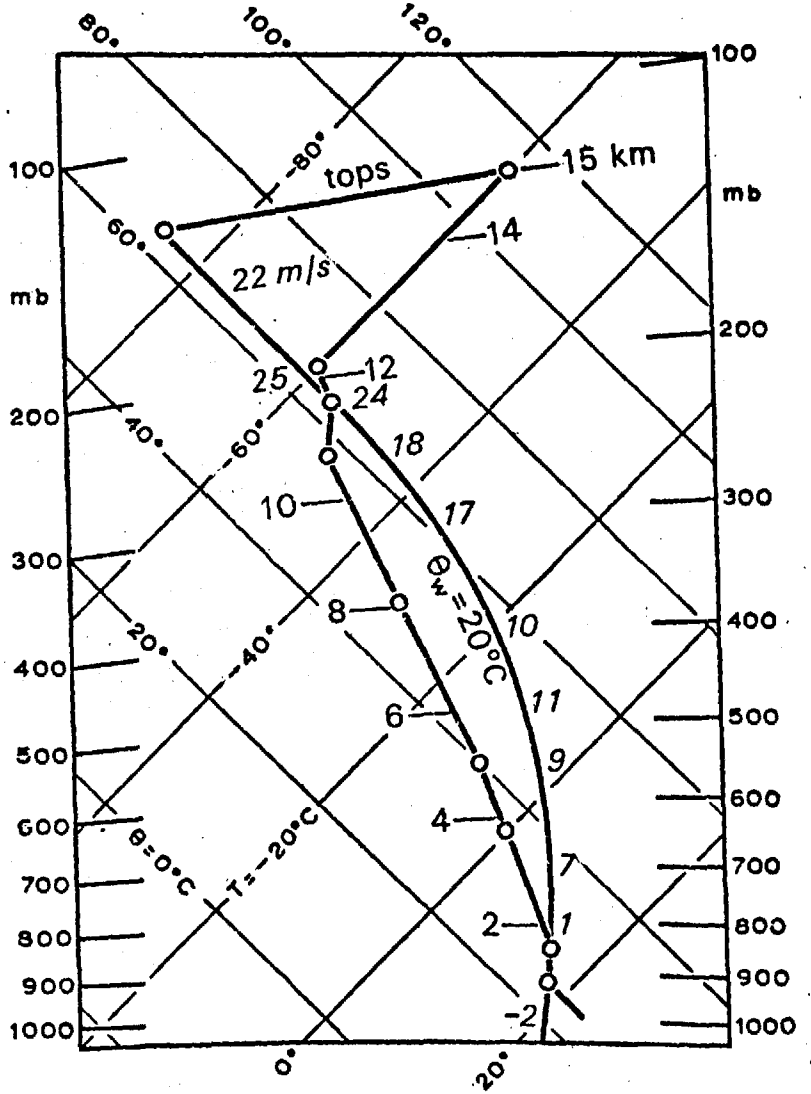

FIG. 3.7 — THE HORSHAM STORM

On these and the following four figures, the velocity component in the direction of propagation is written alongside the θ_w = constant line (the mean θ_w of the lowest kilometre). The height in kilometres is shown alongside the temperature sounding. When available, the maximum cloud top height is shown.

3.4.3 — A SQUALL LINE

This case concerns a squall-line, occurring in the form of a Nor'wester (a convective system associated with Indian pre-monsoonal conditions). The relevant atmospheric conditions are shown in Fig.(3.8) and these give a Richardson Number of -3.2 and $H/H_o = 1.25$. This particular squall-line was tracked on a P.P.I. radar and it can be seen from Fig.(3.9) that during most of its duration was over 200 km in transverse dimension and only about 20 km in cross-sectional width - a markedly two-dimensional system. The speed of propagation measured from the P.P.I. record was 14.5 m s^{-1} to which the 14 m s^{-1} predicted by the theory compares very favourably.

3.4.4 — A PRE-MONSOONAL SEVERE STORM

A severe storm typical of the premonsoonal period in N.E. India was analysed. Fig.(3.10) shows the thermodynamic state of the atmosphere and the velocity profile relevant to this particular situation. From these data the Richardson Number was found to be $Ri = -3.8$ and the density scaling parameter $H/H_o = 1.5$. With these values the propagation speed was predicted to be 13 m s^{-1}, and the steering-level 4.2 km, compared to the observed values of 10 m s^{-1} and about 3.5 km.

3.4.5 — A SEVERE UNITED STATES STORM

This is a case study of a storm occurring in the mid-western states of America. More information relevant to this particular storm can be found in a report by Browning and Fujita (1965). The tephigram and wind profile relevant to this occasion are given in Fig.(3.11). The Richardson Number was calculated to be $Ri = -5.6$ and the density scaling parameter $H/H_o = 1.7$,

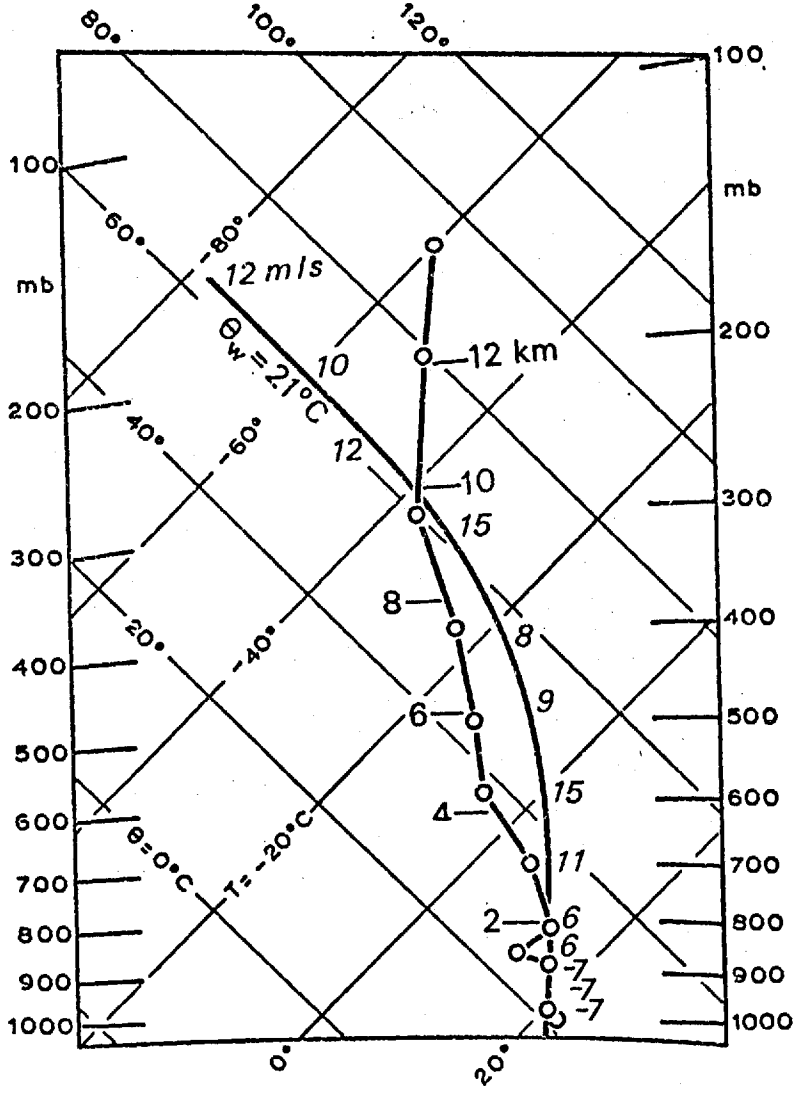

FIG. 3.8 — A SQUALL LINE

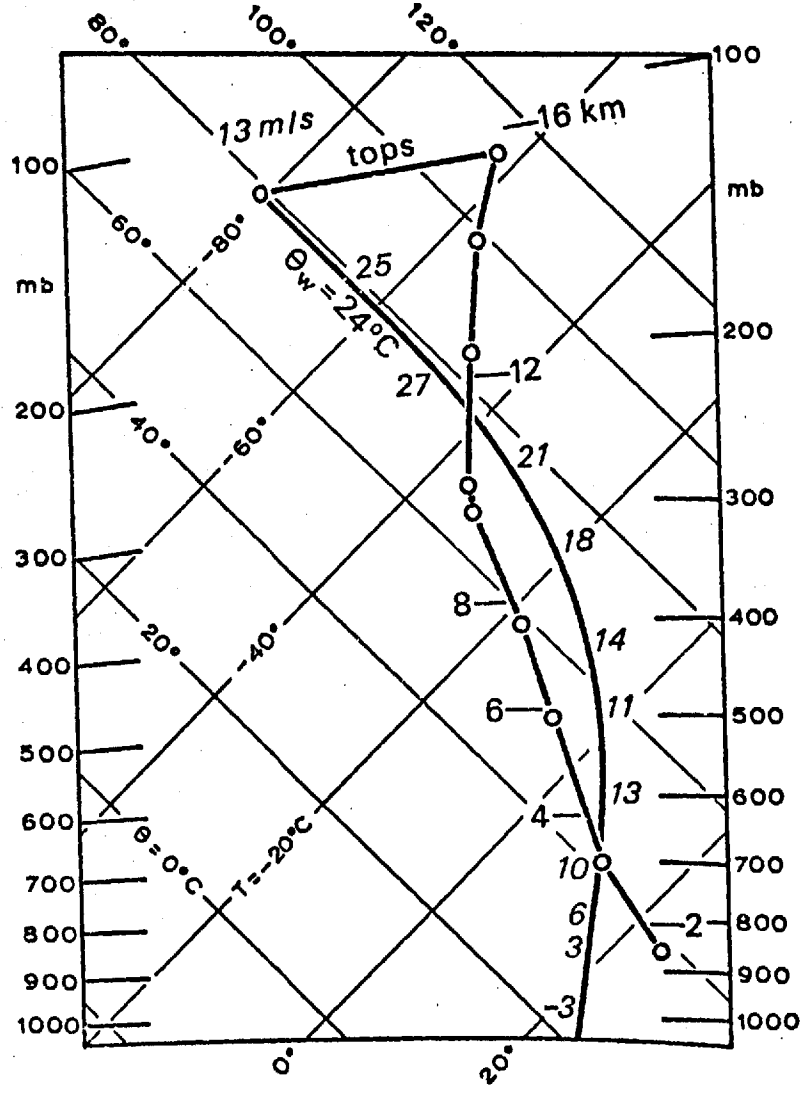

FIG. 3.10 — A PRE-MONSOONAL SEVERE STORM

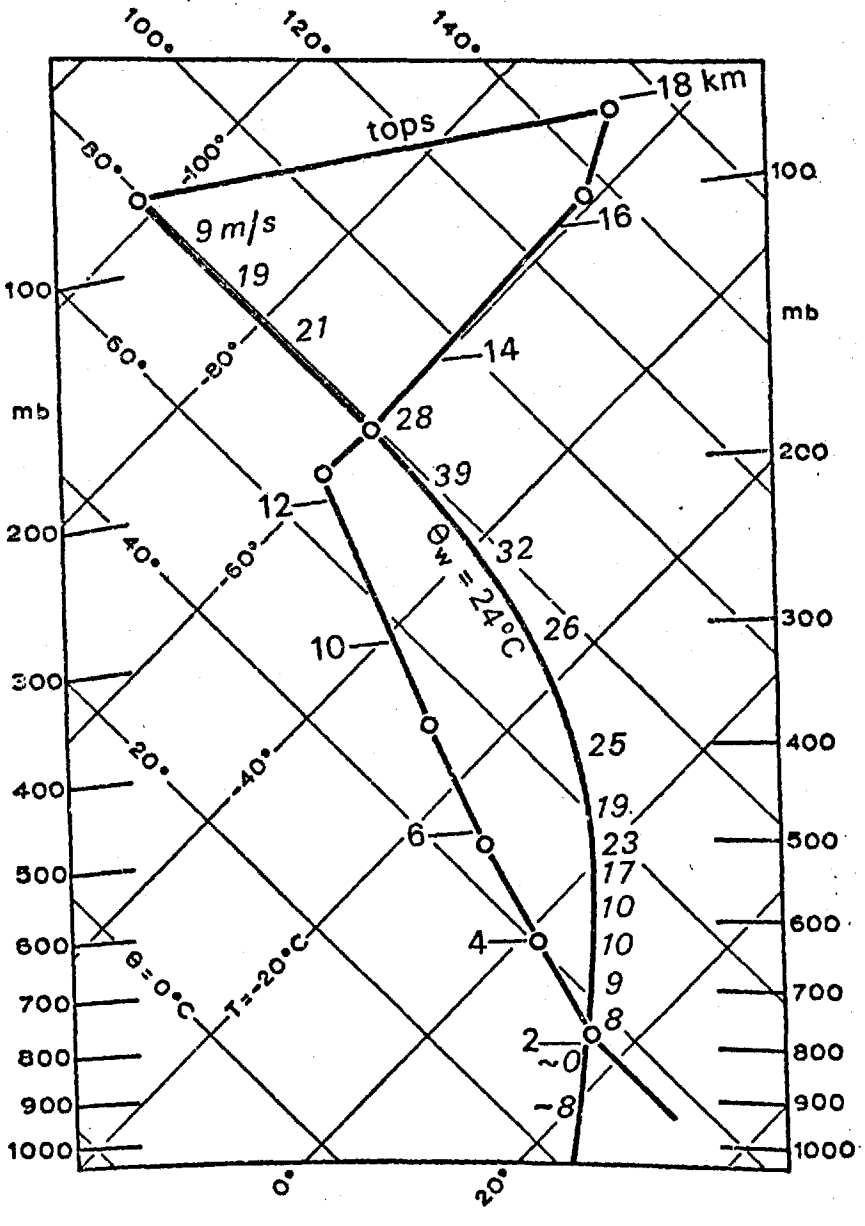

FIG. 3.11 — A SEVERE UNITED STATES STORM

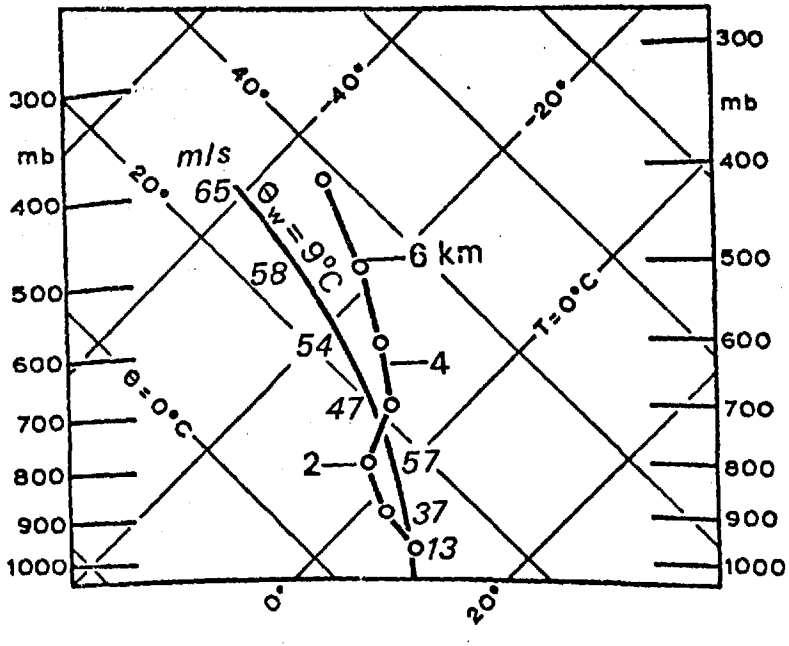

FIG. 3.12 — A COLD FRONT

predicting the propagation speed to be 21 m s^{-1} and the steering-level 5.5 km. It is interesting that this is an example of a case which gives a very poor prediction of the storm motion, since the observed propagation speed was 10 m s^{-1} and the observed steering-level 4.3 km. However, this particular storm was what Browning and Fujita term a "severe right-moving storm", in that it moved at a greater angle to the right of the mean wind than is considered typical of severe storms. Since the error in the observed propagation speed is unlikely to be more than a few metres a second, it is possible that the theory of this chapter is inapplicable to storms of this type, and that there is some additional mechanism (perhaps of three-dimensional nature) responsible. It is not possible to resolve the question at present, but it is hoped to study the effect of three-dimensionality in the future, and perhaps this will provide some insight into the reason for the anomalous prediction given by the present theory.

3.4.6 — A COLD FRONT

A cold front which crossed England on 1st December 1966 has been analysed in considerable detail by Harwood (1969), who from analysis of autographic records, found that the general pattern of the wind field was fairly uniform along the length of the frontal system - in fact a crudely two-dimensional situation. Moreover, Harwood evaluated the normal velocity relative to the frontal axis, and the resulting relative flow pattern is of a form similar to the cumulonimbus circulation of Fig.(1.1).

Consequently the theory previously developed was used to predict the steering-level and hence the propagation speed of the frontal system. Fig.(3.12) gives the relevant state of

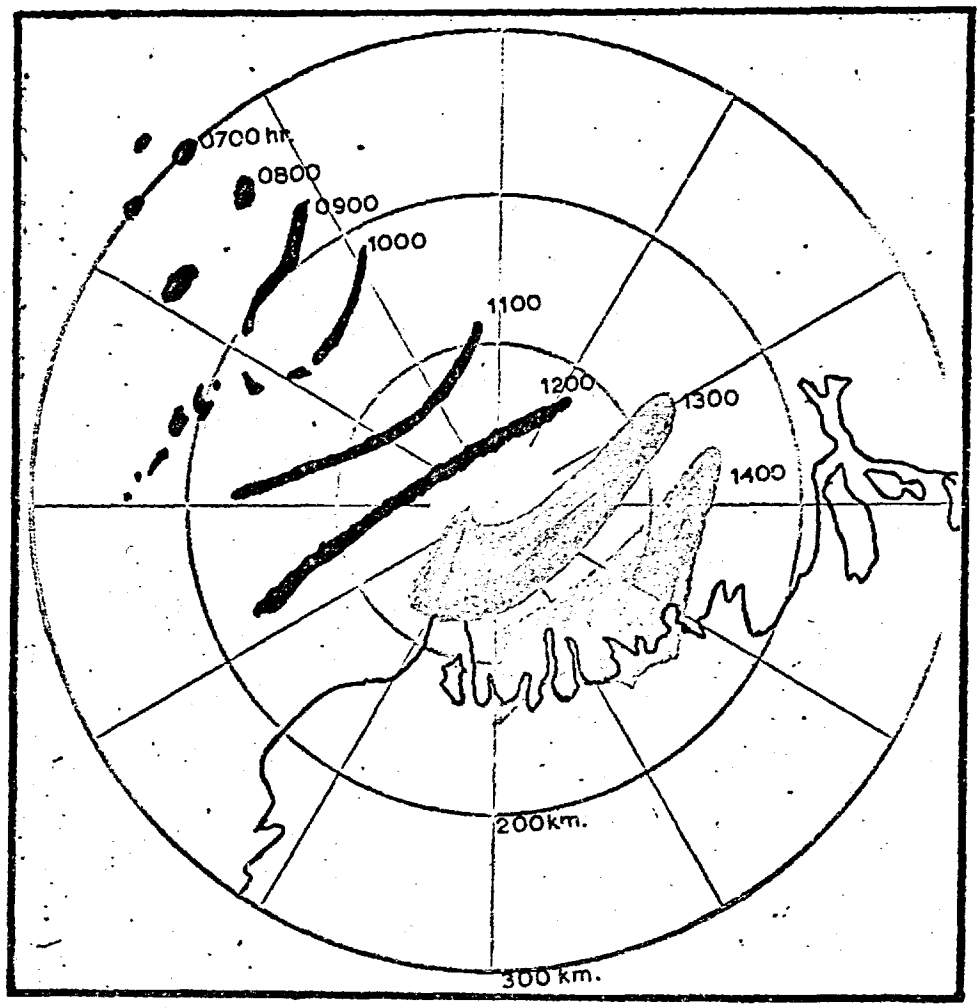

FIG. 3.9 — MOVEMENT OF THE SQUALL-LINE CONSIDERED IN SECTION 3.4.3. (AS RECORDED ON A P.P.I.)

FIG. 3.13 — PREDICTED AND OBSERVED PROPAGATION SPEEDS.

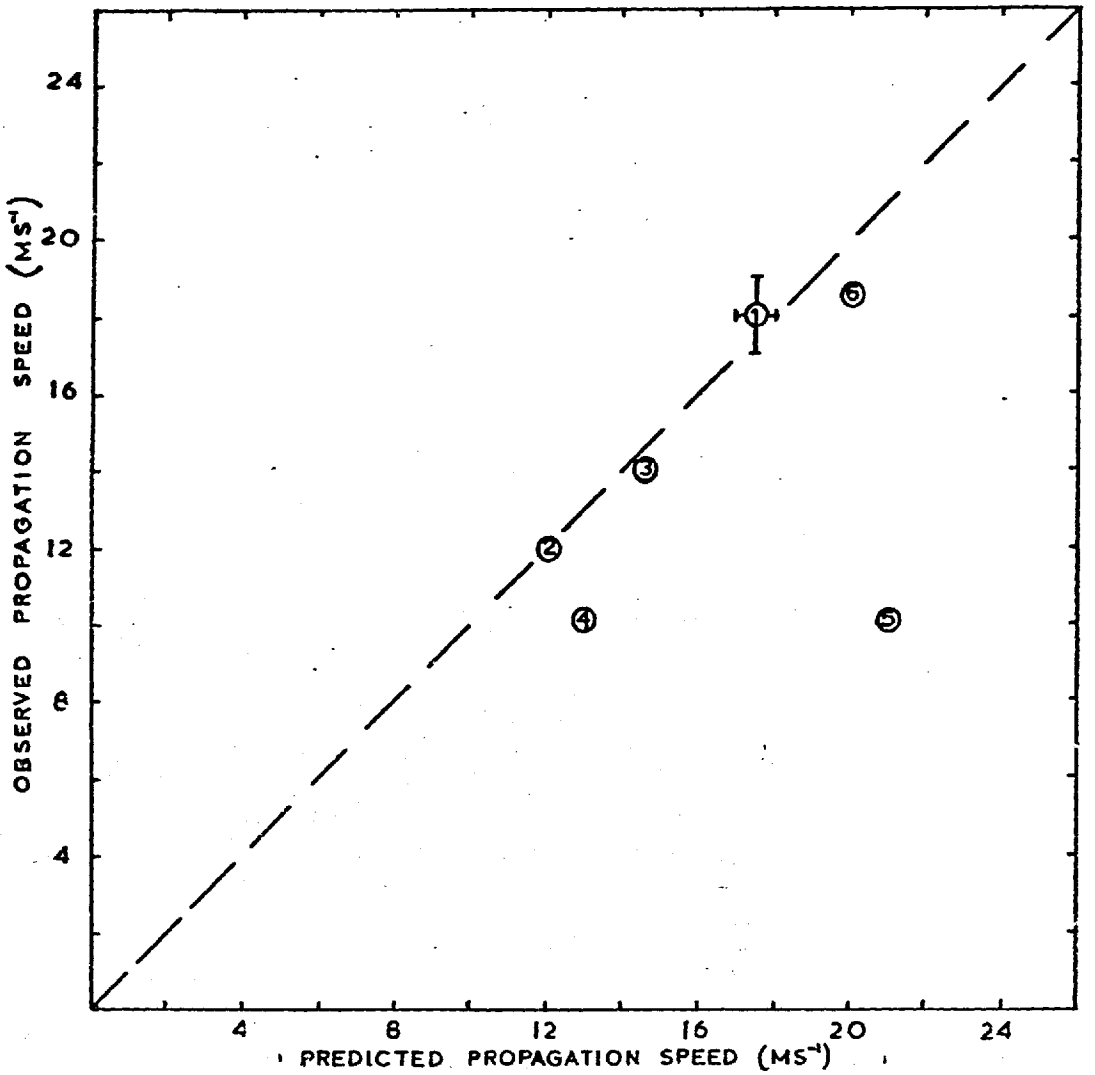

①	WOKINGHAM STORM.	[Ri = -2.3 ; H_o = 1.6]
②	HORSHAM STORM.	[Ri = -14.5 ; H_o = 1.6]
③	SQUALL-LINE.	[Ri = -3.2 ; H_o = 1.6]
④	PRE-MONSOONAL STORM.	[Ri = -3.8 ; H_o = 1.25]
⑤	SEVERE STORM. (U.S.A.)	[Ri = -5.6 ; H_o = 1.7]
⑥	COLD FRONT.	[Ri = -1.6 ; H_o = 0.4]

the atmosphere, from which data the Richardson Number was found to be Ri = -1.6, and the density scaling parameter $H/H_o = 0.4$. The steering-level and propagation speed were predicted to be 1.5 km and 20 m s^{-1} respectively. The observed values were 1.2 km and 18½ m s^{-1}, a favourable agreement.

3.4.7 — GENERAL POINTS

Although storms in mid-latitudes usually travel quite rapidly relative to the surface, this is by no means necessary but is a consequence of the strong mid-tropospheric winds characteristic of these latitudes. Slow moving systems are capable of generating a considerable amount of precipitation at one place and are therefore particularly important. If a storm is to be stationary, the wind relative to the ground must vanish at the steering-level. Consequently the surface wind must at least oppose the direction of the shear. In frontal zones, where the shear is usually about 3×10^{-3} s^{-1}, a typical severe storm with Ri = -2 say and $H/H_o = 1.4$, will have zero propagation speed if the 'surface' windspeed (in a frictionless model) is 13 m s^{-1} and opposed to the shear. This is a fairly strong surface wind, and in any case in frontal zones the shear and the low-level wind are usually in the same general direction, so frontal storms rarely move slowly.

Stationary storms can, however, be found on the poleward side of depressions, where the shear is typically about 1×10^{-3} s^{-1} and the surface wind is usually opposed to the shear. For the above values of Ri (note that although the shear is smaller than in frontal regions, the positive area is often smaller as well so it is valid to consider the same size of Richardson Number in the two regions) and H/H_o, the

surface wind needs only to be about 4 m s^{-1} and opposed to the shear to ensure stationarity.

The theory might also be applied to the movement of precipitation belts associated with cold fronts. Harper and Beimers (1958), studied 51 cases of this type and concluded that the steering-level was typically about 700 mb, with a standard deviation of about 50 mb. It is unfortunate that the temperature soundings are not available from Harper and Beimers studies, and so it is not possible to calculate Ri for their case studies. However with $Ri = -1.0$ and $H/H_o \simeq 0.75$, fairly typical values for such occasions, $z_* = 0.48H$. This gives a steering-level of 3.5 km or 660 mb, not inconsistent with the observational value of 700 mb quoted by Harper and Beimers.

3.5 — HEAT AND MOMENTUM FLUXES

At the present time there is great emphasis on the numerical simulation of the atmosphere on a global scale, and one of the problems raised by this is the difficulty of feeding the fluxes of heat and momentum arising from sub-gridscale processes into numerical models in a dynamically realistic manner. It is essential to take account of these fluxes if the equations of motion are integrated over a time-scale comparable to the lifetime of the large-scale eddies which transport the greater part of the heat and momentum on the global scale, otherwise it is likely that the model eddy kinetic energy will be too small because the available potential energy of the mean flow, from which the eddy kinetic energy is derived, cannot be maintained.

The contents of this section may be useful in the above context, because expressions for the transfer of heat and

momentum by cumulonimbus convection in sheared flow are obtained in terms of parameters which can be measured on the synoptic scale. In formulating these fluxes it is desirable to distinguish two extreme cases. First, where the compensating descent, necessary to preserve mass balance, takes place over an area large compared to that of the updraught. Second, where the downdraught and updraught are of comparable intensity and area. This latter case is probably closer to reality for severe storms, although the dominant regime must be closely related to the maintenance and organisation of steady overturning, a subject which will be attempted in chapters IV and V. (The content of these chapters deals with the details of the overturning process, whereas in this chapter the effect of the convection on the environment is considered.)

3.5.1 — HEAT FLUXES

3.5.1.1 — DESCENT AREA >> ASCENT AREA

Suppose that Fig.(3.14) schematically represents a cumulonimbus updraught cell.

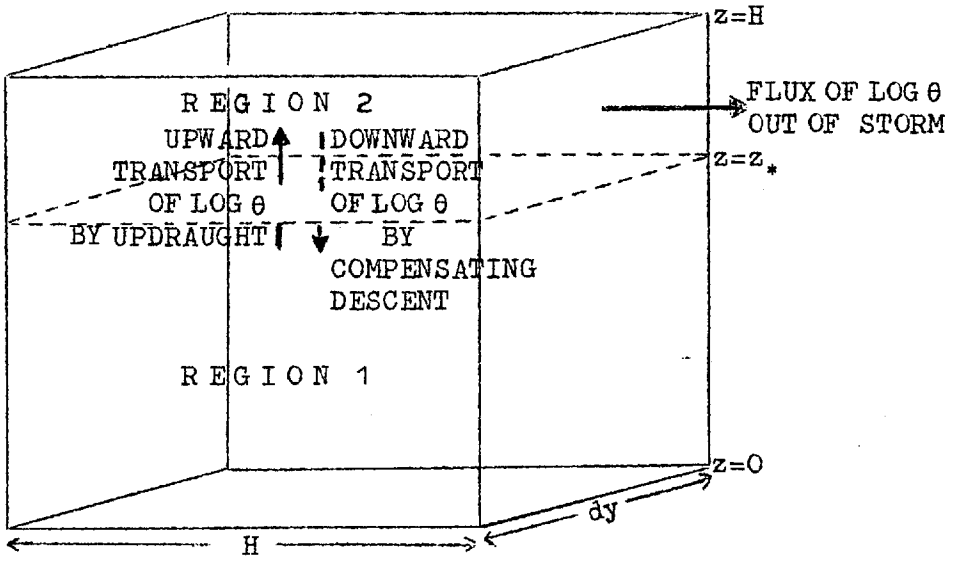

FIG. 3.14 — SCHEMATIC REPRESENTATION OF HEAT TRANSPORT BY CUMULONIMBUS CONVECTION IN SHEAR WHERE UPDRAUGHT AREA << DOWNDRAUGHT AREA

If F_2 is the net flux of $\phi = \log\theta$ into region (2) of this figure, then

$$F_2 = \left\{\int_{x=0}^{H} \rho c_p w \phi \, dx \, dy - \int_A \rho_* c_p w_* \phi_* \, dA\right\} + \left\{\int_{z_*}^{H} \rho c_p u \phi \, dz - \int_{x=0}^{H} \rho c_p w \phi \, dx\right\} dy$$

NET UPWARD TRANSPORT OF ϕ THROUGH THE STEERING-LEVEL $z = z_*$; GENERATION IN REGION (2)

——(3.29)

where w_* is the descent speed of the compensating current at the steering-level, ϕ_* is the log-potential temperature of this air and A is the area of descent. In fact F_2 can be rewrittem a

$$F_2 = \int_{z_*}^{H} \rho c_p u \phi \, dx \, dy - \int_A \rho_* c_p w_* \phi_* \, dA \qquad \text{——(3.30)}$$

FLUX OF ϕ OUT OF STORM ; FLUX OF ϕ THROUGH THE STEERING-LEVEL BY COMPENSATING DESCENT

Since the ascending and descending air must satisfy mass continuity,

$$-\rho_* w_* \, dA = \rho w \, dx \, dy = \rho u \, dy \, dz$$

$$F_2 = \left\{\int_{z_*}^{H} \rho c_p u(\phi - \phi_*) dz\right\} dy \qquad \text{——(3.31)}$$

Using the incompressible model of 3.2.1 as an example,

$$\phi - \phi_* = \left\{\gamma + \beta(\gamma - B)\right\}(z - z_*) \quad \text{and} \quad u = 2A\beta^2(z - z_*),$$

so that the net flux of ϕ into region (2) is

$$F_2 = 2A\rho c_p \frac{H^3}{3}\left\{\gamma + \beta(\gamma - B)\right\}\frac{\beta^2}{(1+\beta)^3} \, dy \qquad \text{——(3.32)}$$

In Eq.(3.32), the term $f_1 = 2A\rho c_p \frac{H^3}{3} \frac{\beta^3}{(1+\beta)^3}(\gamma - B)\, dy$ is the net transport of ϕ through the steering-level, and being a transport

term it is dependent on the temperature difference between the ascending and descending air and independent of the static stability. The term $f_2 = 2A\rho c_p \frac{H^3}{3}\gamma\frac{\beta^2}{(1+\beta)^3}\,dy$ in this same equation is a generation term and unlike f_1 it is directly dependent on the parcel lapse γ. The total flux F_2 is, however, directly related to the static stability of the outflow air, $\Gamma = \gamma+\beta(\gamma - B)$. Note that the outflow shear $2A\beta^2$ appears explicitly in this expression, emphasising its importance in estimating the heat flux. Fig.(3.15) shows the profile of ϕ before and after the passage of the model cumulonimbus, in the case where the descent is dry-adiabatic and covers an area much larger than the updraught.

The net flux into region (1) can also be calculated since it is given by the flux generation in region (1) less the net transport through the steering-level, and

$$F_1 = 2A\rho c_p \frac{H^3}{3} B \frac{\beta^3}{(1+\beta)^3}\,dy \qquad \text{——(3.33)}$$

Note that F_1 and F_2 are of similar form and their ratio is given by

$$\frac{F_1}{F_2} = \beta\frac{B}{\Gamma} \qquad \text{——(3.34)}$$

that is, proportional to the ratio of the static stabilities of the inflow and outflow air, and to the square root of the ratio of outflow to inflow shear. Incidentally this proves that if the motion is dry-adiabatic and neutral ($\gamma = B$), although there is no net transport of $\log\theta$ through the steering-level, there is an equal heating of both layers measured by

$$F_1 = F_2 = 2A\rho c_p \frac{H^3}{24} B\,dy \qquad \text{——(3.35)}$$

It is interesting to find the relative magnitude of the fluxes F_1 and F_2. However Eq.(3.34) is an implicit relationship and

FIG. 3-15 — PROFILE OF ϕ WHERE UPDRAUGHT AREA ≪ DOWNDRAUGHT AREA.

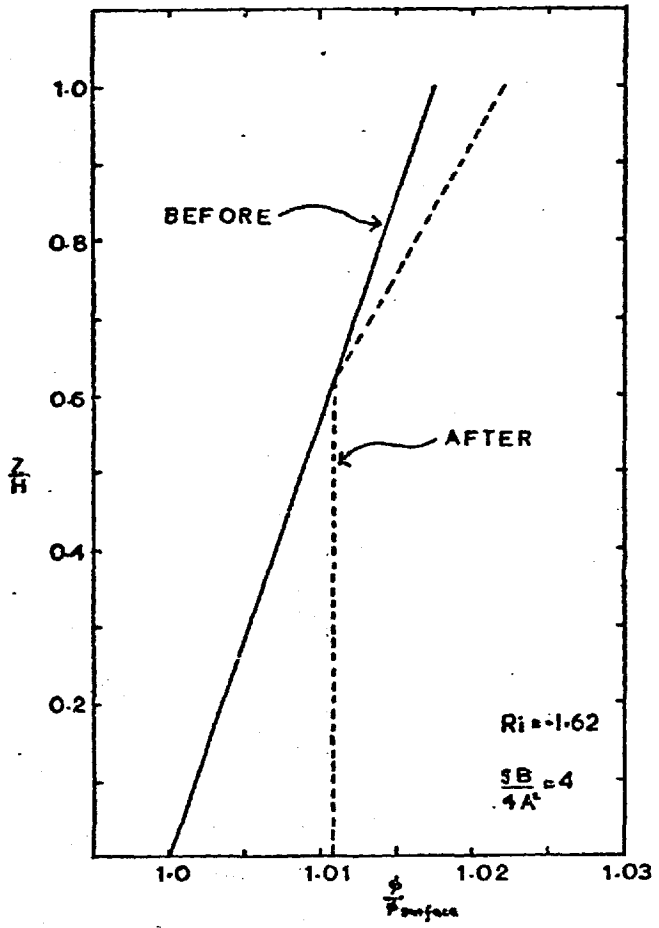

FIG. 3-16 — PROFILE OF ϕ WHERE UPDRAUGHT AREA = DOWNDRAUGHT AREA.

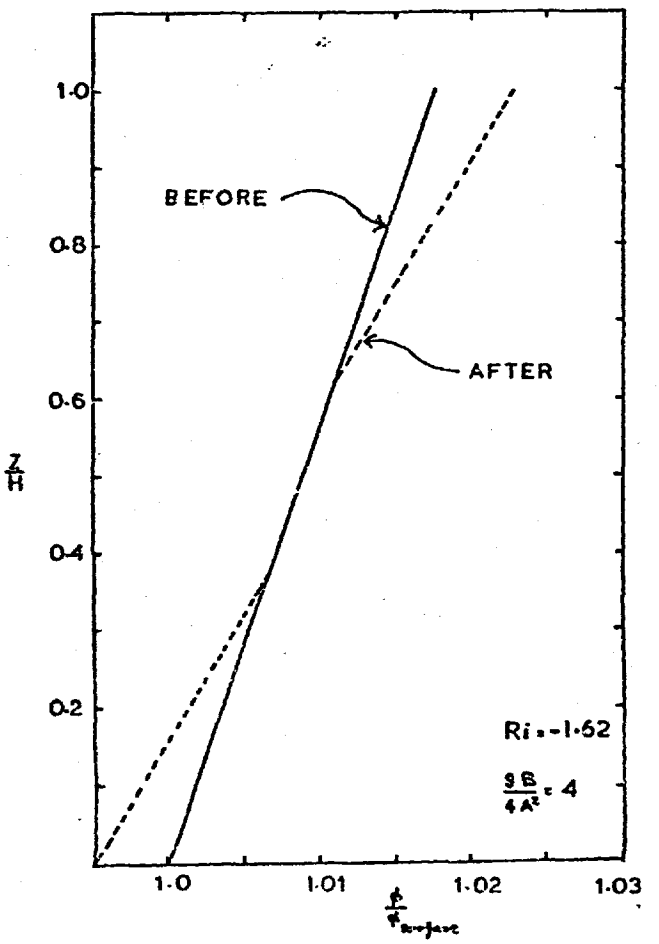

it is more convenient to formulate the problem in terms of the nondimensional number R. It can be shown that $F_1 > F_2$ if the following inequality is satisfied:

$$\frac{gB}{4A^2} \begin{cases} < & 1 + R + (1+4R)^{\frac{1}{2}} \quad \text{if} \quad R > 0 \\ > & 1 + R + (1+4R)^{\frac{1}{2}} \quad \text{if} \quad -1/4 < R < 0 \end{cases} \qquad \text{———(3.36)}$$

Typically $B = 10^{-7}$ cm^{-1} and $2A = 3 \times 10^{-3}$ s^{-1} so that $gB/4A^2 = 10.9$ and by Eq.(3.36) $F_1 > F_2$ if R lies in the range $0 < R < 5.9$. Consequently, for conditions typical of severe storms, if the compensating descent is dry-adiabatic and takes place over an area large compared to the updraught, there will be a net heating of the whole troposphere with the greatest heating in the layer below the steering-level. This is in the opposite sense to the case where the updraught and downdraught is of comparable intensity, for in the latter case the air in the lower layers of the atmosphere is cooled by the evaporation of rain. This second case will now be dealt with.

3.5.1.2 — ASCENT AND DESCENT AREAS EQUAL

The downdraught in this case is supposed to be maintained by evaporative cooling by rain falling out of the updraught. In evaluating the generation and transport of ϕ, it is convenient to consider the three distinct layers shown schematically in Fig.(3.16). Note that in this ideal antisymmetric regime there is no net input of heat over the region as a whole, only a redistribution of the form shown schematically in Fig.(3.17).

The net flux of ϕ into region (2) is given by

$$F_2 = \left[\left\{ \int_{x=\frac{H}{2}-z_*}^{H} \rho c_p w \phi_{*U}\, dx + \int_{x=-H}^{\frac{H}{2}-z_*} \rho c_p w \phi_{*D}\, dx \right\} + \left\{ \int_{z=z_*}^{H} \rho c_p u \phi\, dz - \int_{x=\frac{H}{2}-z_*}^{H} \rho c_p w \phi_{*U}\, dz \right\} - \left\{ \int_{x=-H}^{\frac{H}{2}-z_*} \rho c_p u \phi_{*D}\, dx - \int_{z=z_*}^{H} \rho c_p u \phi_{*D}\, dx \right\} \right] dy$$

TRANSPORT OF ϕ THROUGH THE STEERING-LEVEL $z=z_*$ | GENERATION OF ϕ IN UPDRAUGHT SECTION OF REGION (2) | GENERATION OF ϕ IN DOWNDRAUGHT SECTION OF REGION (2)

———(3.37)

where subscripts [U] and [D] refer to updraught and downdraught respectively. Using mass continuity and for convenience the asymmetry condition

$$F_2 = \left\{ \int_{z=z_*}^{H} \rho c_p u(\phi_{*U} - \phi_{*D})dz + \int_{z=z_*}^{H} \rho c_p u(\phi_U - \phi_{*U})dz + \int_{z_o=0}^{H-z_*} \rho c_p u(\phi_{*D} - \phi_D)dz_o \right\} dy \qquad (3.38)$$

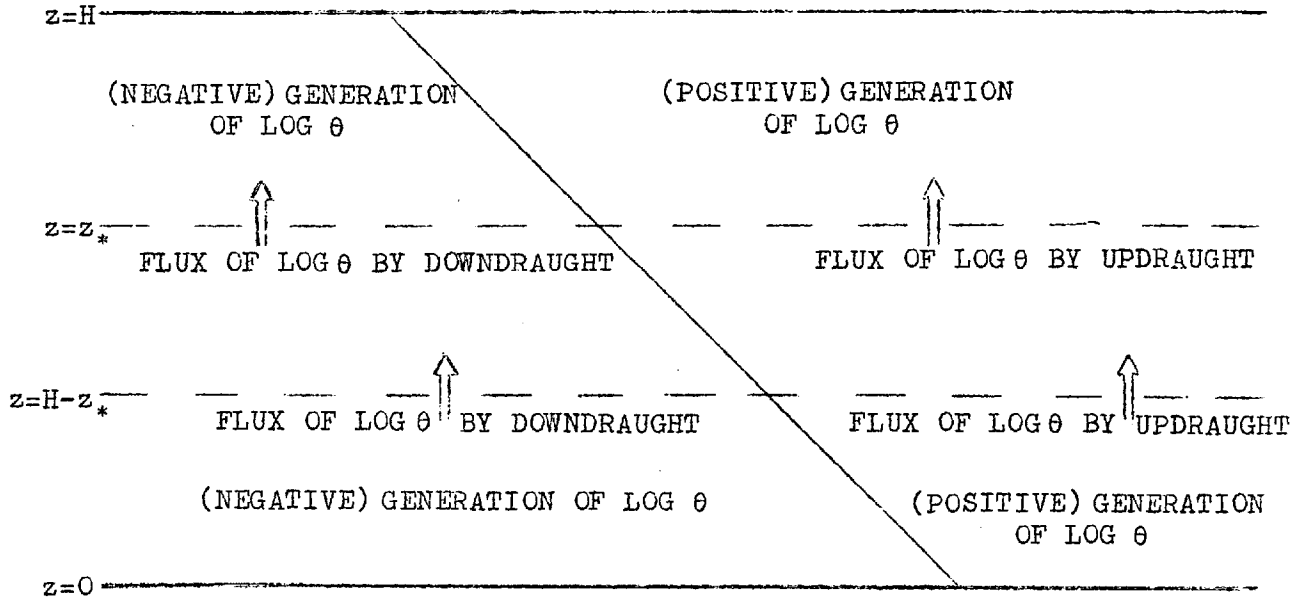

FIG. 3.16 — SCHEMATIC DIAGRAM OF HEAT TRANSPORT AND GENERATION BY CUMULONIMBUS CONVECTION IN SHEAR WHERE UPDRAUGHT AND DOWNDRAUGHT AREAS ARE EQUAL

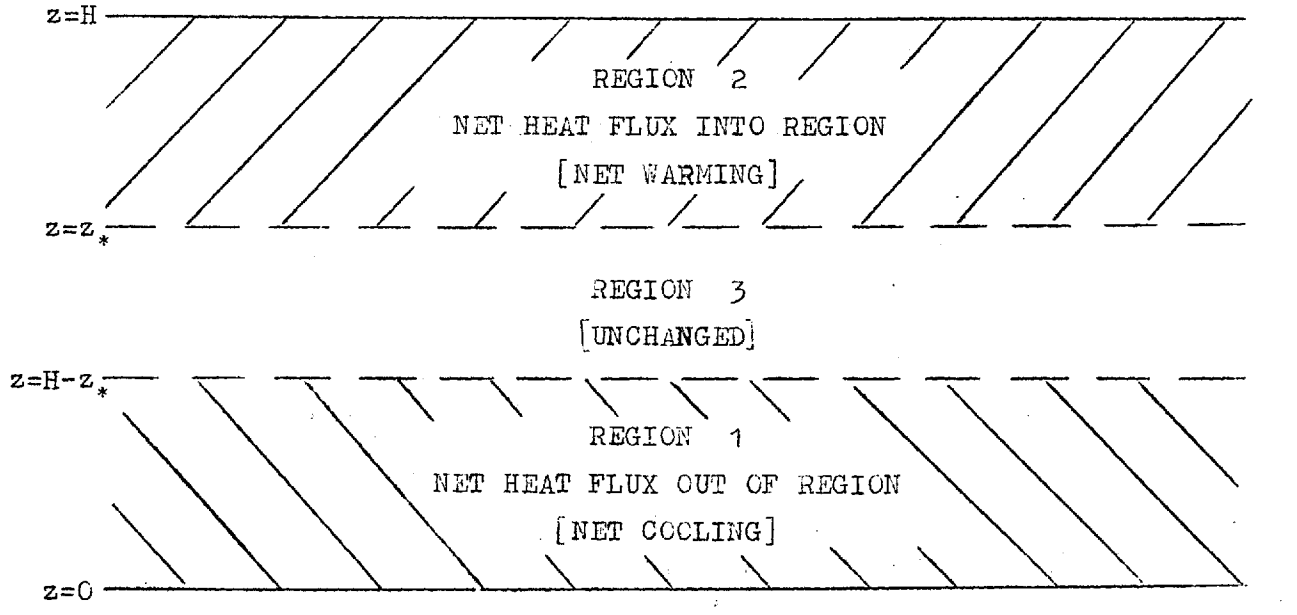

FIG. 3.17 — SCHEMATIC DIAGRAM OF THE EFFECT OF CUMULONIMBUS CONVECTION IN SHEAR ON THE ENVIRONMENT, WHERE UPDRAUGHT AND DOWNDRAUGHT ARE OF EQUAL AREA

Using the incompressible model of section 3.2.1 as an example,

$$\phi_U - \phi_{*U} = \gamma(z - z_*) \quad ; \quad \phi_{D*} - \phi_D = \gamma(H - z_* - z_o)$$

$$\phi_{*U} - \phi_{*D} = \left\{\gamma + \beta(\gamma - B)\right\}(z - z_*) \quad ; \quad u = 2A\beta^2(z - z_*)$$

$$u_o = 2A(z_o - z_*)$$

After some calculation the heat flux is found to be

$$F_2 = 2A\rho c_p \frac{H^3}{3} \frac{\beta 2}{(1+\beta)^3} \left\{\gamma\left(1 - \frac{3}{2\beta} + \frac{1}{2\beta^2}\right) + (\gamma - B)\frac{(\beta+3)}{2}\right\} \qquad (3.39)$$

From the symmetry of the problem obviously the net flux (F_1) into region (1) is $F_1 = -F_2$, and the net flux (F_3) into region (3) is zero. Fig.(3.18) shows the profile of θ before and after the passage of the model cumulonimbus, in the case where the descent and ascent cover an equal area.

Consequently this is a system which cools the lower layers of the troposphere, warms the upper layers but leaves the middle layers unchanged - distinct from the process outlined in section 3.5.1.1 which warms the whole troposphere. Although these are both processes of stabilisation in the sense that the mean static stability is increased, there is an important distinction. This distinction is most important over the sea because in the latter regime, the lower layers are cooled and thus the air/sea temperature contrast increased with the result that the fluxes of heat and moisture across the air/sea interface are enhanced. Therefore this antisymmetric type of system defines a process which is not only efficient in releasing available potential energy, but by cooling the lower layers and (at least over the sea) maximises the surface fluxes of heat and water vapour. That is, it also ensures that the best possible conditions are available

for the smaller scale convective processes to recharge the available potential energy of the mean flow on which fresh cumulonimbi can feed. Over land, the situation is probably more complicated since the small-scale convection must be initiated by surface heating, a factor which depends on larger scale processes in general, and the amount of cloud cover in particular.

The distinction between the regimes of this and the previous section is probably relevant when considering the role cumulonimbus convection plays in the growth and maintenance of hurricane circulations, because over warm tropical oceans, a very efficient way of enhancing the surface heat flux is by depositing a layer of cold air over it. The former case, (3.5.1.1) where there is large-scale, dry-adiabatic descent and the lower layers are heated by the cumulonimbus convection, has the opposite effect of inhibiting the heat transport from the sea surface. The distinction between the effects of the contrasting downdraught processes at least indicates that care is needed in the parameterisation of cumulonimbus processes, for instance in global numerical models.

3.5.2 — DERIVATION OF HEAT TRANSFER COEFFICIENTS FOR STEADY OVERTURNING

The evaluation of convective heat transfer, particularly in small scale turbulence studies, is classically by means of dimensional analysis, a process yielding a constant of proportionality which must be found empirically by observational measurements often requiring sophisticated apparatus. Here, the heat transfer coefficients are determined on a dynamical basis without the necessity of empiricism, essentially by rewriting the flux equations of section 3.5.1.1. The motivation

for this is not only because of general interest, but when rewritten in a certain form, the equations yield a coefficient which is useful as a measure of the efficiency of cumulonimbus convection compared to the smaller scale boundary layer processes which are instrumental in modifying the large scale thermodynamic structure into a form favourable for the development of cumulonimbus convection.

Suppose the heat transfer coefficient is defined as the ratio of the heat flux to the gradient of potential temperature.

$$K_H = \frac{F_H}{\rho c_p} \Big/ \frac{\partial \theta}{\partial z}$$

With the heat flux given by Eq.(3.32) the heat transfer coefficient corresponding to region (2) is

$$K_H = 2A \frac{H^2}{3} \frac{\beta^2}{(1+\beta)^3} \qquad \text{———(3.40)}$$

from which equation it follows that K_H is uniquely determined by R and the undisturbed shear, both of which can be measured by routine synoptic observations.

With typical values of $2A = 3 \times 10^{-3}$ s^{-1}, H = 10 km and R = 1 substituted into Eq.(3.40), $K_H \simeq 4 \times 10^{8}$ cm^2 s^{-1}, which is four orders of magnitude greater than the transfer coefficient typical of the shallow layer where the flux is nearly constant, and nine orders of magnitude greater than the molecular diffusion coefficient. (Incidentally note that the transfer coefficient for steady overturning given by Eq.(3.40) is of the same form as the molecular diffusion coefficient $\nu = \frac{1}{3} c l$, where c and l are the r.m.s. speed and mean free path of the molecules respectively.) The magnitude of the transfer coefficient for steady overturning compared to that of the eddy processes in the constant flux layer can be interpreted as a measure of the relative efficiency of steady

overturning and eddy diffusion as heat transfer mechanisms. The efficiency difference is in fact almost as great as that of eddy compared to molecular diffusion! Moreover, since the surface heat transfer is associated with a transfer coefficient which is much smaller than that of steady overturning, the time-scale required by the surface transfer processes to charge the lower atmosphere with potential energy necessary for the cumulonimbus regime must be correspondingly large. This infers that over any given area, the fraction of the time that convection assumes the cumulonimbus regime must necessarily be small.

Similarly, the heat transfer coefficient corresponding to region (1) in section 3.5.1.1 can be shown to be

$$K_H = \frac{2AH^2}{3} \frac{\beta^3}{(1+\beta)^3} \qquad \text{——(3.41)}$$

Similar conclusions can be drawn when the heat flux formula Eq.(3.40) is compared with the so-called bulk aerodynamic formula,

$$F_H = \rho c_p C_H (u - u_o)(\theta - \theta_o) , \qquad \text{——(3.42)}$$

where u_o, θ_o are the speed and potential temperature at the surface. The 'drag' coefficient C_H, usually obtained empirically as a function of z, has a typical value of about 1×10^{-3} at a height of 10 m in near neutral conditions. The 'drag' coefficient for steady overturning can be evaluated theoretically from Eq.(3.40) since

$$u(H) - u(z_*) = 2A\beta^2 H/(1+\beta)$$
$$\theta(H) - \theta(z_*) = \Gamma H/(1+\beta)$$

giving C_H corresponding to region (2) as

$$C_H = \frac{1}{3(1+\beta)} \qquad \text{——(3.43)}$$

This coefficient is consequently uniquely determined by the

value of R for the undisturbed flow. If $R = 1$, $\beta = 1.62$ so that $C_H = 0.125$, that is two orders of magnitude larger than the coefficient associated with the turbulent heat transfer close to the air/sea interface, leading to the same conclusions about the efficiency of steady overturning as a heat transport mechanism as was given before.

An analogous argument gives C_H for region (1) to be

$$C_H = \frac{\beta}{3(1+\beta)} \qquad \text{——(3.44)}$$

The main value of the flux formulae given by Eqs.(3.32, 3.33, 3.39) arises because they express the total heat flux in terms of parameters which can be readily calculated from standard synoptic observations. The undisturbed stratification and wind field can be obtained from radiosonde ascents, and the parcel potential temperature from assuming adiabatic ascent at a mean θ_w for the surface boundary layer. This gives sufficient information to enable R to be calculated and consequently z_* and β by Eqs.(3.10, 3.11).

3.5.3 — MOMENTUM FLUXES

The solutions on Figs.(3.3, 3.4) show that buoyant overturning acts to increase shear above the steering-level and transfers momentum into the mean flow above this level. The amount of momentum transferred into this layer can be calculated since the outflow speed and the steering-level has been calculated for a given undisturbed state.

This momentum transfer is given by

$$F_M = \int_{z_*}^{H} \rho u^2 \, dz \, dy - \int_{z_*}^{H} \rho u_o^2 \, dz \, dy$$

where u_o is the undisturbed speed. For example, in the

incompressible problem, $u = 2A\beta^2(z - z_*)$ and $u_o = 2A(z - z_*)$ and so for this case,

$$F_M = \int_{z_*}^{H} 4A^2(\beta^4 - 1)\rho(z - z_*)^2 \, dz \, dy$$

$$F_M = \frac{4A^2}{3} \frac{(\beta^4 - 1)}{(1 + \beta)^3} \rho H^3 \, dy \qquad \text{———(3.45)}$$

Eq.(3.45) represents the amount of momentum transferred into the upper levels both in the case where the updraught area is much smaller than the downdraught area and where these areas are equal, the difference being that in the latter case an equal amount of momentum is removed from the surface layer of depth $H - z_*$. The cumulonimbus therefore redistributes momentum.

For typical severe storm conditions with $H = 10$ km, $2A = 3 \times 10^{-3}$ s^{-1} and $R = 1$ so $\beta = 1.62$. Therefore where there is cumulonimbus convection, the amount of momentum transferred into the layer above the steering-level is

$$F_M \simeq 750 \text{ dyne cm}^{-2}$$

This is a very large value compared to the momentum transfere in the surface layers by turbulent eddies, because in this region the corresponding value is about 0.5 dyne cm^{-2}. Cumulonimbus convection is therefore an important momentum transfer mechanism. The implication will be discussed in chapter VI.

3.5.4 — DERIVATION OF A MOMENTUM TRANSFER COEFFICIENT FOR STEADY OVERTURNING

An effective way of comparing the relative efficiency of heat and momentum transfers is to obtain an expression for the ratio of the corresponding transfer coefficients.

A momentum transfer coefficient K_M is defined in a form

analogous to the heat transfer coefficient defined in section 3.5.2

$$\text{i.e.} \quad K_M = \frac{F_M}{\rho} \Big/ \frac{\partial u}{\partial z} \qquad \text{——(3.46)}$$

where $\frac{\partial u}{\partial z}$ is the outflow shear. In the model $\frac{\partial u}{\partial z} \sim 2A\beta^2$, and F_M is given by Eq.(3.45), so it follows that for steady overturning, K_M is given by

$$K_M = 2AH^2 \frac{1}{3} \frac{\beta^4 - 1}{\beta^2(1+\beta)^3} \qquad \text{——(3.47)}$$

The ratio of the heat and momentum transfer coefficients is therefore

$$\frac{K_M}{K_H} = \frac{\beta^4 - 1}{\beta^5} \qquad \text{——(3.48)}$$

Therefore for steady, buoyant overturning ($R > 0$, $\beta > 1$), $K_H > K_M$, (for instance if $R = 1$, $\beta = 1.62$ and $K_M/K_H = 0.53$) so heat is more readily transferred than momentum.

3.5.4 — HEAT AND MOMENTUM FLUXES FOR PARTICULAR STORMS

The flux formulae are used to estimate the heat fluxes by severe storms using actual data to calculate the values of the various parameters. The origin of these data has been discussed in a previous section. The particular values obtained for F_H and F_M quantify the importance of the storms as heat and momentum transfer processes, compared to surface processes.

(a) Wokingham Storm

The surface wet-bulb temperature observed after the passage of this storm suggested that there must have been considerable evaporation of rain into the downdraught, which was vigorous judging by the strength of the gusts behind the squall-front. Therefore, the regime in which the updraught and downdraught are of comparable area is used to estimate the heat flux. From the data the value of the variables are estimated as

$$2A = 5 \times 10^{-3}\ s^{-1}$$

$$B = 1.01 \times 10^{-7}\ cm^{-1}$$

$$\gamma = 1.13 \times 10^{-7}\ cm^{-1}$$

$$H = 11\ km$$

giving the following (incompressible) values for R, β and z_*.

$$R = 0.86$$

$$\beta = 1.43$$

$$z_* = 0.59$$

Using Eqs.(3.39, 3.47) the heat and momentum fluxes in the incompressible model are found to be

$$F_H = 68\ cal\ cm^{-2}\ min^{-1}$$

$$F_M = 2.2 \times 10^{3}\ dyne\ cm^{-2}$$

(b) Horsham Storm

The observations in this case also suggest that the updraught and downdraught were of comparable area and intensity. Using observationsl data

$$2A = 1.8 \times 10^{-3}\ s^{-1}$$

$$B = 0.99\ cm^{-1}$$

$$\gamma = 1.29\ cm^{-1}$$

$$H = 11.5\ km$$

giving the (incompressible values of R, β and z_* as

$$R = 10$$

$$\beta = 3.74$$

$$z_* = 0.79$$

The heat and momentum fluxes in thc incompressible model are thus

$$F_H = 95 \text{ cal cm}^{-2} \text{ min}^{-1}$$

$$F_M = 2.6 \times 10^3 \text{ dyne cm}^{-2}$$

3.6 — EFFECT OF NON-HYDROSTATIC PRESSURE ON STEADY FINITE-AMPLITUDE OVERTURNING

The quantity $\frac{1}{2}\underset{\sim}{v}^2 + \frac{\delta p}{\rho} - \int_{z_o}^{z} g\,\delta\phi_p\,dz$ is conserved along streamlines in steady flow and may be used to find the kinetic energy at a level in terms of the potential energy release, the inflow kinetic energy and the nonhydrostatic pressure field.

Using the fact that if the remote flow is horizontal, then the pressure must be hydrostatic and therefore,

$$\frac{\delta p}{\rho}(x=\infty, z) \sim \frac{\delta p}{\rho}(x=\infty, z_o) + \int_{z_o}^{z} g\,\delta\phi\,dz \qquad \text{——(3.49)}$$

and if the x-component of the momentum equation is integrated at constant z,

$$\frac{\delta p}{\rho}(x,z) = \frac{\delta p}{\rho}(x=\infty, z) + \int_{x}^{\infty} \frac{Du}{Dt}\,dx\,, \qquad \text{——(3.50)}$$

together with

$$\frac{1}{2}\underset{\sim}{v}^2 + \frac{\delta p}{\rho} - \int_{z_o}^{z} g\,\delta\phi_p\,dz = \frac{1}{2}u_o^2 + \frac{\delta p}{\rho}\,, \qquad \text{——(3.51)}$$

it can be shown that

$$\frac{1}{2}\underset{\sim}{v}^2 = \frac{1}{2}u_o^2 + \int_{z_o}^{z} g(\delta\phi_p - \delta\phi)\,dz - \int_{x=0}^{\infty} \frac{Du}{Dt}\,dx \qquad \text{——(3.52)}$$

Eq.(3.52) indicates that the effect of non-hydrostatic pressure, measured effectively by the (positive) term on the extreme R.H.S. of this equation, has the effect of decreasing the updraught kinetic energy thus acting against the enhancing effect of the inflow kinetic energy. The residual $\frac{1}{2}u_o^2 - \int_{x}^{\infty} \frac{Du}{Dt}\,dx$ is in fact a measure of the departure of the updraught kinetic energy from the parcel theory value. It is interesting to deduce a rough measure of this departure. In particular for the limiting

streamline defined by $z_o = 0$ at the steering-level $z = z_*$, since at this level $u\frac{\partial u}{\partial x} << w\frac{\partial u}{\partial z}$,

$$\int_{x=0}^{\infty} \frac{Du}{Dt} dx \simeq H \cdot \overline{w\frac{\partial u}{\partial z}}^{x, z=z_*}$$

$$= \overline{\frac{\partial u}{\partial z}}^{x, z=z_*} \; \overline{u_o}^{z_o} \qquad \text{(by continuity)}$$

$$\simeq \frac{u(x=\infty, z_o=0)}{2z_*} \, z_* \, \frac{u(x=\infty, z_o=0)}{2}$$

$$= \frac{u^2(x=\infty, z_o=0)}{4}$$

$$\therefore \quad \frac{1}{2}\underset{\sim}{v}^2(x=0, z=z_*) \simeq \frac{u^2(x=\infty, z_o=0)}{4} + \int_0^{z_*} g(\delta\phi_p - \delta\phi)dz \qquad \text{———(3.53)}$$

The updraught speed deduced by parcel theory will be in error by about $\frac{u(x=\infty, z_o=0)}{\sqrt{2}}$ at the steering-level when the pressure is non-hydrostatic within the storm, as against $u(x=\infty, z_o=0)$ if the pressure is assumed to be hydrostatic everywhere.

Generalising from these results, non-hydrostatic pressure reduces the updraught speed, and therefore will reduce the growth rate of the developing storm, as compared to that assuming the pressure hydrostatic within the storm. Moreover, the effects of non-hydrostatic pressure and relative inflow kinetic energy are in opposition so the result is to bring the updraught speed close to that estimated from parcel theory. The updraught speeds in the nonhydrostatic and hydrostatic problems are related by

$$|\underset{\sim}{v}'| \simeq \sqrt{\frac{R + 0.5}{R + 1}} \; |\underset{\sim}{v}|$$

where the prime denotes the nonhydrostatic value.

CHAPTER IV — TWO-DIMENSIONAL FREE-BOUNDARY (DISCONTINUOUS) MODELS

The main problem in representing the detailed flow within the storm with a free-boundary approach arises in modelling the boundary layer between updraught and downdraught by suitable boundary conditions. Since observations suggest that in many storms there is a rapid transition from updraught to downdraught over a distance small compared to the length-scale of the storm, boundary conditions implying discontinuities in the dependent variables at an interface between the draughts is a possible way of modelling this boundary layer. The justification of the validity of this discontinuous model is far from trivial.

In chapter II, the fully nonlinear vorticity equation was integrated along streamlines, giving an expression for the vorticity in terms of z and ψ and a corresponding partial differential equation for the streamfunction (Eq.3.1). This equation is elliptic and provided appropriate boundary conditions are defined, the resulting problem is of the free-boundary type in which both the streamfunction and the shape of the updraught/downdraught boundary can be determined. Kinematic boundary conditions determine the streamfunction for a given interface shape, while the shape of this interface is determined by the dynamic boundary condition.

The form of the boundary layer between the draughts, and consequently the nature of this dynamic boundary condition, is crucial to the following analysis. This thesis will be concerned with four distinct forms of boundary layer. The two types examined in this chapter are discontinuous in the sense that the velocity or both the velocity and the temperature are discontinuous at the updraught/downdraught interface. The

distinction between these two forms is important because where the velocity is discontinuous and temperature continuous, there is a finite generation of negative vorticity, a feature which must always be present in the physical problem. However if the temperature is also discontinuous, the interface defines a vorticity generating sheet as well as a vortex sheet, with the result that vorticity of positive sense only is developed within the body of the flow. It will be shown that the validity of a boundary condition having a discontinuity of temperature and velocity is determined by the size of the Richardson Number.

In chapter V, another two types of boundary will be examined. First, where all the variables are continuous - distinct from the discontinuous models of this chapter since vorticity and vorticity generation are everywhere finite. This model leads to the determination of an equivalent discontinuous model for the interfacial boundary layer, a boundary condition which not only implies discontinuities in temperature and velocity at the interface but also a discontinuity of pressure.

4.1 — THE FUNCTIONS F AND G USED IN THE DISCONTINUOUS MODELS

In principle, the free-boundary problem defined by Eq.(3.1) and its boundary conditions can be solved numerically for arbitrary functions F and G, but only at the expense of added labour. Since too much generality only obscures the picture, simple forms for F and G are used to illustrate important features. Subsequently, the function G, the vertical shear of the undisturbed flow remote from the storm, will therefore be taken as $G(\psi) = 2A$, where A is constant. In mid-latitude severe storms, the windspeed does in fact increase approximately linearly with height (although the wind direction, especially in the lowest kilometre,

is far from constant due to the Ekman effect), so in two-dimensional models there is some justification for this simplified form for G.

The function F, the parcel potential temperature, is not so justifiably represented in simple form. The effects of the wet-adiabatic process require representation particularly the release of potential energy, preferably without having to bother about the actual details of the process. If the parcel potential temperature is assumed to be a linear function of height, then this release of potential energy can be at least crudely represented. This form has already been used in chapter III, and this asymptotic case gave acceptable results for the remote flow field, the height of the steering-level, propagation speed and a measure of the heat and momentum transports. Encouraged by these results, the same form for F is used in the determination of the detailed flow within the storm.

$$\text{i.e.} \quad F(\psi, z - z_o) = bz_o + \gamma(z - z_o) \ , \qquad \text{———(4.1)}$$

where $b(z_o)$ is the static stability of the undisturbed flow and γ is the (constant) parcel lapse. In the model where the temperature is allowed to be discontinuous at the updraught/downdraught interface, it is assumed that $b = B$, a constant. Where the draughts form an antisymmetric system, this gives a log-potential temperature discontinuity of $(\gamma - B)H$ at the interface. Fig.(4.1) schematically shows the remote log-potential temperature, before and after convective overturning has taken place.

Since a model having the temperature continuous at the interface is also required, a particular form is taken for the static stability. In the main part of the flow $b = B$ but in a boundary layer of asymptotic inflow depth ϵ, $b = \gamma + (\gamma - B)(\frac{H}{2\epsilon} - 1)$

FIG. 4.1 — ϕ STRUCTURE OF THE MODEL WITH THE TEMPERATURE DISCONTINUOUS AT THE UPDRAUGHT/DOWNDRAUGHT INTERFACE.

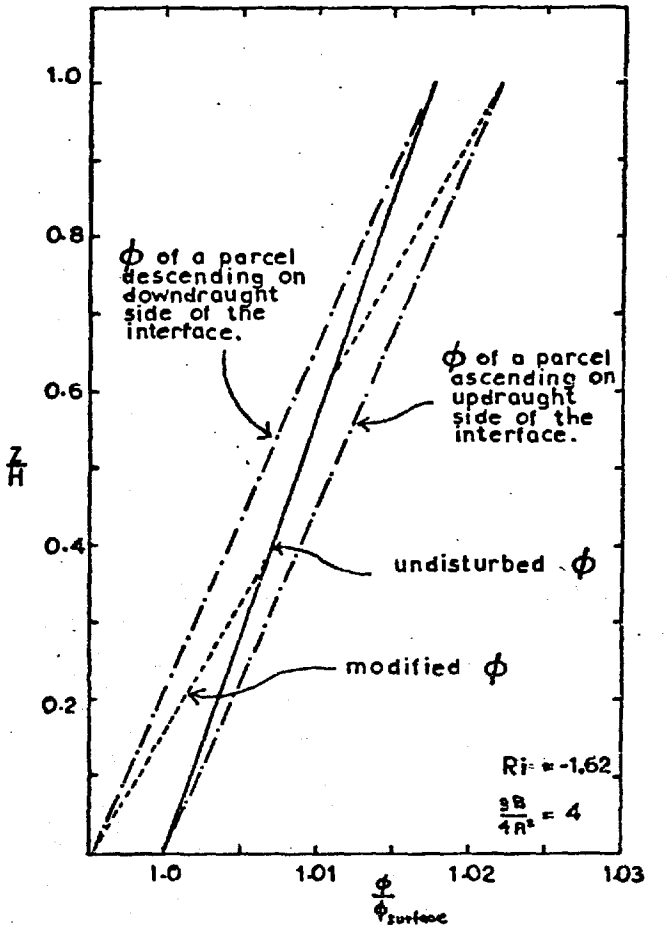

FIG. 4.2 — ϕ STRUCTURE OF THE MODEL WITH CONTINUOUS TEMPERATURE.

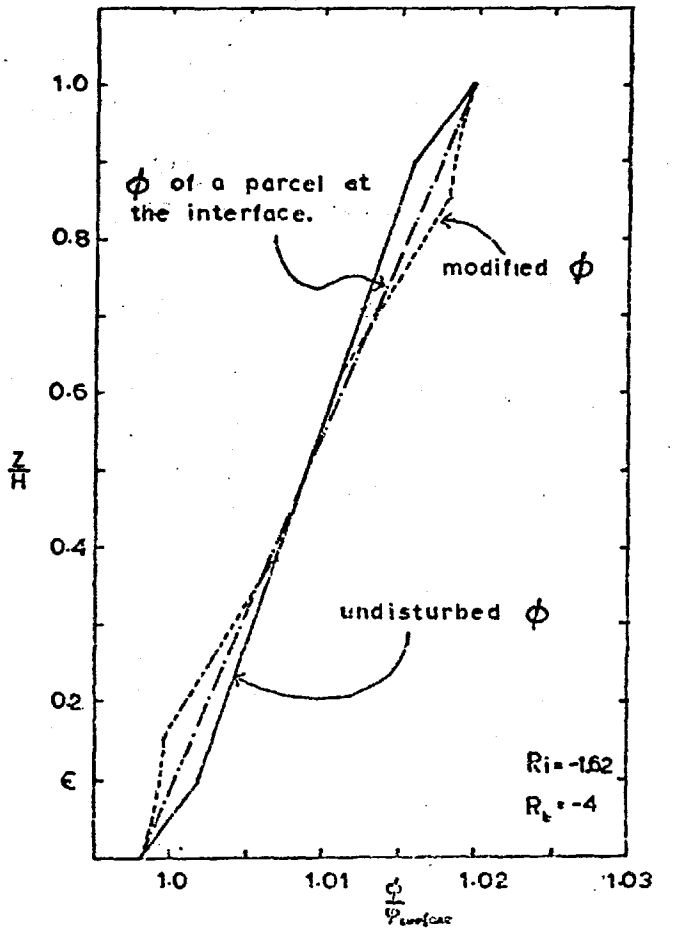

— a form illustrated in Fig.(4.2). Therefore in this case, the temperature is continuous at the interface between updraught and downdraught.

4.2 — THE KINEMATIC BOUNDARY CONDITIONS

Since Eq.(3.1) is elliptic, for a given interface shape it is sufficient to prescribe Dirichlet boundary conditions on ψ to obtain a solution. The convective system studied here is characterised by the inflow and outflow being on the same side, so at the rigid boundaries $z = 0$ and $z = H$ and at the free-boundary defined by the updraught/downdraught interface, the streamfunction must take the same constant value. At these boundaries it is convenient to let $\psi = Az_*^2$. The outflow/inflow boundary condition utilizes the asymptotic solutions obtained in chapter III, or in the case where the temperature is continuous those of section (4.4.1). This completely defines the kinematic boundary conditions shown schematically in Fig.(4.3), and together with Eq.(3.1) these are sufficient to define the streamfunction for a given interface shape.

However, the definition of the additional (dynamic) boundary condition at the interface is the most difficult, and this is the essence of most of the remainder of the analysis.

4.3 — A PARTICULAR ANALYTIC SOLUTION

In general Eq.(3.1) together with its boundary conditions defines a very complicated nonlinear problem. Even the asymptotic form can be solved analytically only for incompressible flow with constant parcel lapse and constant undisturbed shear. Generalisation of this solution to two space dimensions is impossible, not only because of the high degree of nonlinearity

FIG. 4.3 — SCHEMATIC ILLUSTRATION OF THE KINEMATIC BOUNDARY CONDITIONS.

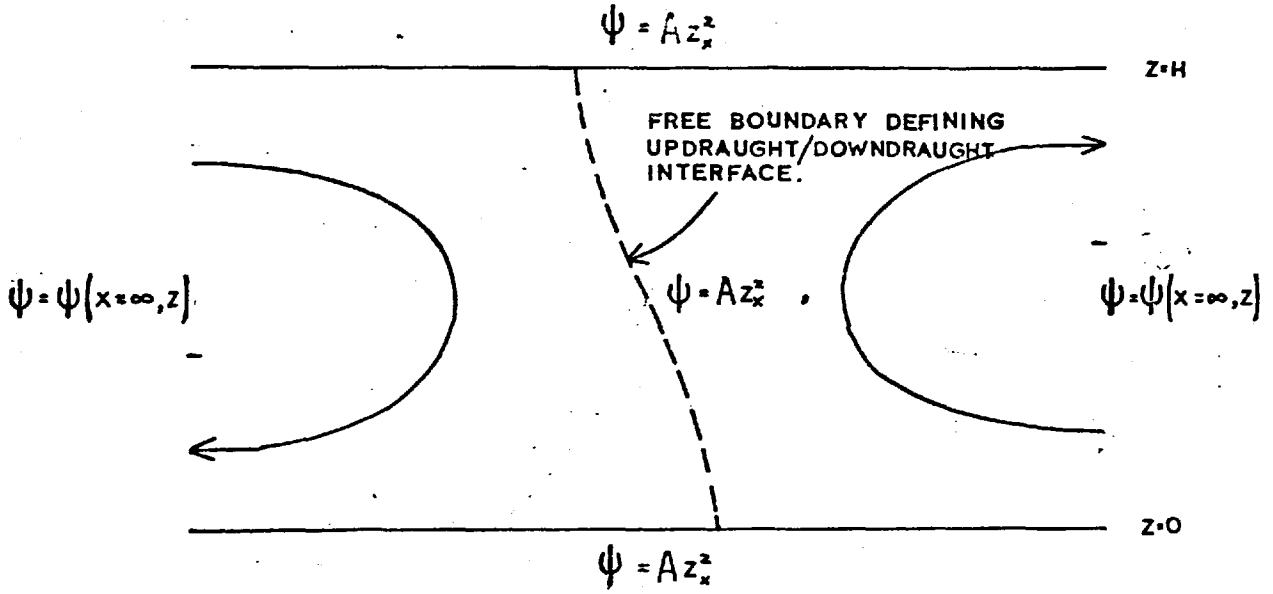

FIG. 4.5 — SCHEMATIC ϕ-STRUCTURE FOR GENERAL INTERFACE CONDITIONS.

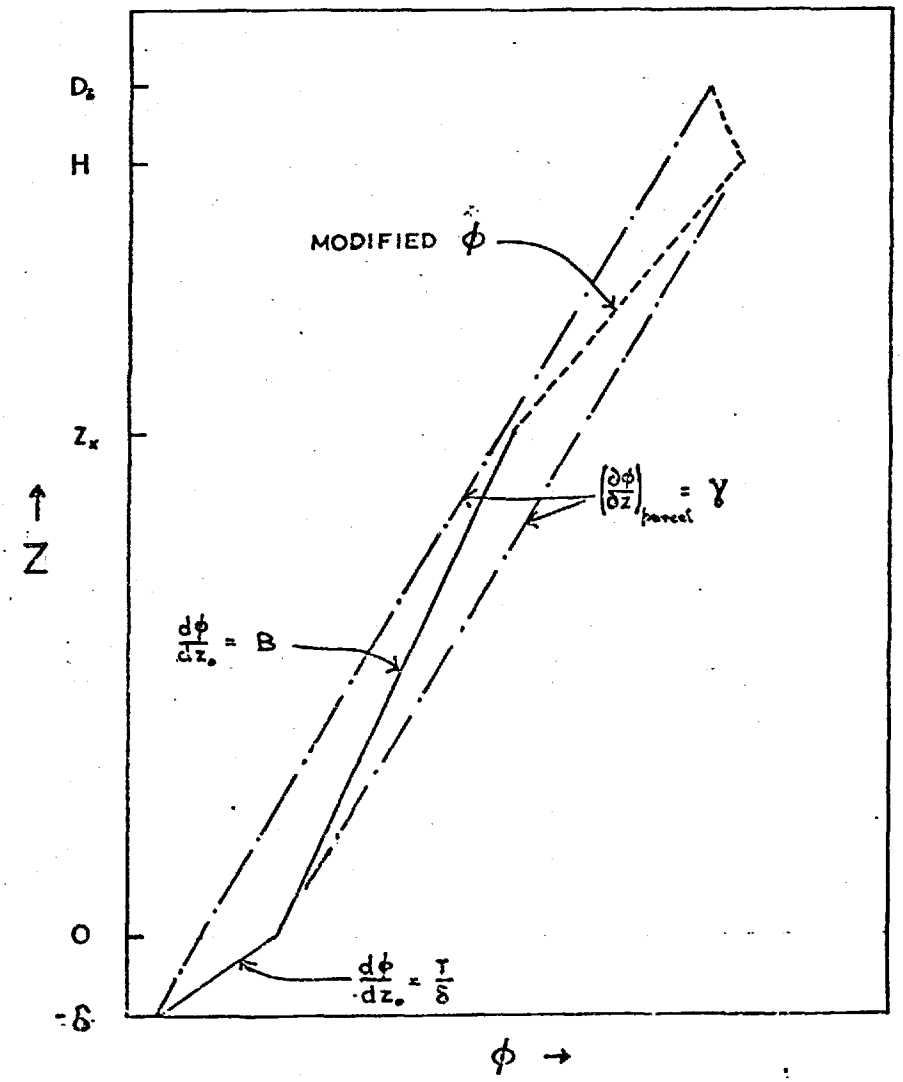

of the equation, but also because of the complicated general shape of the interface.

However for neutral overturning ($\gamma = B$), Eq.(3.1) can be transformed into Laplace's Equation. Solutions of Laplace in two dimensions can be analytically intractable even if the boundary shape is of fairly simple form. Fortunately in incompressible flow, symmetry demands that the interface should be perpendicular, and solutions in this simple case can be found by standard methods.

For incompressible, neutral overturning Eq.(3.1) reduces to a Poisson equation;

$$\nabla^2 \psi = 2A \qquad \text{——(4.2)}$$

and letting $\psi = Az(z - H) + Az_*^2 + \psi'$, the equation for ψ', (the perturbation on the undisturbed flow of constant shear 2A) satisfies Laplace's Equation.

$$\nabla^2 \psi' = 0 \qquad \text{——(4.3)}$$

Using the boundary conditions on ψ, the corresponding conditions on ψ' are

$$\left.\begin{array}{lll} \psi' = 0 & \text{at } z = 0, H \\ \psi' \sim 0 & \text{as } x \to \infty \\ \psi' = Az(H - z) & \text{along the interface } x = 0 \end{array}\right\}$$

A series solution for ψ', found by separation of the variables x and z is

$$\psi'(x,z) = \frac{z}{H} \sum_{n=0}^{\infty} b_n \sin\frac{n\pi z}{H} e^{-n\pi x/H}$$

where

$$b_n = \frac{z}{H} \int_0^H Az(H - z) \sin\frac{n\pi z}{H} \, dz$$

Consequently, the full solution is

$$\psi(x,z) = Az(z-H) + Az_*^2 + \frac{8AH^3}{\pi^3} \sum_{m=0}^{\infty} \frac{1}{(2m+1)^3} \sin(2m+1)\frac{\pi z}{H}\, e^{-(2m+1)\pi x/H} \qquad —(4.4)$$

The vertical velocity at the interface $x = 0$ is given by

$$w = -\frac{\partial \psi}{\partial x} = \frac{8AH^2}{\pi^2} \sum_{m=0}^{\infty} \frac{1}{(2m+1)^2} \sin(2m+1)\frac{\pi z}{H} \qquad ———(4.5)$$

The sum of this series given in Fig.(4.4) indicates that quite a vigorous circulation can persist even in the absence of available potential energy, the draughts being maintained by the inflow kinetic energy. If for instance the shear is 5×10^{-3} s^{-1}, as in the Wokingham storm, then a maximum updraught speed of $w = 18.5$ m s^{-1} could be maintained without any buoyancy. This is a substantial updraught and is a simple example of the importance of shear on the intensity of the circulation.

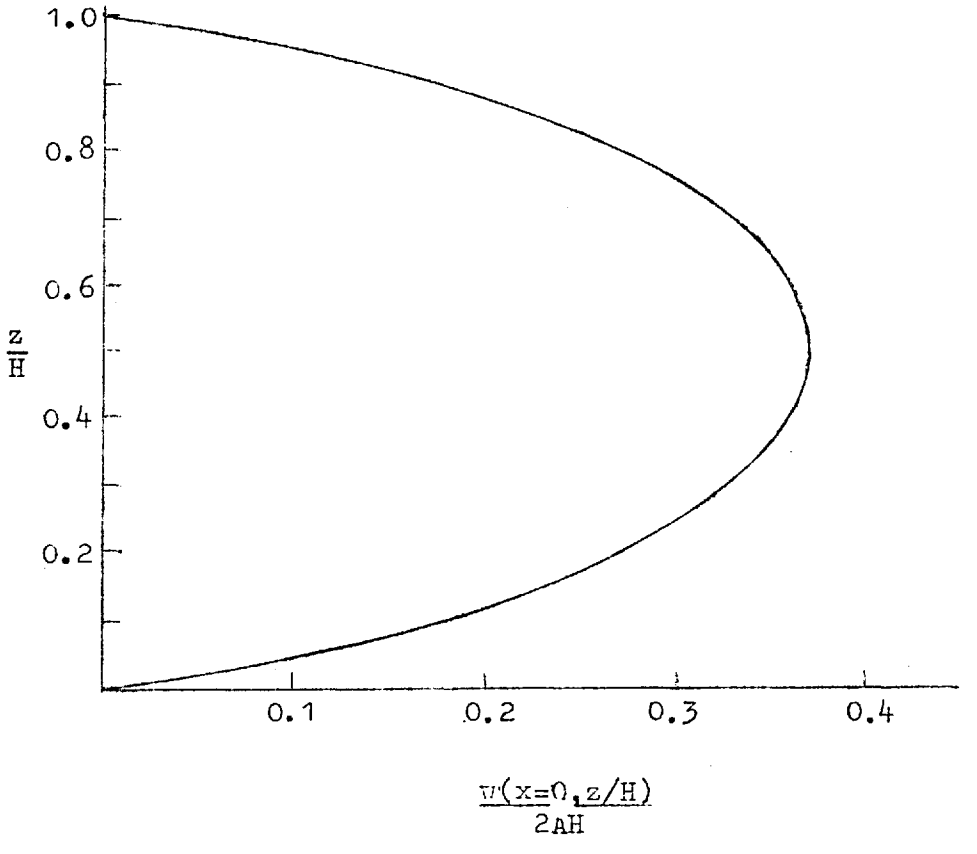

FIG. 4.4 — VERTICAL VELOCITY AT THE INTERFACE FOR Ri=0

4.4 — THE UPDRAUGHT/DOWNDRAUGHT BOUNDARY LAYER AND THE DYNAMIC BOUNDARY CONDITION AT THE INTERFACE

As implied earlier, the effect of negative vorticity generation in the interface region on the orientation of the flow within the cumulonimbus is not obvious. Therefore it is best to proceed rather carefully and using the momentum equations, derive general conditions which have to be satisfied in the boundary layer, particularly for the pressure change across the layer.

For this purpose it is convenient to define a coordinate system ($\underset{\sim}{l}, \underset{\sim}{m}, \underset{\sim}{n}$), where $\underset{\sim}{l}$ is directed along boundary layer axis, $\underset{\sim}{n}$ is the normal to this axis and $\underset{\sim}{m}$ coincides with the $\underset{\sim}{j}$ axis in the ($\underset{\sim}{i}, \underset{\sim}{j}, \underset{\sim}{k}$) coordinate system.

The momentum equation Eq.(1.7) with $f << \frac{D}{Dt}$ can be written as

$$\frac{\partial \underset{\sim}{v}}{\partial t} + \nabla\left(\frac{1}{2}\underset{\sim}{v}^2\right) + \underset{\sim}{\zeta} \wedge \underset{\sim}{v} + \nabla\left(\frac{\delta p}{\rho}\right) - g\,\delta\phi\,\underset{\sim}{k} = 0 \qquad \text{———(4.6)}$$

where the vorticity $\underset{\sim}{\zeta}$ is defined by

$$\underset{\sim}{\zeta} = \left(\frac{\partial v_m}{\partial n} - \frac{\partial v_n}{\partial m}\right)\underset{\sim}{l} + \left(\frac{\partial v_n}{\partial l} - \frac{\partial v_l}{\partial m}\right)\underset{\sim}{m} + \left(\frac{\partial v_l}{\partial m} - \frac{\partial v_m}{\partial l}\right)\underset{\sim}{n} \qquad \text{———(4.7)}$$

The $\underset{\sim}{n}$-component of Eq.(4.6) is

$$\frac{\partial v_n}{\partial t} + \frac{\partial}{\partial n}\left(\frac{1}{2}\underset{\sim}{v}^2\right) + v_l\left(\frac{\partial v_n}{\partial l} - \frac{\partial v_l}{\partial n}\right) + \frac{\partial}{\partial n}\left(\frac{\delta p}{\rho}\right) - g\,\delta\phi\cos\alpha = 0 \qquad \text{———(4.8)}$$

so in steady state, where α is the angle between the $\underset{\sim}{k}$ and $\underset{\sim}{n}$ axes,

$$\frac{\partial}{\partial n}\left(\frac{1}{2}v_n^2 + \frac{\delta p}{\rho}\right) + v_l\frac{\partial v_n}{\partial l} - g\,\delta\phi\cos\alpha = 0 \qquad \text{———(4.9)}$$

Define $r = \frac{1}{v_l}\frac{\partial v_n}{\partial l}$, then r is a measure of the radius of curvature of the streamlines relative to the interface. Integrating across the boundary layer from Δn_1 to Δn_2, in general functions of l, (where subscripts [1] and [2] denote updraught and downdraught variables respectively) the following is obtained

$$\left[\frac{1}{2}v_n^2 + \frac{\delta p}{\rho}\right]_{-\Delta n_2}^{\Delta n_1} = \int_{-\Delta n_2}^{\Delta n_1} g\,\delta\phi\cos\alpha\,dn - \int_{-\Delta n_2}^{\Delta n_1}\frac{v_l^2}{r}\,dn \qquad \text{———(4.10)}$$

The first term on the R.H.S. of Eq.(4.10) is directly related to $\Delta n = \Delta n_1 + \Delta n_2$ and to the temperature difference across the boundary layer, while the second is a measure of the effect of centrifugal accelerations on the pressure field.

At this stage, a distinction must be made between having a <u>real</u> discontinuity in the variables of the physical problem (which is not the case here) and <u>modelling</u> a rapid change over a small distance (which is the object of this exercise). In (subsonic) atmospheric motion, real discontinuities in the temperature, velocity or pressure fields do not persist; for instance a discontinuity in the velocity field would be dynamically unstable according to the summary of chapter I. Consequently, real discontinuities are only of academic interest here, but it is interesting to note that if $\delta\phi$ is finite, a real pressure discontinuity can persist if

$$\left[\frac{\delta p}{\rho} + \frac{1}{2}v_n^2\right]_-^+ + \lim_{\Delta n\to 0}\int_{-\Delta n_2}^{\Delta n_1}\frac{v_l^2}{r}\,dn = 0 \qquad \text{———(4.11)}$$

That is if the limiting normal component of the velocity is different on each side of the interface and/or there exist unbounded centrifugal accelerations at the interface, a possible feature of corner regions. If these do not exist then the pressure must be continuous at the interface.

However, rapid changes over small distances are common in the atmosphere, not only in this cumulonimbus problem but also, for example, in frontal regions, temperature inversions

and jet streams. The rapid change observed in the updraught/downdraught boundary layer of severe storms is, in this chapter, modelled by the boundary condition continuity of pressure at the interface; this condition implies interfacial discontinuities of velocity, vorticity and temperature.

It is convenient in practice to reformulate this boundary condition in terms of kinematic quantities. For this purpose the Bernoulli Equation is used in the form:

$$\frac{1}{2}\underset{\sim}{v}^2 + \frac{\delta p}{\rho} - \int_{z_o}^{z} g\,\delta\phi\,dz = \text{function of } \psi \text{ only} \qquad \text{——(4.12)}$$

Applying this equation to limiting streamlines in the updraught and downdraught branches of flow with the usual subscript notation,

$$\left[\frac{\delta p}{\rho}\right]_2^1 = -\left[\frac{1}{2}\underset{\sim}{v}^2\right]_2^1 + \int_{z_{o1}}^{z} g\,\delta\phi_1\,dz - \int_{z_{o2}}^{z} g\,\delta\phi_2\,dz + f_1(\psi) - f_2(\psi)$$

where $f_1(\psi) = \frac{1}{2}u_{o1}^2 + \frac{\delta p}{\rho}$; $f_2(\psi) = \frac{1}{2}u_{o2}^2 + \frac{\delta p}{\rho}$ are functions of the inflow, and identical if the flow is antisymmetric around $z = H/2$. For the antisymmetric problem considered here it is convenient to let $z_{o1} = z_{o2} = H/2$, in which case

$$\left[\frac{\delta p}{\rho}\right]_2^1 = -\left[\frac{1}{2}v^2\right]_2^1 + \int_{H/2}^{z} g(\delta\phi_1 - \delta\phi_2)dz \qquad \text{——(4.13)}$$

Since for the cases studied in this chapter the pressure is continuous,

$$\left[\frac{1}{2}\underset{\sim}{v}^2\right]_2^1 = \int_{H/2}^{z} g(\delta\phi_1 - \delta\phi_2)dz \qquad \text{——(4.14)}$$

Therefore in kinematic terms, continuity of pressure expresses a balance between the change in the kinetic energy and the change

in the available potential energy across the interface. The analysis of this chapter distinguishes two distinct cases. First, where the temperature is continuous at the interface, Eq.(4.14) shows that the boundary condition to use in practice is continuity of speed. Second, where the log-potential temperature has a discontinuity of magnitude $(\gamma - B)H$ at the interface, Eq.(4.14) becomes

$$\left[\frac{1}{2}\underset{\sim}{v}^2\right]_2^1 = gH(\gamma - B)(z - H/2) \qquad \text{——(4.15)}$$

4.4.1 — THE EFFECT OF NEGATIVE VORTICITY GENERATION IN THE INTERFACE REGION ON THE REMOTE FLOW

The question posed in this section is - under which conditions can the temperature gradient and hence the vorticity gradient be increased in the interfacial boundary layer (by making it narrower) and still maintain steady overturning? It will be shown that it is not always possible to have a discontinuity of temperature at the interface, a limit being set by the size of the Richardson Number.

Negative vorticity generated in the interface region has the effect of decreasing the fluid speed in the neighbourhood of the interface and the outflow speed in a boundary layer. This section will be devoted to examining this effect on the flow remote from the storm. Since the kinematic boundary conditions on the steady flow demand that the outflow speed must be positive for $z > z_*$, for each value of R (defining the flow in the main part of the region) and for each temperature gradient across the interfacial boundary layer (a measure of the negative vorticity generation) there exists a spectrum of boundary layer thicknesses

defining possible outflows. One limiting case was investigated by Green (1962) and this will be considered in greater detail in this section to examine the validity of a boundary condition with a discontinuity of temperature.

The effect of negative vorticity on the remote flow field is represented by a model with the undisturbed log-potential temperature shown in Fig.(4.5), with static stability $b = B$ for $0 \leqslant z \leqslant H$ and $b = \frac{T}{\delta}$ for $-\delta \leqslant z_o < 0$, where T is the temperature difference across the interfacial boundary layer. Constant parcel lapse γ and constant undisturbed shear is assumed, to enable the results of section 3.2.1 to be used in the region $0 \leqslant z \leqslant H$, while in the region $H \leqslant z \leqslant D_\delta$ additional analysis is imposed. For this region

$$F(\psi, z - z_o) = \phi(x=\infty, z=0) + (\gamma - \frac{T}{\delta}) z_o + \gamma z \qquad \text{———(4.16)}$$

giving

$$\left(\frac{\partial F}{\partial \psi}\right)_z = (\gamma - \frac{T}{\delta}) \,/\, 2A(z_* - z_o) \qquad \text{———(4.17)}$$

Substitute Eq.(4.17) into Eq.(3.1) and obtain

$$\frac{\partial^2 \psi}{\partial z^2} \sim 2A + \frac{g(\gamma - T/\delta)}{2A} \left\{ 1 + \frac{z - z_*}{\sqrt{\psi/A}} \right\} \qquad \text{———(4.18)}$$

to define the outflow in $H \leqslant z \leqslant D_\delta$ in terms of the nondimensional number $R_B = \frac{g(\gamma - T/\delta)}{4A^2}$, of the form of a boundary layer Richardson Number. From Eq.(4.18) the ψ distribution can be constructed for $H \leqslant z \leqslant D_\delta$, given the following boundary conditions, obtained (in terms of R) from the solution in $0 \leqslant z \leqslant H$ and continuity of ψ and velocity at $z = H$.

$$\psi \sim A z_*^2$$

$$\frac{\partial \psi}{\partial z} \sim 2A\beta^2 (H - z)$$

Incidentally, in contrast to Eq.(3.6) at $z = z_*$, Eq.(4.18) is nonsingular at $z = H$, so there is no difficulty in obtaining second order starting values for ψ.

The length δ is implicit in this solution, but since by definition, δ and D_δ lie on the same streamline $\psi(x=\infty, z=D_\delta)$, it can be found explicitly by solving

$$\psi(x=\infty, z=D_\delta) = A(z - z_*)^2$$

$$\therefore \quad \delta = z_* \pm \sqrt{\psi(x=\infty, z=D_\delta)}/A \qquad \text{——(4.19)}$$

If for a given R, $-R_B$ is sufficiently large (i.e. a sufficiently steep temperature gradient across the boundary layer) so that the vorticity is negative in $H \leqslant z \leqslant D_\delta$, then for some $z = D$ the outflow speed becomes negative and consequently $D - H$ defines the maximum outflow thickness of the boundary layer. The corresponding maximum inflow thickness (δ_{max}) can of course be found by solving Eq.(4.19) with $D_\delta = D$.

For given values of the parameter R in the 'unmixed' layer $0 \leqslant z \leqslant H$, the continuous lines on Fig.(4.6) define the critical fractional length $\delta_{max}/(D + \delta_{max})$ as a function of $R_B \delta_{max}/(D + \delta_{max})$. This diagram shows that for given values of R and R_B, only values of δ satisfying $\delta \leqslant \delta_{max}$ are permissible in steady, two-dimensional overturning. For given R, the broken lines on this diagram show the fractional length δ as a function of $R_B\, \delta/D$ as defined in the model with the continuous temperature distribution at the interface (in which case $R_B = R\left(\frac{1}{2} - \frac{D_\delta}{2\delta}\right)$). It can be seen from this figure that if in this model $R \leqslant 1$, steady two-dimensional overturning can exist for all lengths δ ranging from δ_{max} down to infinitesimal values; that is, it is permissible to model a steep gradient of temperature by a temperature discontinuity

FIG. 4.6 — THE LIMIT ON STEADY, TWO-DIMENSIONAL OVERTURNING DETERMINED BY THE EFFECT OF NEGATIVE VORTICITY GENERATION IN THE INTERFACE REGION ON THE REMOTE FLOW.

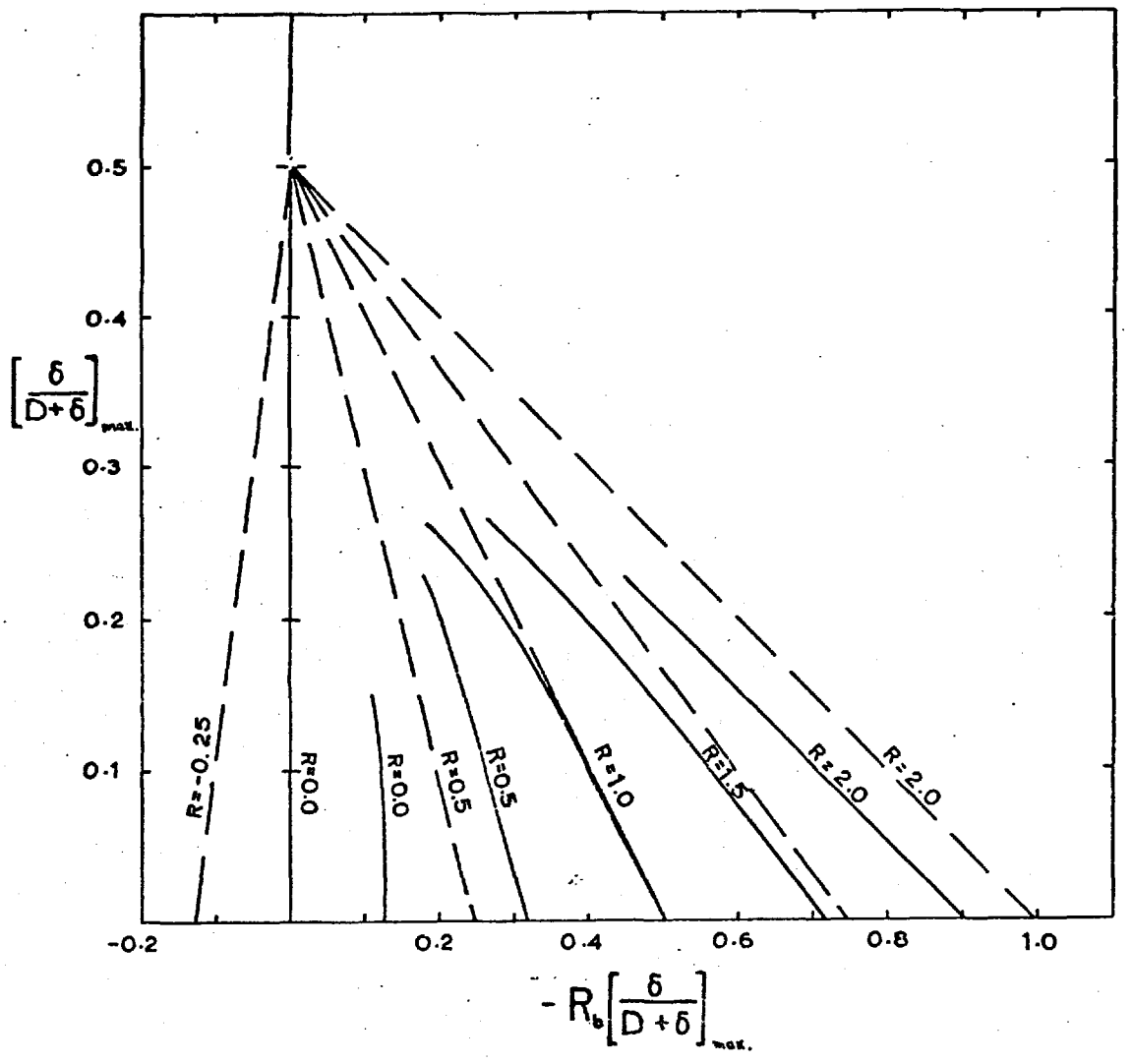

(a) The continuous lines define the maximum possible value of $\delta/(D+\delta)$ as a function of $R_b\delta/(D+\delta)$, a number proportional to the temperature difference across the interfacial boundary layer, in isopleths of R.

(b) The broken lines define the value of ε/H as a function of $R_b\varepsilon/H$ for the particular model of section 4.4-1. The equation of these lines is $R_b\varepsilon/H = R(1 - H/2\varepsilon)$.

(c) The critical value of the Richardson Number for steady, two-dimensional overturning can be seen to be $Ri = -1.62$ (i.e. $R = 1.0$)

for this range of R and still maintain steady two-dimensional overturning. It is difficult to imagine that the origin of δ or the precise details of the distribution of temperature across the interface are crucial, so the conclusion is that steady two-dimensional overturning is only possible if $-0.25 \leqslant R \leqslant 1$, the lower limit being obtained from Eq.(3.10). If $R > 1$ or $R < -0.25$, the flow is presumably not steady or not two-dimensional. Since the Richardson Number is more physically acceptable than R this limit is given alternatively by $-1.62 \leqslant Ri \leqslant 0.75$.

4.4.2 — THE EFFECT OF NEGATIVE VORTICITY GENERATION IN THE INTERFACE REGION ON THE DETAILED OVERTURNING (VELOCITY DISCONTINUOUS AT INTERFACE)

In this section, detailed two-dimensional solutions are found for the model with a continuous pressure and temperature distribution and a discontinuous velocity field at the interface, and the effect of the negative vorticity production in the neighbourhood of the interface deduced from the solutions.

The free-boundary problem to be solved in this section is

$$\frac{\partial^2\psi}{\partial x^2} + \frac{\partial^2\psi}{\partial z^2} = \begin{cases} 2A + \dfrac{g(\gamma - B)}{2A}\left(\dfrac{z - z_o}{z_* - z_o}\right) & 0 \leqslant z_o \leqslant \epsilon \\ 2A + \dfrac{g(\gamma - B)}{2A}\left(1 - \dfrac{H}{2\epsilon}\right)\left(\dfrac{z - z_o}{z_* - z_o}\right) & \epsilon \leqslant z_o \leqslant z_* \end{cases} \qquad \text{——(4.20)}$$

where ϵ/H is a specified fractional inflow depth of the interfacial boundary layer, and is related to the length δ of the last section by $\epsilon/H = \delta/(D_\delta + \delta)$, (the difference between ϵ and δ is only one of scale). z_o is defined by $z_o = z_* - \sqrt{\psi/A}$. The kinematic boundary conditions are those given in section 4.2, with the inflow/outflow conditions being obtained by scaling the asymptotic solutions of section 4.4.1, and continuity of pressure is the

dynamic boundary condition at the interface.

This free-boundary problem was solved numerically for various values of R and $R_B = R\left(1 - \frac{H}{2\epsilon}\right)$. A selection of solutions are shown in Figs.(4.7 - 4.9).

From these solutions, as the temperature gradient across the interfacial is increased, the interface is progressively more tilted into the updraught. This behaviour may be visualised as follows: In the updraught boundary layer, a particle tends to be retarded by the effect of negative vorticity as it ascends, but the dynamic boundary condition (continuity of pressure) in effect demands continuity of speed, so the interface has to be tilted into the updraught squashing the streamlines closer together i.e. generating a local pressure field to accelerate the fluid to counteract the slowing due to the negative vorticity, and thereby satisfy the boundary conditions.

4.4.3 — VELOCITY AND TEMPERATURE DISCONTINUOUS AT THE INTERFACE

It was shown in section 4.4.1 that the finite vorticity generation in a boundary layer across which there is a finite gradient of temperature can be validly modelled by a temperature discontinuity, at least if $-1.62 \leqslant Ri \leqslant 0.75$. In this section therefore, detailed solutions are obtained for the model with a continuous pressure field but with the velocity and temperature fields discontinuous at the interface. That is, the free-boundary problem defined by the partial differential equation,

$$\frac{\partial^2\psi}{\partial x^2} + \frac{\partial^2\psi}{\partial z^2} = 2A + \frac{g(\gamma - B)}{2A}\left(\frac{z - z_o}{z_* - z_o}\right) \qquad \text{———(4.21)}$$

together with the kinematic and dynamic boundary conditions of the previous section, except that the inflow/outflow boundary condition is in this case given by the asymptotic solution of section 3.2.1.

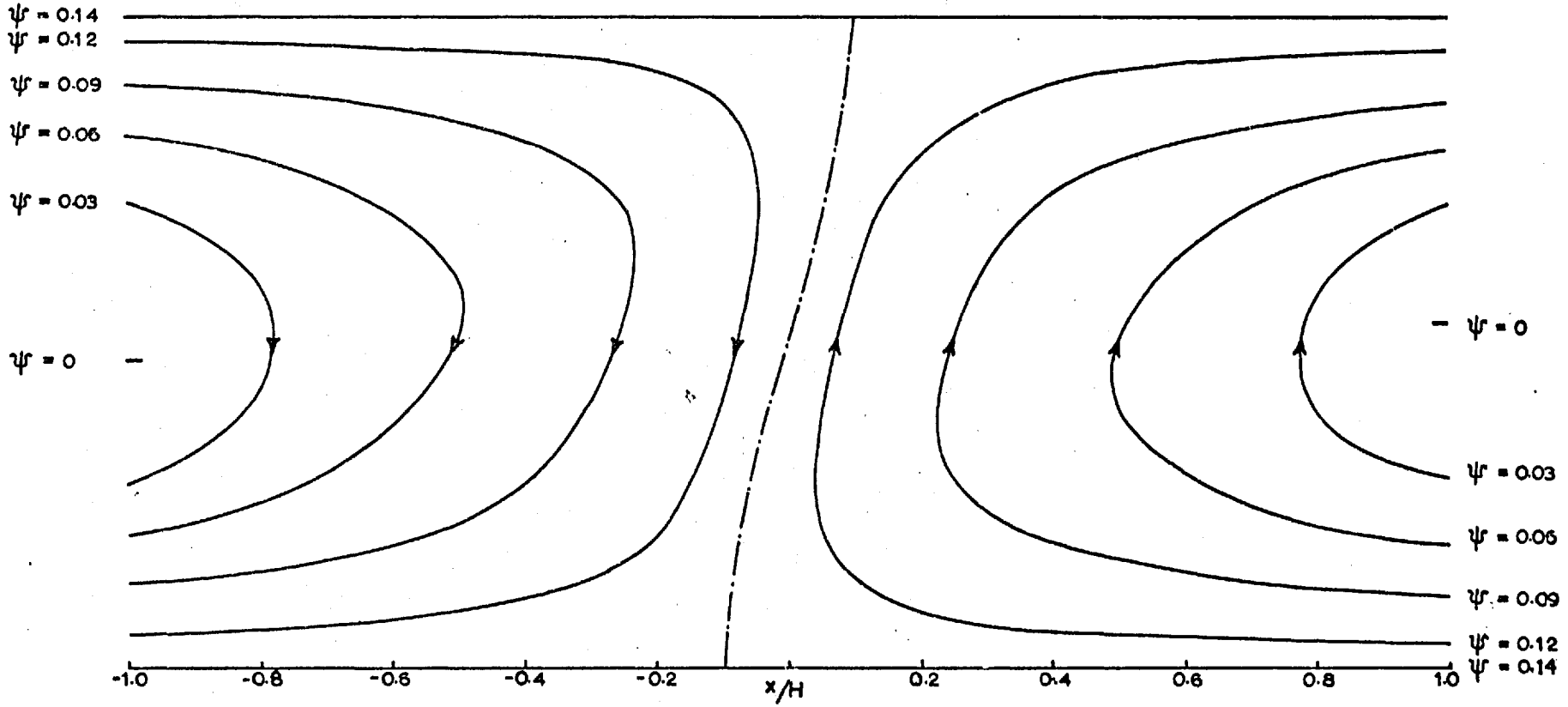

FIG. 4.7 — SOLUTION TO FREE-BOUNDARY PROBLEM WITH VELOCITY DISCONTINUOUS BUT TEMPERATURE & PRESSURE CONTINUOUS AT THE INTERFACE FOR Ri = -0.94 (R = 0.5) AND R_b = -0.33 (ε = 0.3H). THE POSITION OF THE FREE-BOUNDARY IS SHOWN BY THE BROKEN LINE.

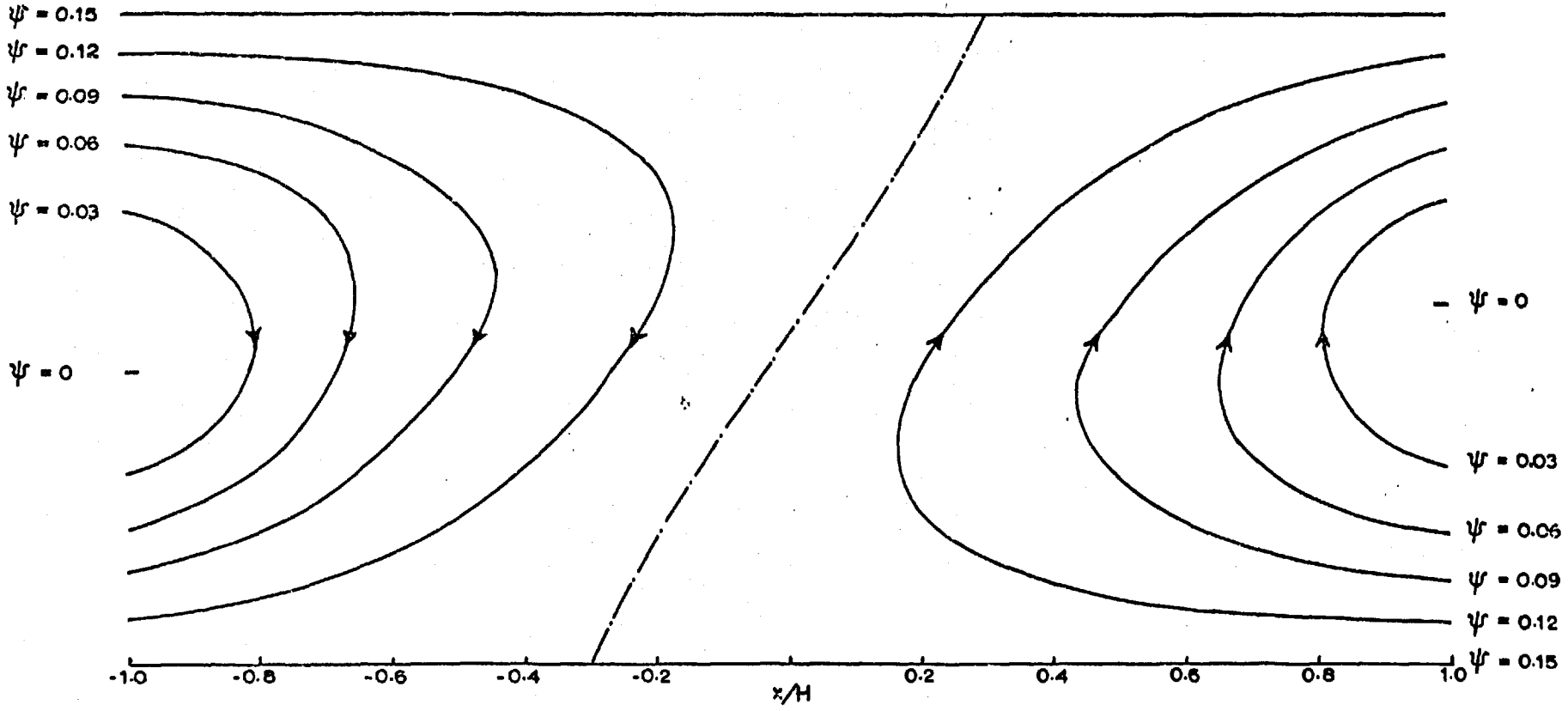

FIG. 4.8 — SOLUTION TO FREE-BOUNDARY PROBLEM WITH VELOCITY DISCONTINUOUS BUT TEMPERATURE & PRESSURE CONTINUOUS AT THE INTERFACE FOR Ri = -0.91 (R = 0.5) AND R_b = -0.75 (ε = 0.2H). THE POSITION OF THE FREE-BOUNDARY IS SHOWN BY THE BROKEN LINE.

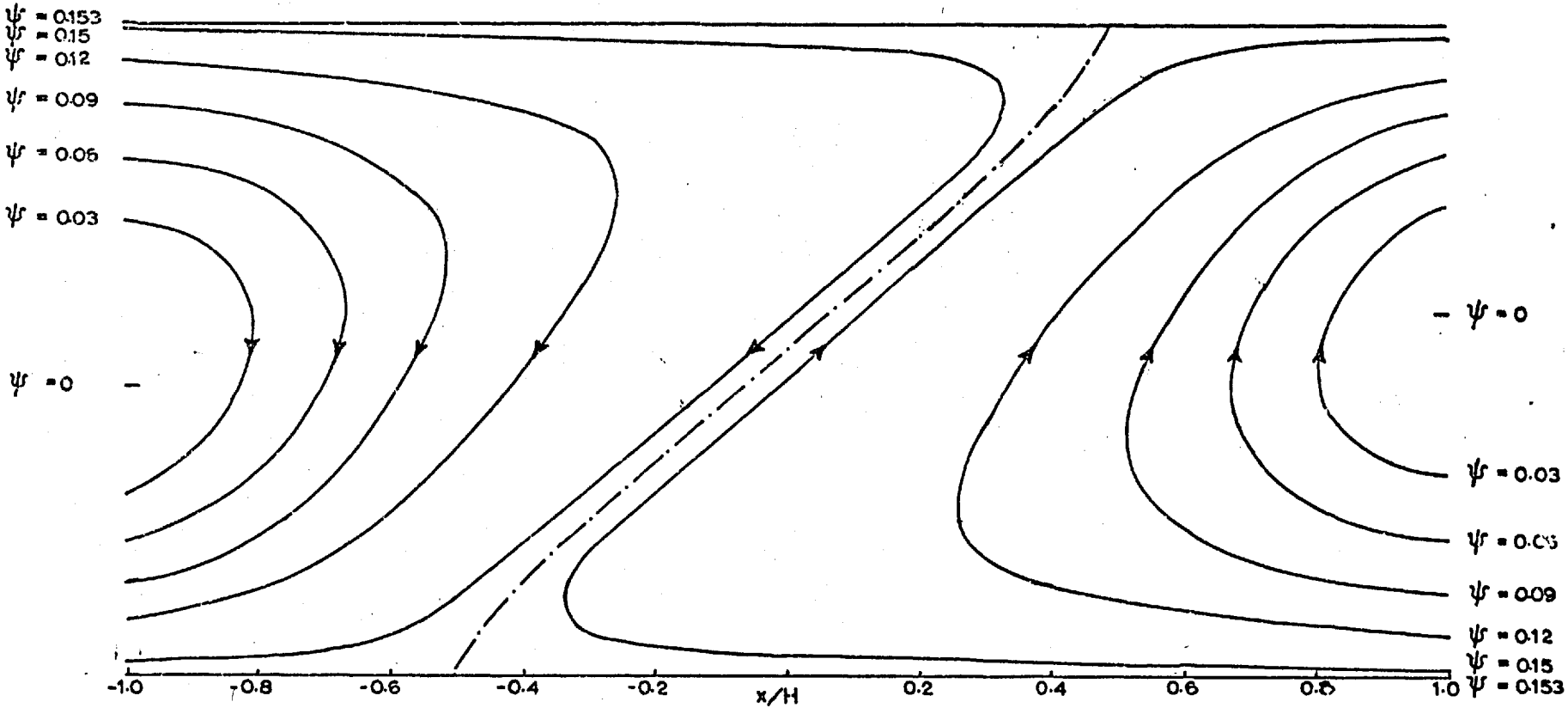

FIG. 4.9 — SOLUTION TO FREE-BOUNDARY PROBLEM WITH VELOCITY DISCONTINUOUS BUT TEMPERATURE & PRESSURE CONTINUOUS AT THE INTERFACE FOR $Ri = -0.9$ ($R = 0.5$) AND $R_t = -2.0$ ($\varepsilon = 0.1H$). THE POSITION OF THE FREE-BOUNDARY IS SHOWN BY THE BROKEN LINE.

The solutions to this problem for representative values of the nondimensional number R are given in Figs.(4.10-4.14). From these solutions, if $R > 0$ (i.e. buoyant overturning with a release of potential energy) the flow is orientated with the updraught lying below the downdraught, the angle of tilt increasing with R. For negative R with $-0.25 \leqslant R \leqslant 0$, (i.e. overturning generating potential energy), the orientation is in the opposite sense with the updraught sloping over the downdraught. A more detailed discussion of the implications will be given in the following section.

4.5 — CONCLUSIONS ON THE DISCONTINUOUS MODELS OF CHAPTER IV

Assisted by the solutions of the previous section, it is possible to prove a necessary condition for the existence of a solution to the free-boundary problem considered in that section. Since continuity of pressure at the interface demands that the kinetic energy change across the interface is equal to $gH(\gamma - B)(z - H/2)$, and from the solutions in Figs.(4.10-4.14), $z = H$ is a stagnation point for the downdraught at the interface, the condition to be satisfied at $z = H$ on the updraught side of the interface must be

$$|\underset{\sim}{v}| = \sqrt{g(\gamma - B)}\, H \qquad \text{——(4.2?)}$$

The asymptotic outflow speed at $z = H$ is

$$|\underset{\sim}{v}| \sim 2A \frac{\beta^2}{1+\beta} H , \qquad \text{——(4.23)}$$

and so from the form of the solutions it is readily seen that a solution to the free-boundary problem can exist only if:

$$\sqrt{g(\gamma - B)} \leqslant 2A \frac{\beta^2}{1+\beta} \qquad \text{——(4.24)}$$

i.e. only if $$R^{1/2} \leqslant \frac{\beta^2}{1+\beta} \qquad \text{——(4.25)}$$

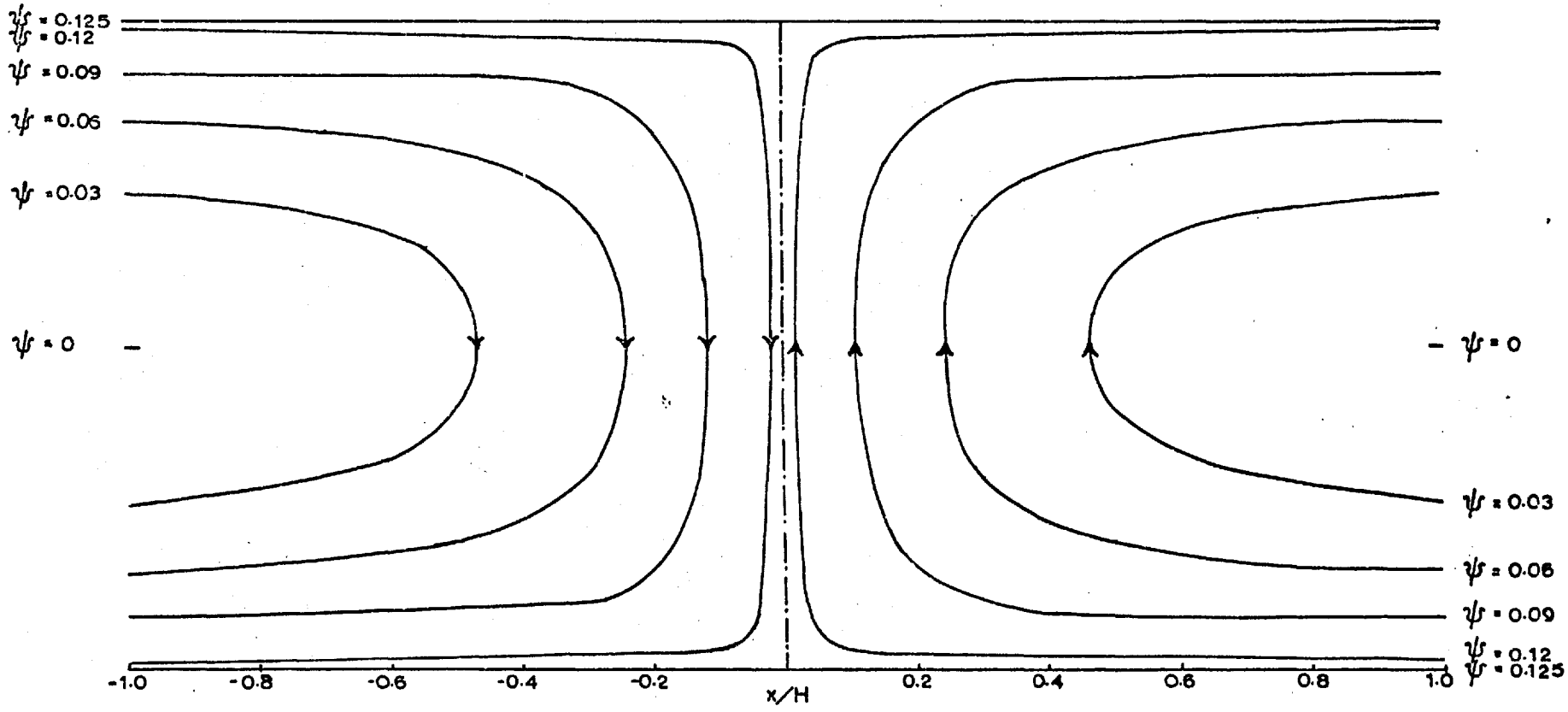

FIG. 4.10 — SOLUTION TO FREE-BOUNDARY PROBLEM WITH VELOCITY & TEMPERATURE DISCONTINUOUS BUT PRESSURE CONTINUOUS AT THE INTERFACE FOR Ri = 0 (R = 0). THE FREE-BOUNDARY IS SHOWN BY THE BROKEN LINE.

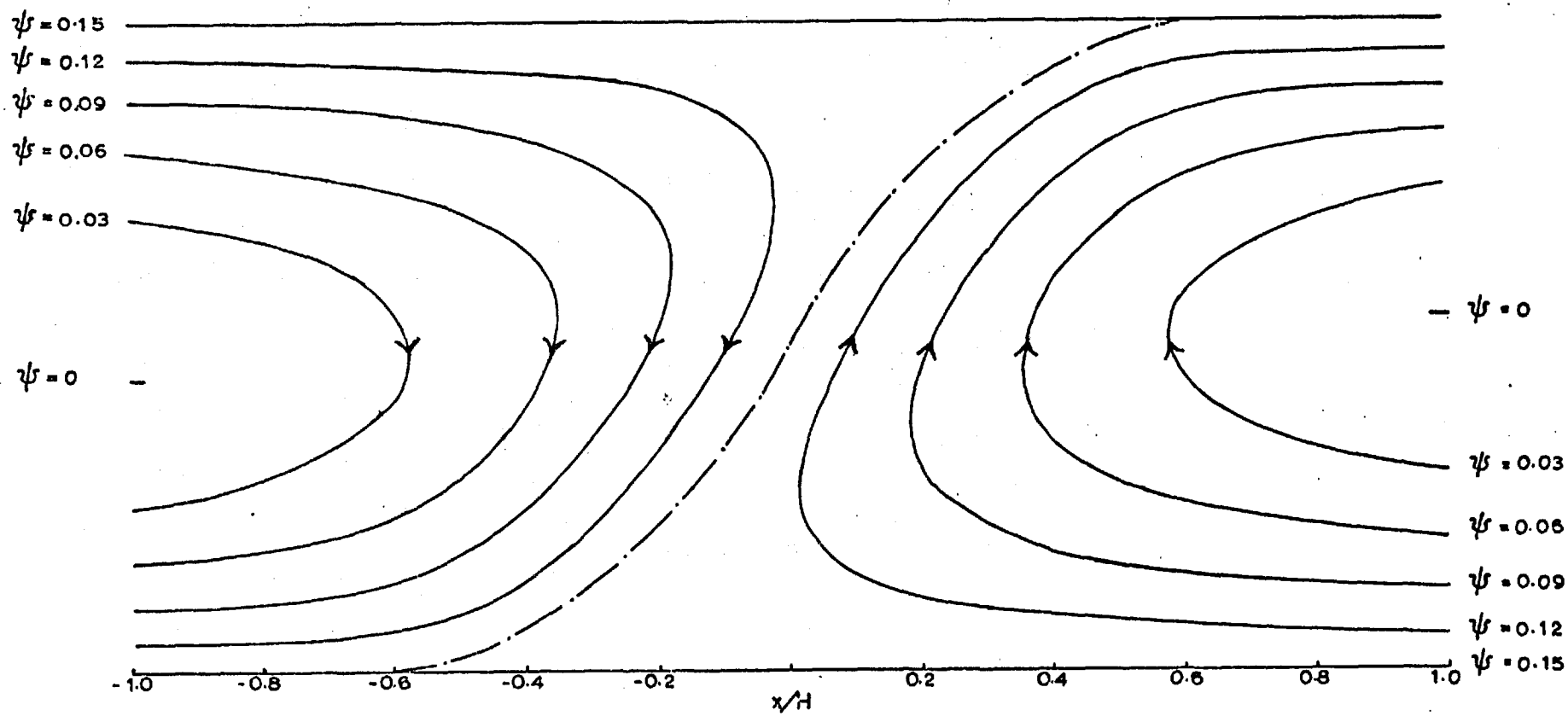

FIG. 4.11 — SOLUTION TO FREE-BOUNDARY PROBLEM WITH VELOCITY & TEMPERATURE DISCONTINUOUS BUT PRESSURE CONTINUOUS AT THE INTERFACE FOR Ri = -0.55 (R=0.25). THE FREE-BOUNDARY IS SHOWN BY THE BROKEN LINE.

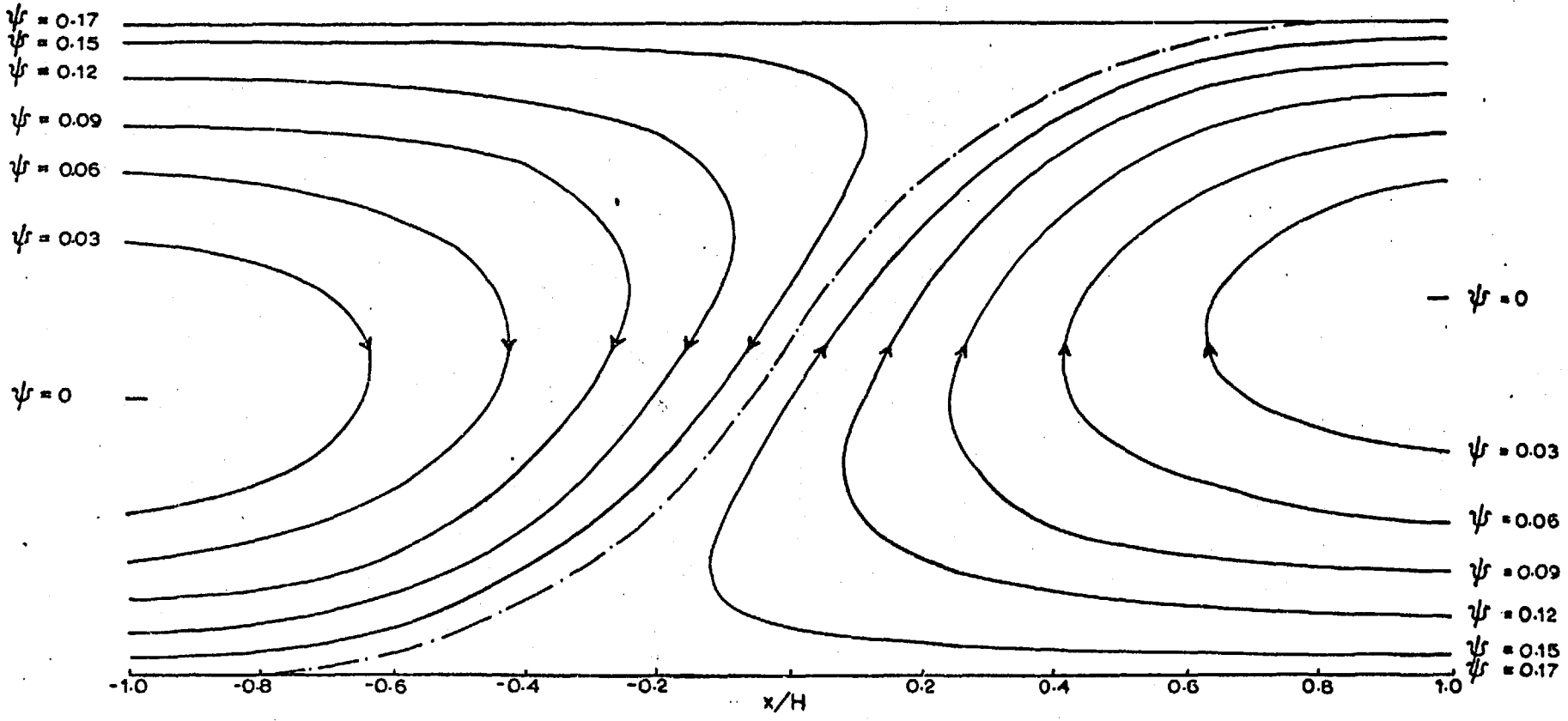

FIG. 4.12 — SOLUTION TO FREE-BOUNDARY PROBLEM WITH VELOCITY & TEMPERATURE DISCONTINUOUS BUT PRESSURE CONTINUOUS AT THE INTERFACE FOR Ri = -0.87 (R = 0.5). THE FREE-BOUNDARY IS SHOWN BY THE BROKEN LINE.

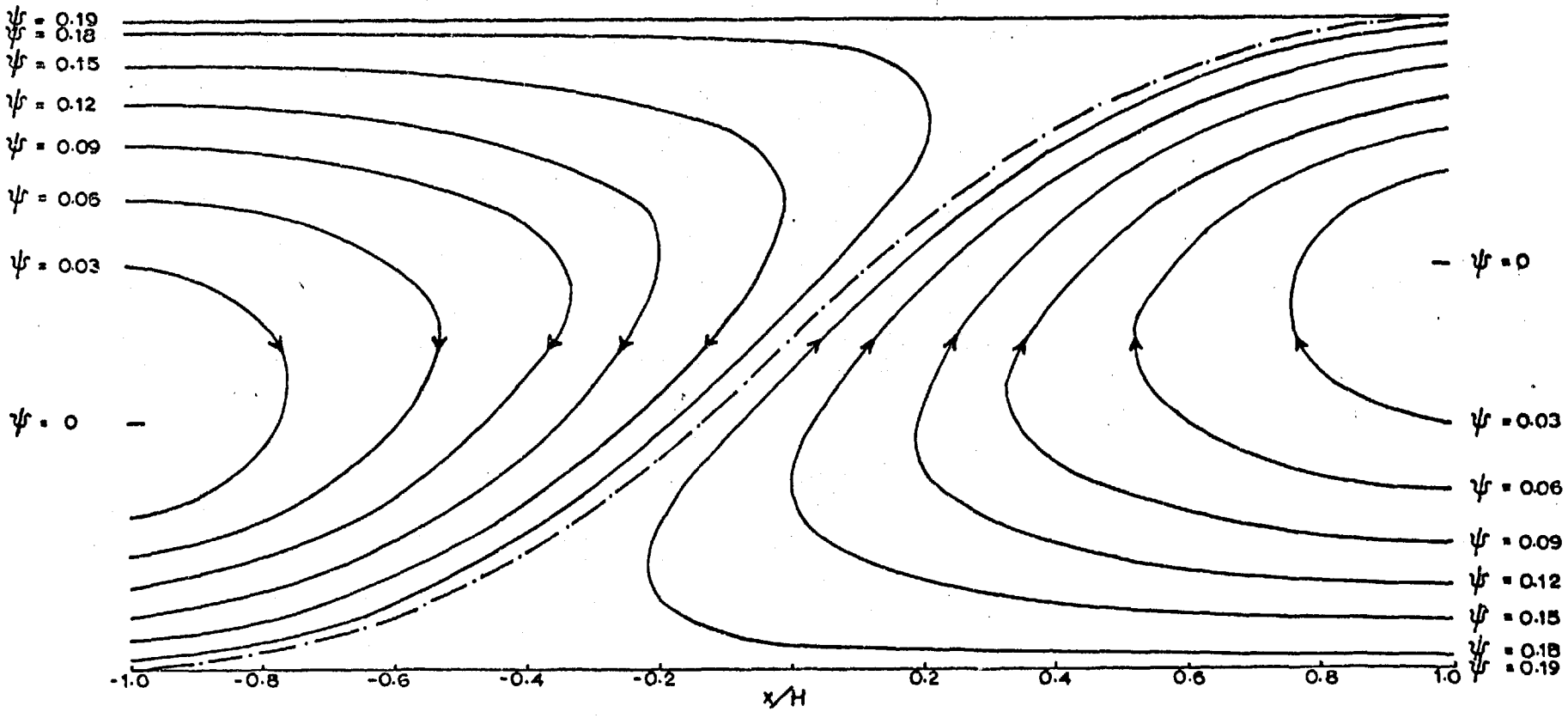

FIG. 4.13 — SOLUTION TO FREE-BOUNDARY PROBLEM WITH VELOCITY & TEMPERATURE DISCONTINUOUS BUT PRESSURE CONTINUOUS AT THE INTERFACE FOR Ri = -1.62 (R = 1). THE FREE-BOUNDARY IS SHOWN BY THE BROKEN LINE.

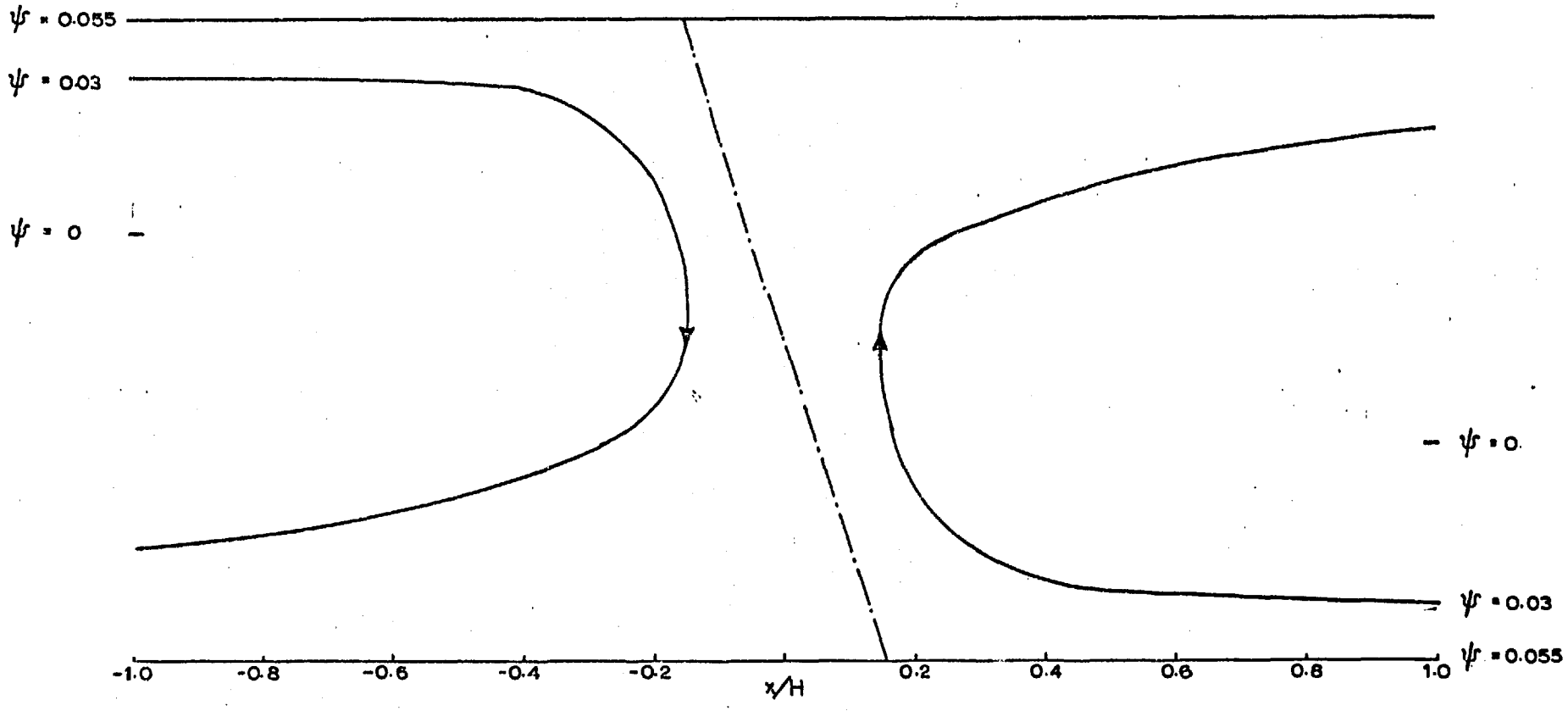

FIG. 4.14 — SOLUTION TO FREE-BOUNDARY PROBLEM WITH VELOCITY & TEMPERATURE DISCONTINUOUS BUT PRESSURE CONTINUOUS AT THE INTERFACE FOR Ri = 0.75 (R = -0.25). THE FREE-BOUNDARY IS SHOWN BY THE BROKEN LINE.

A little algebra shows that the limit on R from the existence of a solution to the free-boundary is defined by the solution of

$$R^{\frac{1}{2}} = \frac{1 + 2R + (1 + 4R)^{\frac{1}{2}}}{3 + (1 + 4R)^{\frac{1}{2}}} \qquad \text{——(4.26)}$$

It can be shown that $R = 1$ defines this upper limit, with the result that a necessary condition for the existence of a solution to the free-boundary problem of the last section is $-0.25 \leqslant R \leqslant 1$. It follows that $R = 1$ defines an upper limit to steady, two-dimensional overturning, a condition obtained independently in section 4.4.1.

Comparing the model solutions of sections 4.4.2 and 4.4.3, it is clear that the presence of a finite generation of negative vorticity in the interface region, (through a continuous temperature distribution) does not alter the general orientation of the flow within the storm - the updraught lies under the downdraught in both models. This verifies the generalisation from the asymptotic argument of section 4.4.1, where it was concluded that a rapid change of temperature (and hence vorticity) could validly be modelled by a temperature discontinuity (a vorticity generating sheet).

The results so far suggest that this orientation of the flow with the updraught/downdraught boundary sloping downshear is a feature of steady, two-dimensional, wet-adiabatic flow of Richardson Number satisfying $-1.62 \leqslant Ri \leqslant 0.75$. However, before being committed to this conclusion, it is necessary to ensure that a discontinuity of velocity at the interface is a valid way of modelling the shear across the interfacial boundary layer, and also to examine if in fact continuity of pressure is, in general, an adequate dynamic boundary condition to model

the interfacial boundary layer in the two-dimensional, steady convection at present being studied.

With these problems in mind, the next chapter deals with initial value problems in which flow fields are generated by given sources and sinks of heat, with steady-state solutions being of particular interest for comparison with the discontinuous models of this chapter.

CHAPTER V — TWO-DIMENSIONAL CONTINUOUS MODELS

The updraught/downdraught boundary layer examined in the first part of this chapter is distinct from that of the previous models in that the velocity, temperature and vorticity are all continuous. It is interesting to examine the effect of different sources and sinks of heat on the orientation of the flow, and in order to model the updraught/downdraught boundary layer, the solutions are used to define an alternative dynamic boundary condition to continuity of pressure. This new boundary condition implies a discontinuity of velocity, temperature, vorticity and pressure at the interface, and models a physical process in the boundary layer - cooling of the low-level and warming of the high-level inflow air in this region. It is used in one of the free-boundary models of the last chapter and the solution compared to that of the continuous models.

5.1 — THE GROWTH OF SMALL-AMPLITUDE DISTURBANCES IN UNSTABLY STRATIFIED SHEAR FLOW

The convective overturning in its steady-state form is essentially of finite amplitude since the vertical displacement of particles is comparable to the height scale of the system. Nevertheless during its initial development from the undisturbed condition, the motion must be of small amplitude and hence the linearised theory applicable.

The following set of equations,

$$\frac{D\eta}{Dt} + \eta \operatorname{div} \underset{\sim}{v} + g\frac{\partial(\delta\phi)}{\partial x} = 0 \qquad \text{——(5.1)}$$

$$\operatorname{div}(\rho \underset{\sim}{v}) = 0 \qquad \text{——(5.2)}$$

$$\frac{D(\delta\phi)}{Dt} = w(\Gamma' - B) \qquad \text{where } \Gamma > B\,, \qquad \text{——(5.3)}$$

is linearised in the classical way by introducing small perturbations on the undisturbed, horizontal flow, and ignoring variations in the y-direction. Since Eq.(5.2) allows the definition of a streamfunction in the form,

$$\rho u = \frac{\partial \psi}{\partial z} \quad ; \quad \rho w = -\frac{\partial \psi}{\partial x} \qquad \text{——(5.4)}$$

it is convenient to linearise the equations with respect to

$$\psi = \psi_o + \text{Real part of } \left\{ h(z) \exp i(\lambda x - at) \right\} \qquad \text{——(5.5)}$$

$$\phi = (\Gamma - B)z + \text{Real part of } \left\{ g(z) \exp i(\lambda x - at) \right\} \qquad \text{——(5.6)}$$

Substituting Eqs.(5.5, 5.6) into Eqs.(5.1 - 5.3) and ignoring second-order terms, the following equations for h(z) and g(z) are obtained:

$$\frac{d^2h}{dz^2} - \frac{1}{H_o}\frac{dh}{dz} - \left\{ \frac{\frac{d\eta_o}{dz} + \frac{\eta_o}{H_o}}{u_o - \sigma/\lambda} + \frac{g(\Gamma - B)}{(u_o - \sigma/\lambda)^2} + \lambda^2 \right\} h = 0 \qquad \text{——(5.7)}$$

$$g(z) = \frac{(\Gamma - B)\, h}{(u_o - \sigma/\lambda)} \qquad \text{——(5.8)}$$

Using the transformation

$$h(z) = \omega(z) \exp\left(\frac{z}{2H_o}\right) \qquad \text{——(5.9)}$$

Eq.(5.7) can be written as

$$\frac{d^2\omega}{dz^2} - \left\{ \frac{\left(\frac{d\eta_o}{dz} + \frac{\eta_o}{H_o}\right)}{u_o - \sigma/\lambda} + \frac{g(\Gamma - B)}{(u_o - \sigma/\lambda)^2} + \lambda^2 + \frac{1}{4H_o^2} \right\} \omega = 0 \qquad \text{——(5.10)}$$

This equation for the amplitude of the perturbation appears extensively in the linearised theory of mountain waves, cyclone waves etc. As in the previous analysis let the undisturbed shear η_o be constant and equal to 2A, and $u_o = 2A(z - H/2)$ making flow stationary with respect to $z = H/2$.

$$\therefore \quad \frac{d^2\omega}{dz^2} - \left\{ \frac{1}{H_o(z - H/2 - \sigma/2A)} + \frac{g(\Gamma - B)}{4A^2(z - H/2 - \sigma/2A\lambda)^2} + \lambda^2 + \frac{1}{4H_o^2} \right\} \omega = 0$$

$$\text{——(5.11)}$$

Eq.(5.11) is a confluent hypergeometric equation, and thus $\omega(z)$ is given in terms of Whittaker Functions, in general of complicated series form. If however, the incompressible form of Eq.(5.11) (obtained by setting $H/H_o = 0$) is taken, considerable simplification results, because using the substitution

$$S = \lambda z - \lambda H/2 - \sigma/2A$$

Eq.(5.11) reduces to

$$\frac{d^2\omega}{dS^2} - \left\{1 + \frac{R}{S^2}\right\}\omega = 0 \qquad \text{——(5.12)}$$

General solutions to Eq.(5.12) exist in the form

$$\omega = S^{1/2}[A I_n(S) + B K_n(S)]$$

where in classical notation $I_n(S)$ and $K_n(S)$ are Bessel Functions of order $n = (1/4 + R)^{1/2}$ and imaginary argument. The constants A and B can of course be evaluated using boundary conditions at S_o and S_1. The condition for non-zero solutions of Eq.(5.12) is given by the characteristic equation

$$C(S_o, S_1) = I_n(S_o)\, K_n(S_1) - I_n(S_1)\, K_n(S_o) = 0 , \qquad \text{——(5.13)}$$

the roots of which give the amplification rate σ and the phase-velocity $c = \sigma/\lambda$ in terms of the wavenumber λ and R. These solutions can be obtained fairly easily in closed form if $n = N + \frac{1}{2}$, where N is an integer, but otherwise solutions are difficult to obtain. Some solutions of the characteristic equation for nonintegral values of N have been found by Kuo (1963). Green (1962) obtained solutions for $N = 1$, with boundary conditions $W = 0$ at $S_o = -\lambda H/2 - \sigma/2A$ and $S_1 = \lambda H/2 - \sigma/2A$ ($z = 0$ and $z = H$ respectively). He found that the fastest growing wave is that of wavenumber $\lambda H = 1.61$

with an amplification rate of $\sigma/2A = 0.155$. This solution indicates an orientation of the temperature extremes with a slope of about 45° with the warm air above the cold. However, since the value of $R = 2$, corresponding to $N = 1$ is outside the range considered in the previous two-dimensional solutions, and in any case the results of the linearised analysis cannot be expected to be directly applicable to the finite amplitude state (especially considering the findings of section 3.2.2) it is not possible to obtain any reliable conclusion about the orientation of the flow in the cumulonimbus from this analysis. Consequently, the nonlinear problem must be solved in detail in order to determine the orientation of the flow.

5.2 — THE NONLINEAR CONTINUOUS PROBLEM

As in the previous chapters, the general dynamical features of convection in shear are investigated, particularly the orientation of the updraught/downdraught boundary, and the details of the precipitation process avoided. Initial value problems are posed and the effect of certain distributions of sources and sinks of heat on an initially horizontal, /sheared flow considered.

Since the effects of compressibility can be allowed for by the scaling procedure adopted in chapter III, and in order to avoid unnecessary complication, the flow is assumed to be incompressible ($H/H_o \ll 1$). To be able to make comparisons with previous analysis, constant undisturbed shear is retained in this chapter. In the continuity equation the term $\frac{\partial \rho}{\partial t}$ may be neglected by comparison with the other terms, and a streamfunction $\psi(x,z,t)$ defined as

$$u = \frac{\partial \psi}{\partial z} \quad ; \qquad w = -\frac{\partial \psi}{\partial x} \quad .$$

The mathematical problem involves the solution of the vorticity and energy equations,

$$\frac{D}{Dt}(\nabla^2\psi) + g\frac{\partial(\delta\phi)}{\partial x} = 0 \qquad \text{———(5.14)}$$

$$\frac{D}{Dt}(\delta\phi) = Q \qquad \text{———(5.15)}$$

where $Q = Q_o q(x,z)$ (say) is the distribution of sources and sinks of heat.

It can be shown that the nondimensional number which determines the flow is

$$r = \frac{g}{4A^2}\frac{Q_o}{2AH} \qquad \text{———(5.16)}$$

r is evidently closely associated with the nondimensional number R arising in the free-streamline formulation of previous chapters. For example, adopting the usual notation, if $Q_o = \Gamma - B$ and $q = w$, the vertical velocity, then r and R are numerically equal (i.e. in quasi- wet-adiabatic flow).

The initial conditions on the problem are

$$\psi(x,z,t=0) = Az(z-H),$$

$$Q(x,z) = rq(x,z), \text{ for a given r and } q(x,z)$$

$$\delta\phi(x,z,t=0) = 0;$$

that is a heat source stationary with respect to $z = H/2$ in an initially horizontal flow of constant shear 2A.

At the rigid boundaries at top and bottom, it is sufficient to prescribe the streamfunction as $\psi(x,z=0,t) = \psi(x,z=H,t) = 0$. The outflow/inflow boundary condition is not so straightforward to define because the flow at this boundary is influenced by the development of the storm circulation. Accordingly, the boundary condition has to be changed as the circulation develops from the

initial state. This adjustment of the flow in the vicinity of the outflow/inflow boundaries is communicated from the source region in the interior of the system by internal gravity waves (sound waves have been eliminated by neglecting the elastic compressibility effect $\frac{\partial \rho}{\partial t}$ in the continuity equation). Consequently the time taken by the longest (fastest) gravity wave to travel from the source region to the outflow/inflow boundary is a measure of the time at which it first becomes necessary to adjust the initial streamfunction distribution at the boundary. The relative phase speed of an internal gravity wave is

$$U \pm C = \left(\frac{g \frac{\partial \phi}{\partial z}}{\lambda^2 + \nu^2} \right)^{1/2} \qquad \text{——(5.17)}$$

where λ and ν are the horizontal and vertical wave numbers respectively, and for the system under consideration the longest wave is given by $\lambda \simeq \nu = \frac{2\pi}{H}$

$$\frac{(U \pm C)}{2AH} = \frac{1}{\sqrt{2}\,\pi} \frac{\left(g \frac{\partial \phi}{\partial z} \right)^{1/2}}{2A}$$

With $2A = 3 \times 10^{-3}\ s^{-1}$ and $\frac{\partial \phi}{\partial z} = 10^{-7}\ cm^{-1}$, $U \pm C = 14\ m\ s^{-1}$. Consequently the initial inflow/outflow boundary condition can be retained until a simulated time of about 5 minutes, after which time this boundary condition must be modified. This was done successfully by setting the values of θ and ψ at the outflow/inflow boundary equal to those at grid points a predetermined number of mesh lengths into the interior of the flow.

The above initial-value problem was solved numerically for different distributions of sources and sinks of heat, using a staggered-grid computation scheme which is of second order accuracy in time. The details of the different heat source/sink distributions and the solutions are given in the appropriate sections.

5.2.1 — STATIONARY HEAT SOURCE IN FLOW OF CONSTANT SHEAR

This section examines the effect of a heat source, stationary at $z = H/2$ with respect to flow of constant shear. The heat source is of the form $q(x,z) = \sin \pi z/H \, e^{-4|x|}$ where $-H \leqslant x \leqslant H$; $0 \leqslant z \leqslant H$ and its strength determined by the value of r. The heat source was chosen to be proportional to $\sin \pi z/H$ because with the vertical velocity zero at top and bottom an approximately constant parcel lapse is produced. The steady-state solution for a sample value of $r = 0.5$ is shown in Fig.(5.1). Since the temperature and streamline patterns are known from these solutions, it is possible to calculate the equivalent value of Ri. This was done not only because it is easier to make a comparison with the free-boundary solutions, but also because the analysis of chapters III and IV show Ri to be a physically meaningful and fundamental parameter in steady, two-dimensional overturning. On the other hand r does not have any simple physical interpretation.

The solutions indicate that the updraught has a definite slope in the direction of shear. Although the intensity of the circulation depends on the size of the Richardson Number, the orientation of the updraught does not depend critically on this parameter. The downdraught circulation is weak by comparison with the updraught, a feature presumably associated with the absence of positive vorticity generation in this region.

These solutions, showing the effect of a heat source on sheared flow is not directly comparable with the free-boundary solutions of the previous chapter, since the latter imply the existence of a heat source and sink. Since Eq.(4.10) suggests that the orientation of the updraught/downdraught boundary is closely related to the form of the pressure field in the boundary

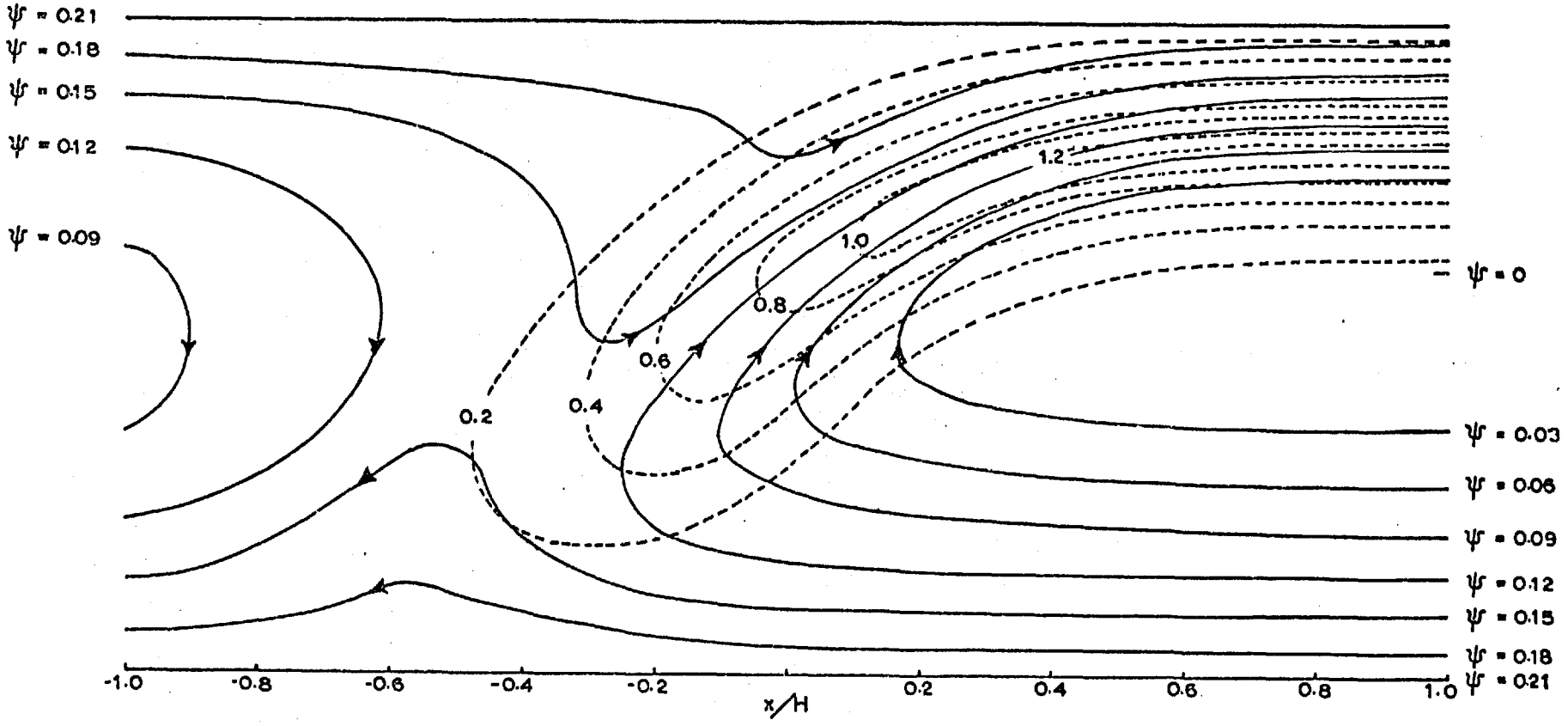

FIG. 5.1 — STEADY SOLUTION TO THE INITIAL-VALUE PROBLEM WITH A STATIONARY HEAT SOURCE IN FLOW OF CONSTANT UNDISTURBED SHEAR. THE RICHARDSON NUMBER IS $Ri = -1.5$, AND THE BROKEN LINES SHOW THE POTENTIAL TEMPERATURE EXCESS IN UNITS OF $\frac{4A^2\theta H}{g}$.

layer and for purposes of comparison with the free-boundary solutions, the next section examines the effect of a stationary heat source and sink on flow of constant undisturbed shear. Before the development of a downdraught by the evaporative cooling of rain, a cumulonimbus is effectively a heat source and therefore the above simple model is at least relevant to this initial stage of development.

5.2.2 — STATIONARY HEAT SOURCE AND SINK IN FLOW OF CONSTANT SHEAR (WET-ADIABATIC MODEL)

This section has two distinct purposes. First, to verify that discontinuity of velocity used in the free-boundary problems of chapter IV is a valid way of modelling the shear across the interfacial boundary layer. Second, the more direct problem of examining the effect of a stationary heat source and sink on sheared flow, particularly in relation to the orientation of the flow.

The first problem requires setting up an equivalent continuous analogue of the free-boundary problem of section 4.4.2 — i.e. generating quasi-steady flow of constant parcel lapse in flow of initially constant shear. More explicitly, the vorticity equation and the energy equation $\frac{D\phi}{Dt} = w\gamma$, where γ is the constant parcel lapse defined in chapters III and IV, must be satisfied. For this purpose, flow was generated using a heat source/sink distribution defined by

$$Q(x,z) = r\cos\pi(z - H/2)\frac{x}{a}\exp\left(-\frac{1}{2q^2}(x^2 - a^2)\right) \qquad \text{——(5.18)}$$

Since Q is proportional to $\cos\pi(z - H/2)$ and the vertical velocity vanishes at $z = 0,H$, an approximately constant parcel lapse is produced. The distribution of Q has a maximum of r at

$(x = a, z = H/2)$ and a minimum of $-r$ at $(x = -a, z = H/2)$. When the flow developed its finite amplitude form, the following (quasi-wet-adiabatic) source was used

$$Q(x,z,t) = R'w \qquad \text{——(5.19)}$$

where R' is a constant calculated from the finite amplitude flow with Q given by Eq.(5.18). The steady-state solution of this problem is then compared to the free-boundary solution with $R = R'$.

The continuous and free-boundary solutions are shown in Fig.(5.2) and Fig.(4.14) respectively for $r = 0.25$, and it can be seen that discontinuity of velocity is a valid model of the boundary layer, particularly regarding its orientation. Consequently, the main features of this quasi- wet-adabatic continuous model are represented by the free-boundary solutions of chapter IV, indicating that the down-shear slope of the interface is a feature of steady, two-dimensional quasi-wet-adiabatic flow, of Richardson Number satisfying $-1.62 \leqslant Ri \leqslant 0.75$.

5.2.3 — STATIONARY HEAT SOURCE AND SINK IN FLOW OF CONSTANT SHEAR (COOLING OF LOW-LEVEL INFLOW)

Examination of the Wokingham Storm tephigram indicates that over the first three kilometres of ascent, the low-level inflow air in the lower part of the updraught must be cooler than its surroundings and negatively buoyant. The flow pattern can nevertheless be maintained by utilisation of the inflow kinetic energy. Moreover, even assuming an upshear slope for the interface, the high level inflow air in the model cannot be significantly cooled by precipitation until it has descended over a considerable distance. (Note that the Ludlam-Browning descriptive model avoids this latter possibility by implying

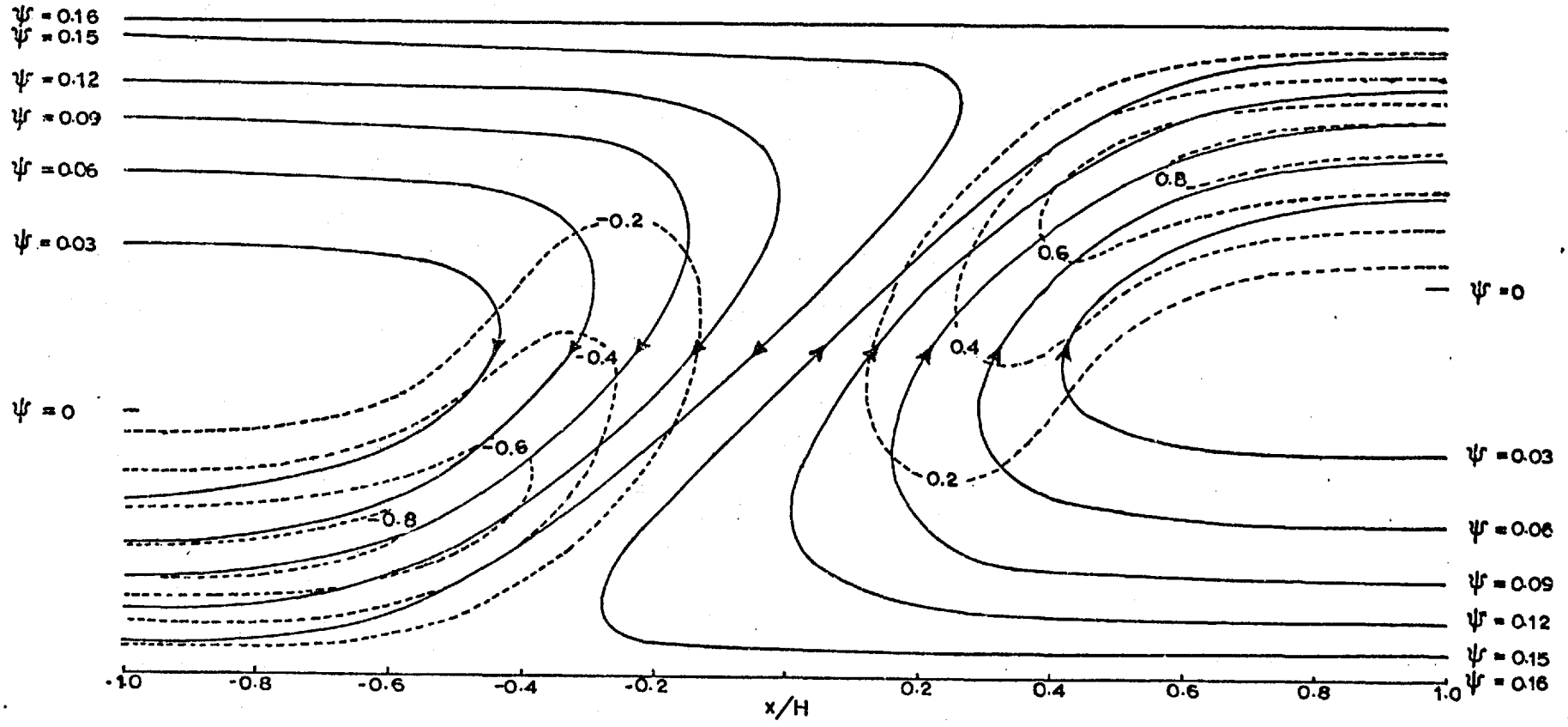

FIG. 5.2 — STEADY SOLUTION TO THE INITIAL-VALUE PROBLEM WITH STATIONARY HEAT SOURCE & SINK IN FLOW OF CONSTANT UNDISTURBED SHEAR. THE RICHARDSON NUMBER IS Ri $\propto$ -1.0, AND THE BROKEN LINES SHOW THE POTENTIAL TEMPERATURE EXCESS IN UNITS OF $\frac{4A^2\theta H}{g}$.

that the downdraught originates from mid-levels - a feature which demands that the flow is dependent on three space dimensions, a possibility excluded from the present analysis.) This section examines the effect of introducing cooling of the low-level and warming of the high-level inflow air, with particular interest in the orientation of the flow.

A convenient way of demonstrating the effect of inflow warming/cooling is to examine the effect of the following Q-distribution on flow if initially constant shear:

$$Q(x,z) = r\left[\sin\left(\frac{2\pi z}{H}\right)\exp-\left(\frac{ax^2}{H}\right)+\sin\left(\frac{2\pi x}{H}\right)\exp-\left(b(z-H/2)^2\right)\right] \qquad (5.20)$$

for $-H \leqslant x \leqslant H$; $0 \leqslant z \leqslant H$, where a and b are constants determining the shape of the heat source/sink distribution.

A sample integration with $a = 4$, $b = 6$, $r = 2$ is shown in Fig.(5.3), and the equivalent value of Richardson Number determined from these solutions is $Ri \simeq 1.5$. This case shows that the updraught/downdraught boundary is inclined upshear, with the updraught above the downdraught, as is implied by observation of real storms.

After intensive examination of two-dimensional finite amplitude overturning induced by given distributions of sources and sinks of heat, it is concluded that in two-space dimensions, a flow orientation with the updraught inclined over the downdraught is peculiar to a model with cooling in the low-level and warming in the high-level inflow.

5.3 — THE PRESSURE FIELDS IN THE INTERFACIAL BOUNDARY LAYERS OF THE CONTINUOUS MODELS

With the object of modelling the boundary layers of the continuous models of this chapter in terms of dynamic boundary

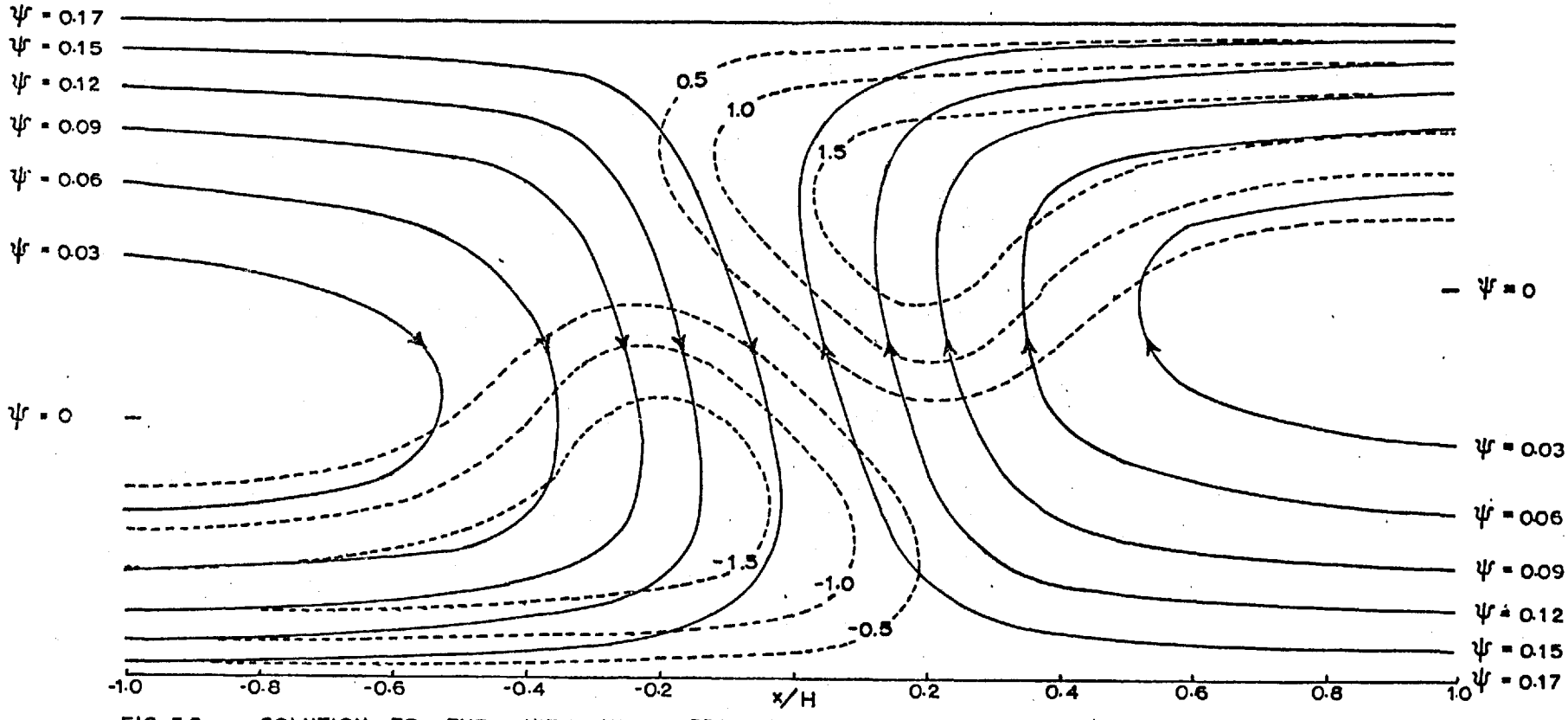

FIG. 5.3 — SOLUTION TO THE INITIAL-VALUE PROBLEM WITH A HEAT SOURCE & SINK SIMULATING COOLING OF THE LOW-LEVEL AND WARMING OF THE HIGH-LEVEL INFLOW AIR, IN FLOW OF CONSTANT UNDISTURBED SHEAR. THE RICHARDSON NUMBER IS $Ri \propto -1.6$ AND THE BROKEN LINES SHOW THE POTENTIAL TEMPERATURE EXCESS IN UNITS OF $\frac{4A^2\theta_0 H}{J}$.

conditions for the free-boundary problem, the interface orientations are now interpreted in terms of the pressure change across the boundary layers. It will be shown that the quasi- wet-adiabatic and boundary layer warming/cooling models of sections 5.2.2 and 5.2.3 respectively have distinctive boundary layer pressure fields.

The Bernoulli equation can be applied along streamlines to define the pressure difference across the interfacial boundary layer. In particular since the flow is antisymmetric with respect to $z = H/2$ and approximately steady, the pressure change across the boundary layer at height z can be shown to be

$$\Delta P(z) = \left(\frac{\delta p}{\rho}\right)_1 - \left(\frac{\delta p}{\rho}\right)_2 = \int_{H/2}^{z} g(\phi_1 - \phi_2)dz - \left(\frac{1}{2}\underset{\sim}{v}_1^2 - \frac{1}{2}\underset{\sim}{v}_2^2\right) \qquad \text{——(5.21)}$$

where the subscripts [1] and [2] refer to variables on the updraught and downdraught sides of the boundary layer respectively. The pressure difference across the boundary layer is therefore equal to the change in the difference between the potential and kinetic energies.

Fig.(5.4) and Fig.(5.5) show the pressure change across the interfacial boundary layer in the models of sections 5.2.3 and 5.2.4 respectively. It is clear that in the former case, flow with a forward sloping interface is characterised by a small pressure change across the boundary layer, whereas the latter case with a backward sloping interface is characterised by a relatively large pressure change.

5.4 — AN ALTERNATIVE DYNAMIC BOUNDARY CONDITION AND EQUIVALENT FREE-BOUNDARY MODEL

In a real physical situation the variables, velocity, temperature and pressure must be continuous (as in the continuous

FIG. 5.4 — THE KINETIC & AVAILABLE POTENTIAL ENERGY CHANGES ACROSS THE INTERFACIAL BOUNDARY LAYER IN THE MODEL OF SECTION 5.2.3.

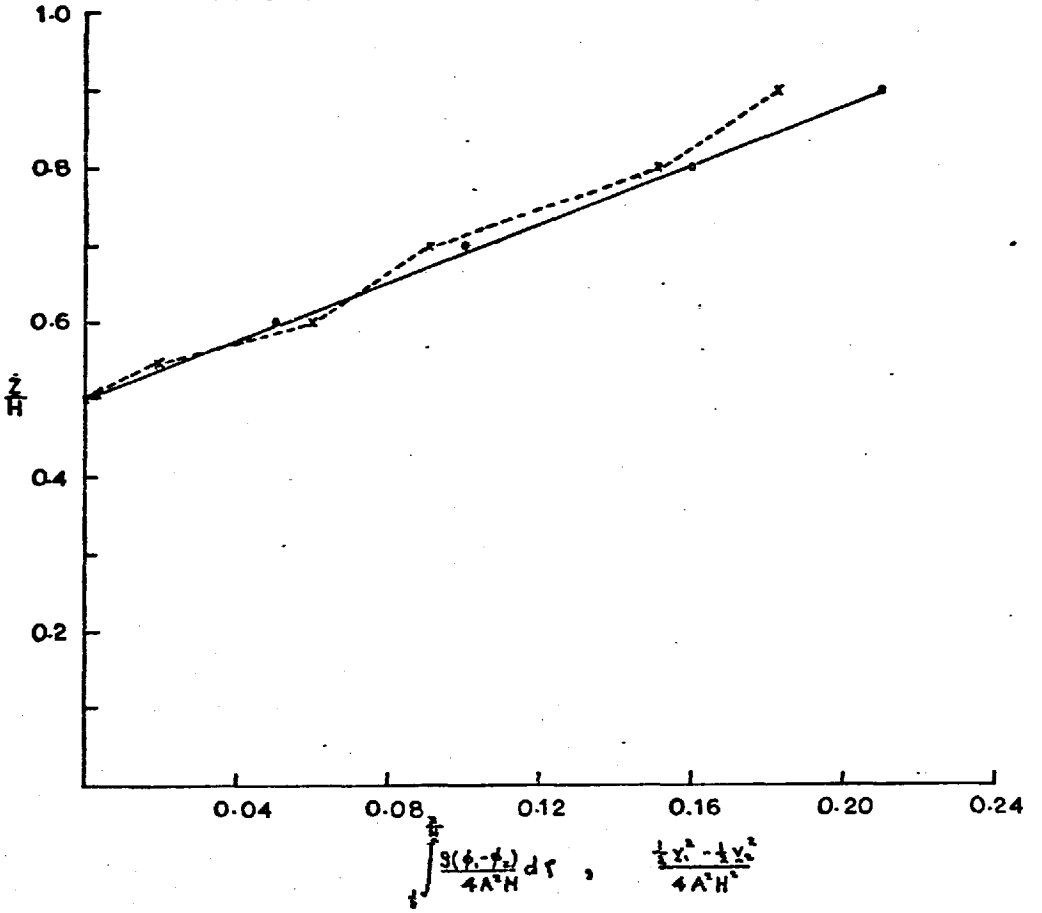

FIG. 5.5 — THE KINETIC & AVAILABLE POTENTIAL ENERGY CHANGES ACROSS THE INTERFACIAL BOUNDARY LAYER IN THE MODEL OF SECTION 5.2.4.

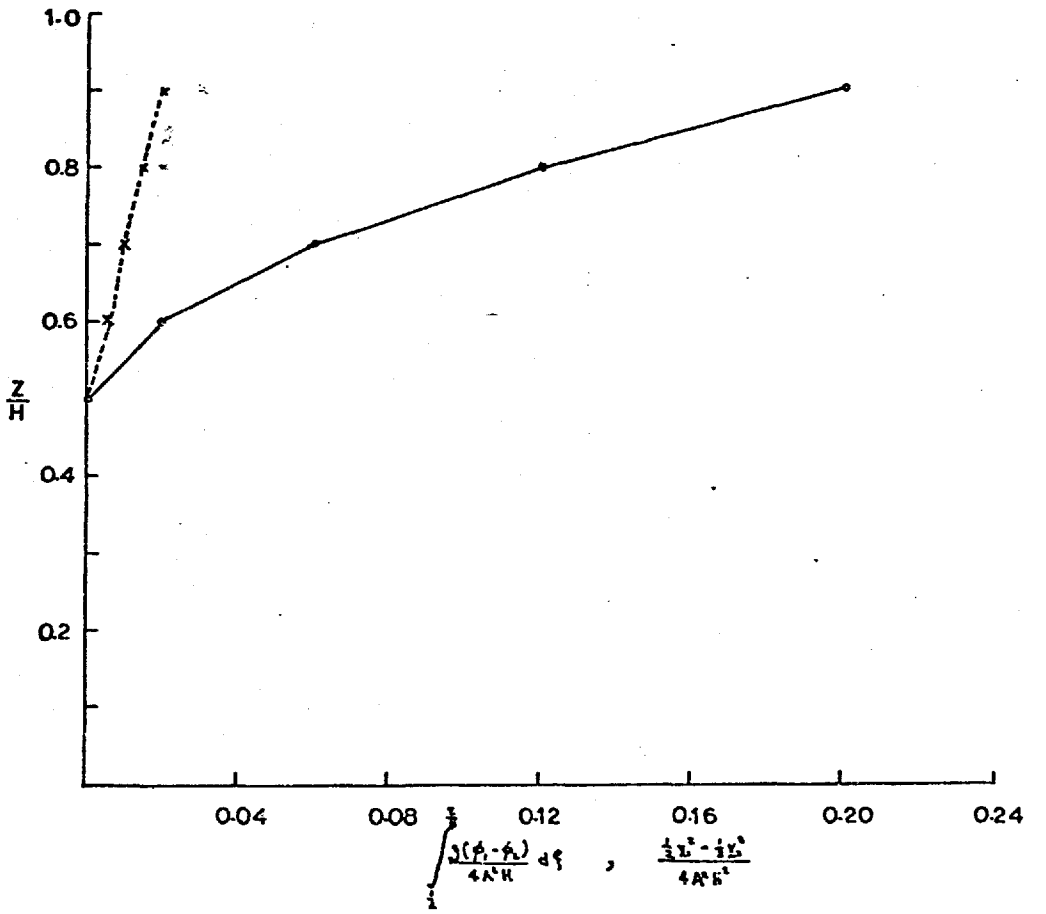

IN THE ABOVE FIGURES, THE BROKEN LINES SHOW THE K.E. CHANGE AND THE SOLID LINES THE P.E. CHANGE.

models of this chapter), otherwise the flow would be dynamically unstable and would readjust itself to smooth out the discontinuities. However, it has already been shown that large gradients in the velocity and temperature fields can be justifiably modelled mathematically by discontinuities, without adversely affecting the physical nature of the flow. Further, it will be shown in this section that a large gradient of pressure can also be modelled by a discontinuity of pressure.

The (wet-adiabatic) model of section 5.2.2 is characterised by flow with a small pressure change across the interfacial boundary layer, and intuitively it should be possible to represent this boundary layer and the general flow pattern by a free-boundary model with continuity of pressure at the interface.

Comparison of the solutions to the free-boundary problems of chapter IV and the continuous, wet-adiabatic model of section 5.2.2 show that this is indeed acceptable.

Likewise, it is not unreasonable to expect that the relatively large pressure change across the boundary layer in the continuous model of section 5.2.3 could be modelled by a pressure discontinuity in the equivalent free-boundary model. Since the solution on Fig.(5.3) shows that the 'pressure' change across the boundary layer is approximately $\int_{H/2}^{z} g(\phi_1 - \phi_2)dz$, the alternative boundary condition is defined as

$$\Delta P(z) = \left(\frac{\delta p}{\rho}\right)_1 - \left(\frac{\delta p}{\rho}\right)_2 = \int_{H/2}^{z} g(\phi_1 - \phi_2)dz$$

i.e. $$\Delta P(z) = g(\gamma - B)(z - H/2) \qquad \text{———(5.22)}$$

The free-boundary problem defined by Eq.(4.21) and the usual kinematic boundary conditions together with the alternative dynamic condition Eq.(5.22) at the interface, was solved for

the value of Ri defined in the continuous model. This solution is shown in Fig.(5.6).

Comparing the free-boundary solution in Fig.(5.6) with the continuous solution in Fig.(5.3), it can be seen that important features such as the interface slope, updraught speed and steering-level are represented to a reasonable accuracy by the equivalent free-boundary analogue. There is therefore considerable justification for representing the continuous boundary layer by a discontinuity of velocity, temperature, and pressure in this free-boundary analogue.

5.5 — GROWTH RATES OF FINITE-AMPLITUDE OVERTURNING IN SHEAR

It is interesting to compare the maximum growth rates of small-amplitude waves in unstably stratified flow of constant shear, obtained from solutions of the characteristic equation Eq.(5.12), with the growth rates of finite amplitude flow, obtained from the numerical solution of the nonlinear equations. (The growth rate of the finite-amplitude disturbance is defined as the reciprocal of the time taken to develop the finite amplitude state from initially horizontal flow.) Fig.(5.7) shows both sets of growth rates and it can be seen that the finite amplitude flow has the fastest growth rate.

Now $[g(\gamma - B)]^{-\frac{1}{2}}$ is the time-scale arising via the linear analysis of convection, while $\frac{1}{2A}$ is that appropriate to the linear theory of convection in sheared flow. It turns out that a simple combination of these time-scales gives a time-scale appropriate to finite amplitude overturning in shear because the growth rate is very nearly linear in $R^{\frac{1}{2}}$. Explicitly

$$\sigma / 2A(1+\sqrt{R}) \simeq \text{constant} = 0.7 \qquad \text{——(5.23)}$$

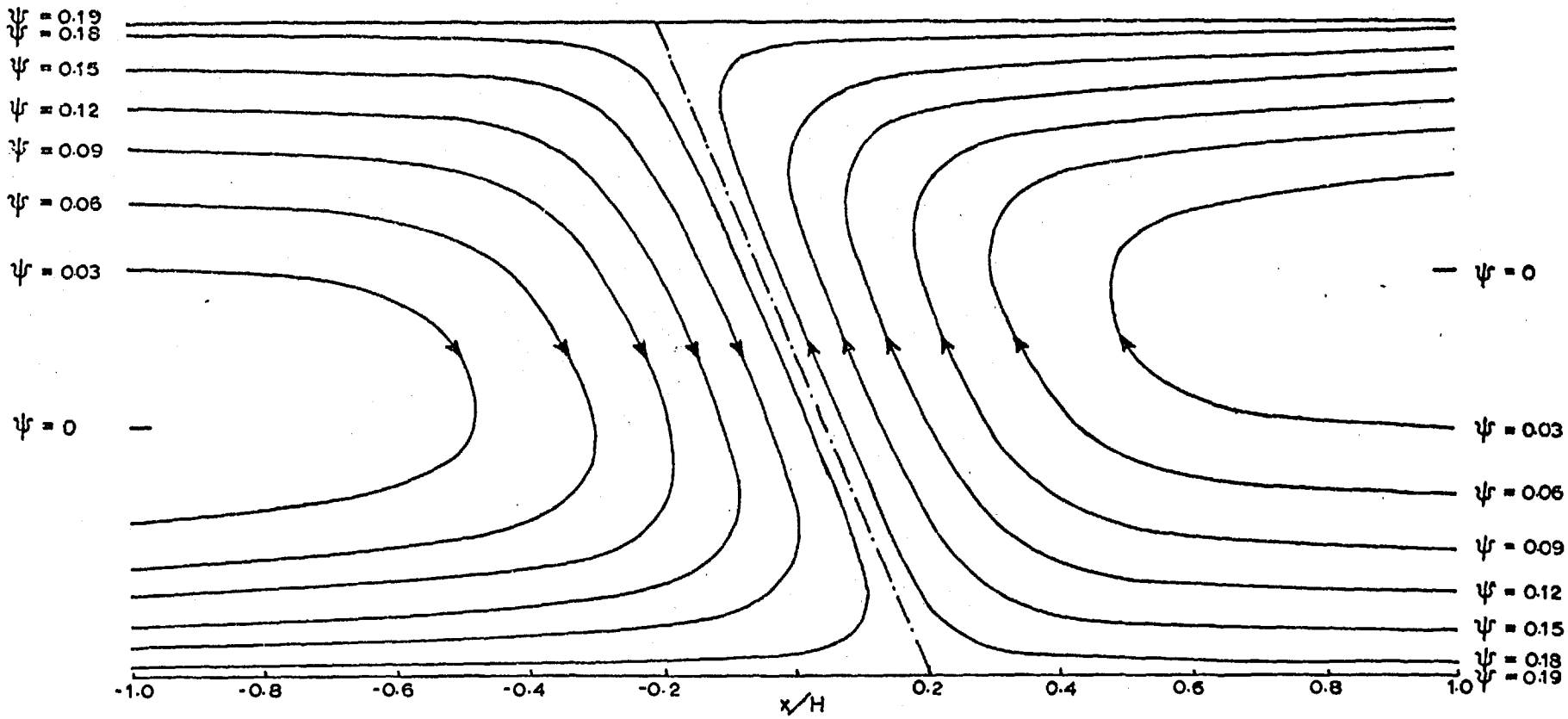

FIG. 5.6 — SOLUTION TO FREE-BOUNDARY PROBLEM WITH VELOCITY, TEMPERATURE & PRESSURE DISCONTINUOUS AT THE INTERFACE FOR Ri = -1.62 (R = 1). THE DYNAMIC BOUNDARY CONDITION IS DEFINED BY EQN.(5.22). THE POSITION OF THE FREE-BOUNDARY IS SHOWN BY THE BROKEN LINE.

gives a simple estimation of the growth rate associated with flow of the form shown in Fig.(5.8), as a function of 2A and $R = \frac{g(\gamma - B)}{4A^2}$. This distinction in growth rate is another example of the incompatibility of the linearised and finite amplitude theories of convective overturning in shear.

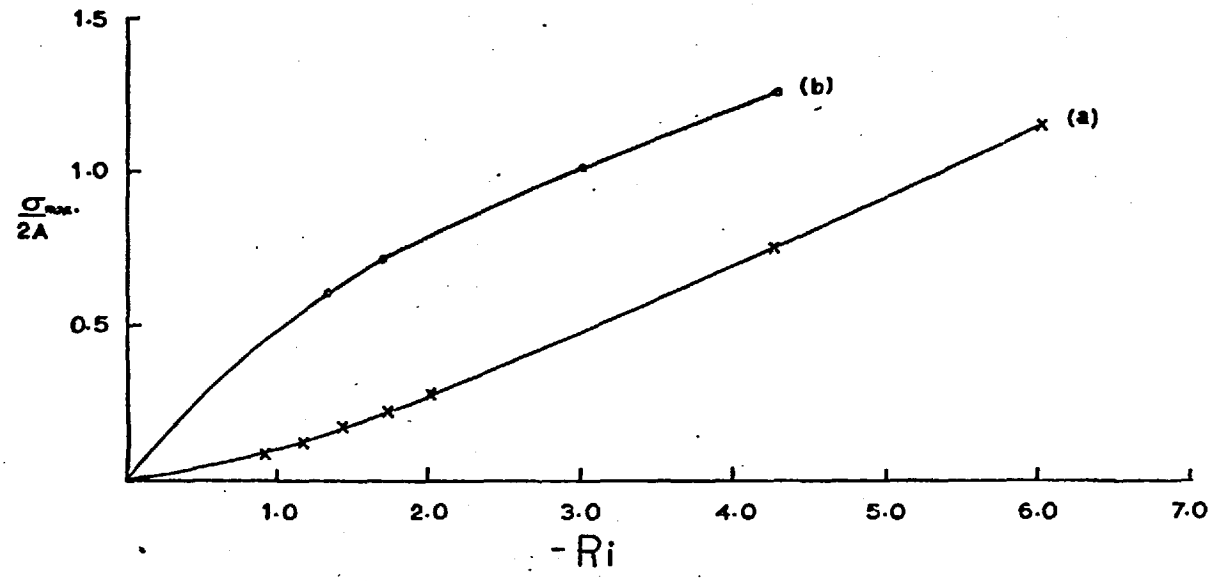

FIG.5.7 — THE GROWTH-RATE AS A FUNCTION OF THE RICHARDSON NUMBER. CURVE (a) INDICATES THE MAXIMUM-GROWTH RATE OF SMALL AMPLITUDE PERTURBATIONS & CURVE (b) THE FINITE AMPLITUDE GROWTH-RATE, IN UNSTABLY STRATIFIED FLOW OF CONSTANT UNDISTURBED SHEAR 2A.

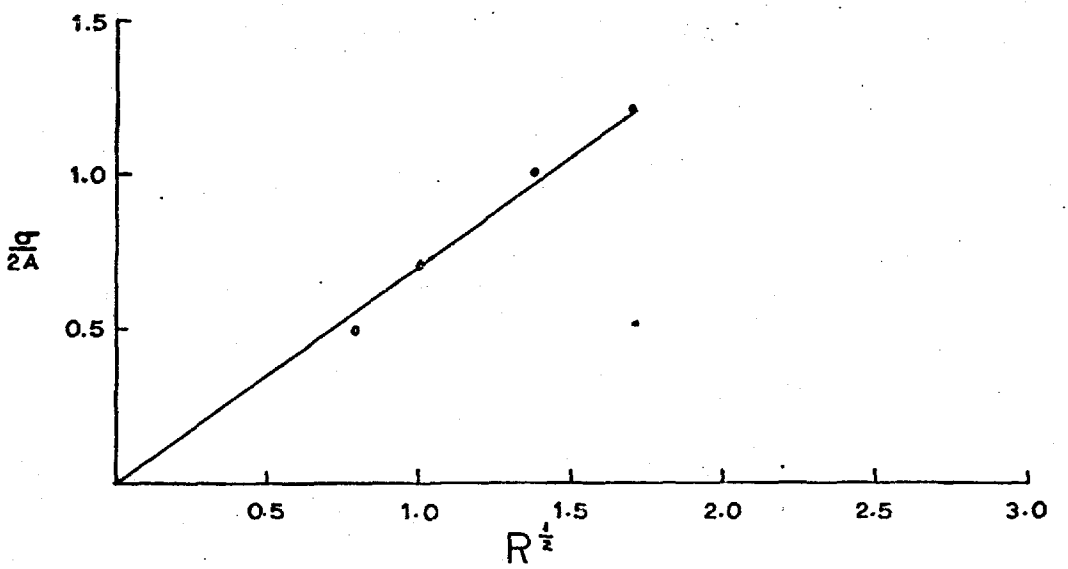

FIG.5.8 — THE GROWTH-RATE OF FINITE AMPLITUDE DISTURBANCES IN FLOW OF CONSTANT UNDISTURBED SHEAR 2A, AS A FUNCTION OF $R^{\frac{1}{2}}$

CHAPTER VI — CONCLUSIONS WITH REGARD TO FUTURE WORK

Most of the conclusions have already been summarised in the abstract or at stages throughout the analysis, and so it is unnecessary to repeat them here. However, important points such as the momentum transfer and the orientation of the flow within the system are worthwhile summarising at this stage.

The momentum transfer in the model described in this thesis is contrary to the conventional ideas of cumulus and cumulonimbus convection, because in the model momentum is transferred from the slower moving fluid to the faster (i.e. against the velocity gradient), whereas vertical convection is usually presented as being a process which transfers momentum downgradient (a contrasting mechanism resulting in the mean shear being decreased). Basically, the reason for the increased shear and the direction of momentum transfer is a feature of the energetics of the cumulonimbus model - the energy exchange is from the available potential energy of the undisturbed flow to the kinetic energy of the modified flow, the effecting mechanism being the cumulonimbus. This effects an increase in the mean shear and also the direction of the momentum transfer. Moreover, the quantification of section 3.5.3 shows that the momentum transfer is large by comparison with the smaller scale boundary-layer processes. Indeed, the fact that cumulonimbus convection in shear involves large energy and momentum transfers makes it an important field of study in meteorology.

The interface orientation with the downdraught above the updraught is characteristic of steady, two-dimensional, wet-adiabatic flow of Richardson Number satisfying $-1.62 \leqslant Ri \leqslant 0.75$, and not a feature of the mathematical representation of a continuous updraught/downdraught boundary layer by discontinuities in the

velocity, temperature or vorticity fields. This has been shown in detail throughout the analysis of chapters IV and V.

Introduction of cooling in the low-level updraught air and warming of the high-level downdraught air generates a pressure field requiring flow with the updraught inclined over the downdraught, the orientation implied by observational evidence to exist in real storms. In a rather extensive analysis of two-dimensional overturning, this is the only physical process found to induce this orientation. This configuration with cooling of the inflow air in low-levels is interesting, because Pearce (1962) also found that cooling had to be introduced in the lower part of the updraught to maintain his assumed backward-sloping interface.

However, when the implications of these contrasting interface orientations are examined in terms of a momentum budget, the conclusion suggests that a complete answer is not likely to be so simple, but that other (probably three space-dimensional) physical processes have to be accounted for: Consider a momentum budget over the shaded region in Figs.(6.1 and 6.2). In case 6.1, with the downshear sloping interface, integration of the x-component of the momentum equation in flux form shows that since $U_1 > U_2$ remote from the storm and $\overline{UW} > 0$ within the storm, the momentum budget can be satisfied without a net pressure difference existing along the length of the storm. However in case 6.2 with the upshear sloping interface, since $U_1 > U_2$ remote from the storm and $\overline{UW} < 0$ within it, the momentum budget can only be satisfied if there is a relatively large net pressure difference along the length of the storm. Consequently taking the Coriolis effect into consideration, a non-negligible transverse (y-directional) circulation is likely to be induced by

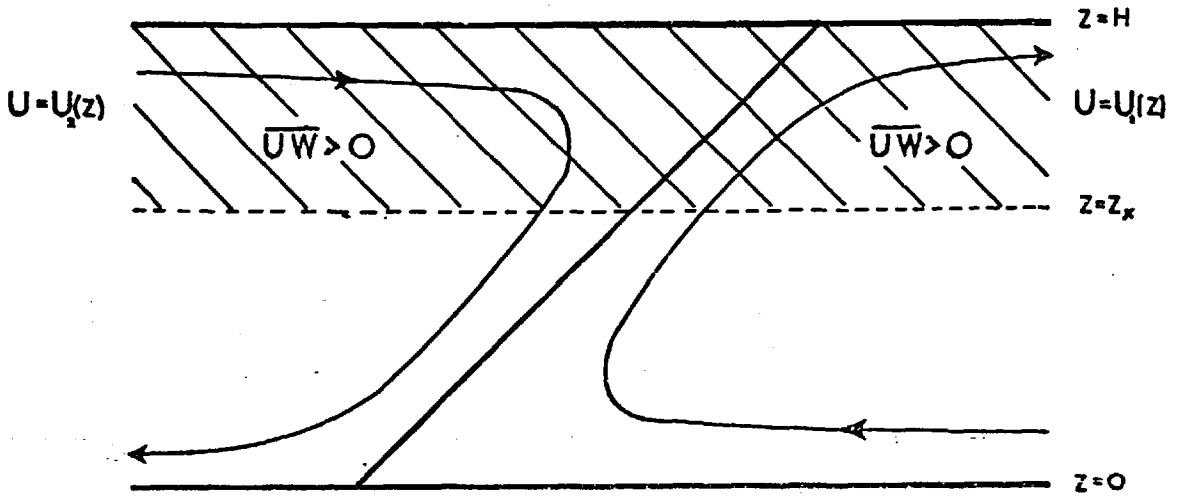

FIG.6.1 — SCHEMATIC DIAGRAM SHOWING $\overline{UW}$ FOR SYSTEM WITH A DOWNSHEAR-SLOPING INTERFACE. (U IS POSITIVE FROM LEFT TO RIGHT IN THIS FIGURE.)

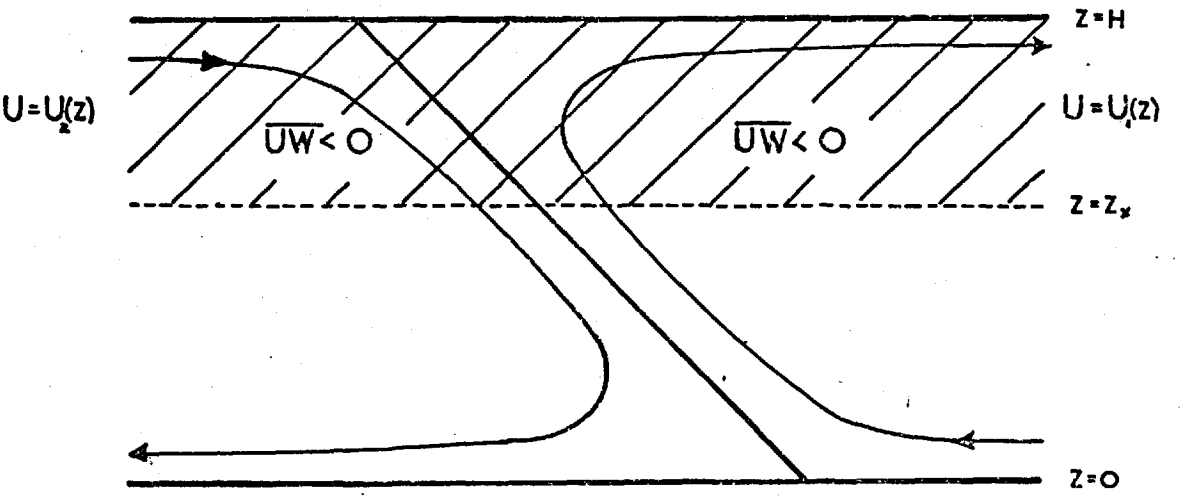

FIG. 6.2 — SCHEMATIC DIAGRAM SHOWING $\overline{UW}$ FOR SYSTEM WITH AN UPSHEAR-SLOPING INTERFACE. (U IS POSITIVE FROM LEFT TO RIGHT IN THIS FIGURE.)

the storm — in which case a three space-dimensional study could reveal additional physical processes. This possibility is worthy of closer study, especially since real storms do in fact feature three-dimensional structure, in particular the propagation to the right of the undisturbed wind field. From this evidence, time spent in developing a theory of three space-dimensional circulation would be justified, a problem which will be subsequently tackled.

Although cumulonimbus convection has been specifically dealt with in this thesis, this is not the only form of convection in shear relevant to this analysis. For instance, application to the prediction of the movement of lines of showers associated with cold-front zones has already been made in chapter III. Moreover, observational studies suggest that structure exists in sub-cloud layer circulations. A similar formulation for the dynamical theory of convection in this sheared region is conceivable. This would be useful since a dynamical theory of the transfer of heat and momentum is necessary, particularly through the requirements of global numerical models.

REFERENCES

Atlas, D.	1963	Severe local storms. Meteor. Monog. 5 American Met. Soc., Boston, Mass.
Brooks, C.F.	1922	The local or heat thunderstorm. Mon. Weath. Rev. 50 p.281.
Browning, K.A.	1962	Air motion and precipitation development in severe local storms. Ph.D. Thesis, Imperial College, London.
Browning, K.A. and Ludlam, F.H.	1962	Airflow in convective storms. Quart. J. R. Met. Soc. 89 p.117.
Browning, K.A. and Fujita, T.	1965	Air Force Cambridge Research Lab. Special Report No.32.
Byers, H.R. and Braham, R.R.	1949	The Thunderstorm. Washington D.C., U.S. Government Printing Office.
Carlson, T.N.	1965	Large scale conditions for the occurrence of severe local storms. Ph.D. Thesis, Imperial College, London.
Case, K.M.	1960	Stability of inviscid plane Couette flow. Phys. Fluids 3 p.155.
Davies, W.M.	1953	Elementary Meteorology. Ginn & Co., Boston, Mass. p.355.
Drazin, P.G.	1958	The stability of heterogeneous shear flows. J. Fluid Mech. 4 p.214.
Dyson, F.J.	1960	Stability of an idealised atmosphere. I - Discussion of results p.140 II - Zeros of the confluent hypergeometric function. p.155. Phys. Fluids 3.
Findeisen, W.	1938	Über die Entstehung der Gewitterelektrizität. Meteor. Z. 57 p.201.
Flügge, S. and Truesdell, C.	1960	Encyclopedia of Physics. Vol.IX. Fluid Dynamics III pp.311-437. Springer-Verlag, Berlin.
Goldstein, S.	1931	On the stability of superposed streams of fluid of different densities. Proc. Roy. Soc. 132A p.524.
Green, J.S.A. and Pearce, R.P.	1962	Cumulonimbus convection in shear. Tech. Note 12, Dept. Meteor., Imperial College, London.
Harper, W.G. and Beimers, J.G.D.	1958	The movement of precipitation belts as observed by radar. Quart. J. R. Met. Soc. 84 p.483.

Harwood, R.S.	1969	Vorticity patterns in extra-tropical cyclones. Ph.D. Thesis, Imperial College, London.
Howard, L.N.	1961	Note on a paper of John W. Miles. J. Fluid Mech. 10 p.509.
Kaimal, J.C. and Businger, J.A.	1970	Case studies of a convective plume and a dust devil. J. Appl. Met. 9 p.612.
Kuo, H.L.	1963	Perturbations of plane Couette flow in stratified fluids and origin of cloud streets. Phys. Fluids 6 p.195.
Lamb, H.	1932	Hydrodynamics. Dover Publications, New York.
Lempfert, R.G.K. and Corlers, R.	1910	Line squalls and associated phenomena. Quart. J. R. Met. Soc. 36 p.135.
Letzmann, J.	1930	Cumulus pulsationen. Meteor. Z. 47 p.236.
Ludlam, F.H.	1962	A case study of thunderstorms on an occasion of small wind shear. Tech. Note 11, Dept. Meteor., Imperial College, London.
Ludlam, F.H.	1963	Severe local storms: A review. Met. Monog. 5 p.1.
Miles, J.W.	1961	On the stability of heterogeneous shear flows. J. Fluid Mech. 10 p.496.
Möller, M.	1884	Meteor. Z. 1 p.230.
Newton, C.W. and Newton, H.R.	1959	Dynamical interactions between large convective clouds and the environment with vertical shear. J. Met. 16 p.483.
Prohaska, K.	1907	The hailfall of 6 July 1905 in the east Alps. Meteor. Z. 24 p.193.
Rayleigh, Lord	1890	Proc. Lond. Math. Soc. 11 p.57.
Suekstorff, G.A.	1939	Die Ergebnisse der Untersuchungen an tropischen Gewittern. Gerlands Beitr. z. Geophys. 55 p.138.
Taylor, G.I.	1931	Effect of variations of density in the stability of superposed streams of fluid. Proc. Roy. Soc. 132A p.499.
Wegener, A.	1911	Thermodynamik der Atmosphäre. J. A. Barth, Leipzig.
Whittaker, E.T. and Watson, G.N.	1927	A course of modern analysis. Cambridge University Press.

ACKNOWLEDGEMENTS

The author is indebted to Dr. J.S.A. Green for introducing an interesting and enjoyable line of research and for constructive criticism throughout. Thanks are also expressed to Miss Marion Street for typing the thesis. The work was supported by a N.E.R.C. Research Studentship.